

Molecular and Cellular Mechanisms Underlying Spatial Learning

Mohammad Reza Hojjati

Hojjati, Mohammad Reza
Molecular and Cellular Mechanisms Underlying Spatial Learning
Printed by: Box Press Company

This thesis contains 4 previously published papers and 1 submitted manuscript for publication, presented in chapters 2 to 6.

Acknowledgements: The research presented in this thesis was carried out at the Department of Neuroscience, Erasmus Medical Center in Rotterdam, The Netherlands. The Iranian Ministry of Health, Treatment, and Medical Education financially supported the researcher, MR Hojjati during his Ph.D. study.

Molecular and Cellular Mechanisms

Underlying Spatial Learning

**Moleculaire en cellulaire mechanismen die ten grondslag liggen aan
spatieel leren**

Proefschrift

ter verkrijging van de graad van doctor aan de
Erasmus Universiteit Rotterdam
op gezag van de
rector magnificus

Prof.dr. S.W.J. Lamberts

en volgens besluit van het College voor Promoties.

De openbare verdediging zal plaatsvinden op
woensdag 14 november 2007 om 9:45 uur

door

Mohammad Reza Hojjati

geboren te Najafabad, IRAN

Promotiecommissie

Promotor: Prof.dr. C.I. de Zeeuw

Overige leden: Prof.dr. J.G.G. Borst
Prof.dr. F.G. Grosveld
Prof.dr. M. Verhage

Copromotor: Dr. Y.Elgersma

*Human beings are members of a whole,
In creation of one essence and soul*

*If one member is afflicted with pain,
Other members uneasy will remain*

*If you have no sympathy for human pain,
The name of human you cannot retain*

Iranian poet Sa'di Shirazi

*for my wife and
my children...*

<i>Content</i>	<i>Page</i>
1 General introduction	9
1.1 Hippocampus	11
1.2 Hippocampal function	11
1.2.1 Hippocampal function in humans	12
1.2.2 Hippocampal function in rodents	12
<i>Lesion studies</i>	13
<i>Pharmacological</i>	13
<i>Genetic studies</i>	13
1.2.3 Hippocampal sensitive tasks	14
<i>Reference memory water maze task (RMWT)</i>	14
<i>Fear conditioning</i>	15
1.3 Extra-hippocampal structures implicated in spatial learning	15
1.4 Hippocampal network	16
1.5 Synaptic plasticity	18
1.5.1 Short-term synaptic plasticity	18
<i>Molecular mechanisms modulating short-term plasticity</i>	19
1.5.2 Long-term synaptic plasticity	20
<i>LTP</i>	20
<i>LTD</i>	26
1.6 Hippocampal impairment in human diseases	27
1.6.1 Angelman Syndrome (AS)	27
1.6.2 Neurofibromatosis (NF1)	28
1.7 Scope of the thesis	29
1.8 References	30
2 Modulation of presynaptic plasticity and learning by the H-ras/extracellular signal-regulated kinase/synapsin I signaling pathway	39
3 Kinase activity is not required for αCaMKII-dependent presynaptic plasticity at hippocampal CA3-CA1 synapses	55
4 Rescue of neurological deficits in a mouse model for Angelman syndrome by reduction of alphaCaMKII inhibitory phosphorylation	69
5 The neuron-specific NF1 exon 9a is essential for theta frequency LTP and learning	85
6 Spatial navigation impairment in mice lacking cerebellar LTD: a motor adaptation deficit?	97
7 General discussion	115
7.1 General discussion	117

<i>Content</i>	<i>Page</i>
Summary	125
Samenvatting (Summary in Dutch)	126
List of publications	127
Curriculum Vitae	128
Acknowledgments	129

Chapter 1

General Introduction

1.1 Hippocampus

The hippocampus is situated in the medial temporal lobe (Figure 1) of the brain. It derived its name from its curved shape in coronal sections of the brain, which bears some resemblance with a seahorse (Greek: *hippo* = *horse*, *kampi* = *curve*). Although the hippocampus lies beneath the cerebral cortex it is not truly a subcortical structure. It is also referred to as archicortex, because it is much older and more primitive than the surrounding neocortex.

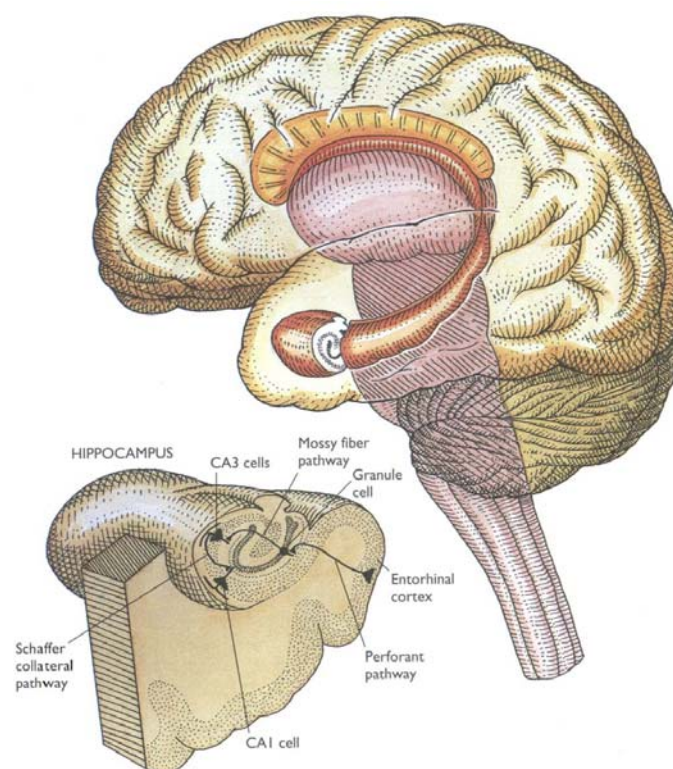


Figure 1- Diagram of the hippocampal formation. The hippocampus is located deep in the medial temporal lobe. Adapted from (Squire and Kandel, 1999).

1.2 Hippocampal function

The hippocampus plays several important roles. One of these functions is memory consolidation, which means converting short-term memory into long-lasting memory. This function is not restricted to the hippocampus. Other areas of the brain also play a role in consolidation of several forms of learning and memory (Lynch, 2004).

Two main types of memory have been described in the mammals: 1) Declarative memory (also called explicit memory) is a form of hippocampal-dependent memory for facts and events, like memory for people, places, and objects;

2) Non-declarative memory (also called implicit memory) functions independently of hippocampus and involves the non-conscious recollection of skills. The main difference between these two forms of memory is that declarative memory is conscious and non-declarative memory is unconscious (Squire, 1994; Milner et al., 1998). Each form of memory is associated with specific brain structures.

Hippocampal function has also been described by a spatial map theory (O'Keefe, 1979). According to this theory the hippocampus of an animal makes a representation or map from the animal environment. The existence of place cells (cells that only fire upon entering a specific place) in the hippocampus have provided ample support for this theory.

1.2.1 Hippocampal function in humans

Hippocampal damage in humans leads to two devastating consequences: loss of the ability to form new declarative memories (anterograde amnesia) and a loss of recently formed memories (retrograde amnesia). Numerous studies have demonstrated the role of the hippocampus in memory (Scoville and Milner, 1957; Morris et al., 1982); reviewed by (Eichenbaum et al., 1992). One of these studies has been done on H.M. patient, who suffered from severe seizures and underwent an experimental bilateral-medial temporal lobe surgery to reduce the severity of the seizures (Scoville and Milner, 1957). After the surgery, H.M. was unable to form any new memories and due to the loss of two-thirds of his hippocampal formation, he suffered from subsequent severe anterograde amnesia. Similar deficits have been reported in patients undergoing unilateral hippocampal resection with prior concomitant damage to the contralateral hippocampus (Penfield and Mathieson, 1974).

Another case study is about a patient called R.B. who was introduced by Zola-Morgan, Squire and Amaral in 1986. He suffered from an ischemic episode and experienced severe anterograde amnesia that was similar to that of H.M. Following his death, his brain was examined to evaluate the extent and regional specificity of the damage. A lesion was found in the CA1 region of the hippocampus with little damage found in other areas of the brain. The R.B. case was one of the first reported cases of memory impairment following damage limited to the hippocampus. These are some of the studies in humans that clearly show the hippocampus is one of the main brain areas involved in declarative memory formation.

1.2.2 Hippocampal function in rodents

In parallel to human studies, compelling animal research has been done to offer insights into the function of the rodent hippocampus. In these studies, several lines of research have been used, such as innovative lesioning techniques, localized pharmacological treatment, and molecular genetic interventions.

Lesion studies

For a long time scientists have been using lesioning techniques in rodents to find out the hippocampal functions. These studies have shown that following the hippocampal lesions, animals demonstrate spatial learning and memory deficits (Morris et al., 1982; Sutherland et al., 1983). By improving lesioning techniques, researchers have been able to investigate the effects of more selective hippocampus damages in distinct hippocampal subregions. For instance, it has been shown that specific lesions of CA3 (Handelmann and Olton, 1981) or dentate gyrus (DG) (Whishaw, 1987; Xavier et al., 1999) lead to spatial memory deficits. These are some examples from a huge number of lesion studies that have been done to identify the role of hippocampal function in the rodents (See (Martin and Clark, 2007) for a review).

Pharmacological studies

Pharmacological manipulation has also been used to study the function of the hippocampus in learning and memory in more detail and to get insight into the critical molecular mechanisms underlying hippocampal function. It has been shown that pharmacological blockade of hippocampal NMDA receptors impairs memory formation (Morris et al., 1990a; Danysz et al., 1995; Martin et al., 2000). In some of these studies, NMDA receptor antagonists have been used in specific region of the hippocampus. For example, infusion of AP5 into the dentate gyrus or CA1 region impairs spatial working memory; in contrast, infusion of AP5 into CA3 area have a transient effect that disappears with further training (Lee and Kesner, 2002; Martin and Clark, 2007). Morris and colleagues showed that intraventricular infusion of AP5 impaired spatial learning of a new task; however the impairment was reversible after removing AP5 (Morris et al., 1986).

Genetic studies

The development of mouse genetic manipulation techniques has provided a unique opportunity to comprehensively address many fundamental issues in cognitive neuroscience that are very difficult to study by using the traditional pharmacological or neurosurgical approaches. Generally, genetic manipulation can be divided into four approaches (Nakajima and Tang, 2005). In the **transgenic** approach (also called gain-of-function) a gene or DNA sequence is added to the genome. One example is over-expression of the NR2B gene in neurons of the forebrain in mice. These transgenic mice show higher long-term potentiation (LTP) in CA1 region and interestingly, they showed increased learning and memory (Tang et al., 1999). In the **knockout** approach (also called loss-of-function) an endogenous gene is deleted from the genome. An example for this approach is NMDA receptor knockout in CA1 region. These mutant mice show spatial learning and memory impairment and also LTP deficit at the Schaffer collateral-CA1 pathway (Tsien et al., 1996). Two other approaches are a **knockdown** approach, by which expression level of a target gene has not completely inhibited, but some expression level is left (McDevitt et al., 1997).

and a **knock-in** approach, by which an endogenous gene is replaced by a manipulated/changed version of the original gene. Although genetic approaches have some limitations, they have led to revolutionary progress in the understanding of the role of genes in different biological and pathological events.

1.2.3 Hippocampus sensitive tasks

Reference memory water maze task (RMW)

Maze studies have been used to examine the role of the hippocampus in learning and memory. The Morris water maze task is presently the most commonly used paradigm to evaluate hippocampal-dependent learning abilities in rats and mice. Richard G.M. Morris first designed this task. In this special navigation task, animals swim in a pool containing opaque water to find a platform that is hidden just below the water surface. Animals use external visual cues to locate the platform (Figure 2). In this task rodents are highly motivated to escape from a water environment by the quickest and the most direct route. There are many different protocols for using the Morris water maze task. Typically, training is 3 to 10 days, each day consists 1-6 trials of 1 to 2 minutes each.



Figure 2- Morris water maze task.

During training, normal mice swim toward the hidden platform with an increasingly direct swim path, therefore they decrease the latency time to reach the platform. Decreasing the latency indicates that the animal has acquired the task. At the end of training period, each mouse is tested on a probe trial, which assesses the ability of the animal to identify the spatial location that previously contained the platform. The platform is removed from the pool and the amount of time spent in the previous location of the platform, is measured as the amount of the learning. If the mouse has acquired the task, it will swim straight to the target quadrant and spend more time close to the former platform location. The Number of platform crossings and time spent in the platform area must be significantly greater when compared to naive

(untrained) mice performance. As a control, a visible water maze task is typically performed to check whether motor performance or motivation to escape is normal. Normal performance in the visible platform task but bad performance in the hidden platform task indicates learning and memory impairment.

Fear Conditioning

Fear conditioning, a form of classical conditioning, is a useful task that can be used to explore hippocampal-dependent learning and memory. Two forms of fear conditioning task have been used in rodents. The cued and contextual fear conditioning tasks measure the ability of the animal to learn and remember an association between an aversive experience (mild electrical foot shock) and spatial or environmental cues (place, sounds, lights) (Fanselow, 1980; Fanselow and Tighe, 1988; LeDoux, 1995). During the conditioning trial, rodents are placed in a cage (context) with a metal grid on the bottom of it and after a specific time (for example 2.5 minute) a cue is presented (usually a sound) and then a mild foot shock are given to the animals. At a later time (for example 24 hour), the animal is placed in the same context in which had been shocked and freezing time is measured. Freezing is operationally defined as a lack of any movement other than that caused by respiration for 2 continuous seconds (Kushner et al., 2005). Similar brain areas involved in the Morris water maze task seem also implicated in the fear conditioning experiments. Indeed, the hippocampus, subiculum, perirhinal cortex and the medial temporal lobe appear to mediate contextual fear conditioning in rodents (Eichenbaum et al., 1996; Squire and Zola, 1996; Logue et al., 1997). However, these brain areas are modulated by the emotional pathways such as the amygdala (McGaugh et al., 1996; LeDoux, 2000). An important control to the contextual fear conditioning could reveal the involvement of the hippocampus: cued fear conditioning is not dependent on the hippocampus, but contextual fear conditioning seems to depend more on the hippocampus than the amygdala (Phillips and LeDoux, 1992). So, if the animal shows impaired contextual fear conditioning but not cued fear conditioning, it is likely that the impairment is the result of hippocampal malfunctioning.

1.3 Extra-hippocampal structures implicated in spatial learning

Many experiments have demonstrated that the hippocampus plays a role in learning and processing of spatial and contextual information, but evidently the hippocampus is not the only structure involved in spatial learning. Other structures, such as the dorsal striatum (McDonald and White, 1994; Devan et al., 1996), the subiculum (Morris et al., 1990b), subcortical structures (Whishaw et al., 1987; Sutherland and Rodriguez, 1989) or the parietal (Save et al., 1992) and entorhinal cortex (Schenk and Morris, 1985) have also been implicated in spatial memory (Smith and Milner, 1989). The literature in humans suggests that the parahippocampal gyrus (PHG) is another structure, which may play an important role in spatial memory (Bohbot et al., 1998).

Recently, a role for the medial thalamus has been suggested in learning water maze behavioral strategies (Cain et al., 2006).

Experiments in mutant mice with cerebellar degeneration suggest that the cerebellum has a role in spatial learning as well (Lalonde and Botez, 1986; Lalonde, 1987; Lalonde et al., 1988). However, most of these experiments suffer from some limitations in examining the role of the cerebellum in spatial learning, which may interfere with spatial learning paradigms. In Chapter 6, we will address this issue using L7-PKCI transgenic mice, which do not show a motor performance deficit (De Zeeuw et al., 1998; Burguiere et al., 2005).

1.4 Hippocampal network

The hippocampus together with the amygdala, cingulate gyrus and a set of other structures forms the limbic system. The limbic system derived its name (*limbus* is Latin for rim) from its location that is around the thalamus, just under the cerebral cortex (Purves et al, 2001). The hippocampal formation comprises four regions. These include the dentate gyrus (DG), the hippocampus proper (which can be divided into three sub-fields, namely CA3, CA2 and CA1), the subicular complex and the entorhinal cortex (Amaral and Witter, 1989). The hippocampus and DG appear as an elongated structure medially in the temporal horn of the lateral ventricle (Figure 3), produced by the invagination of the ventricular wall by the hippocampal sulcus (Amaral and Witter, 1989). They have a simplified laminar pattern compared with the neocortex.

The hippocampus has three major excitatory pathways (Figure 4). The first pathway is called the perforant pathway (PP), which projects from the entorhinal cortex (EC) to the granular cells of the dentate gyrus (DG). This pathway is generally considered the main source of input to the hippocampus. Axons from layers II/IV of the entorhinal cortex project to the granule cells of the dentate gyrus and pyramidal cells of the CA3 region, while those from layers III/V project to the pyramidal cells of the CA1 and the subiculum. The perforant path is divided into lateral and medial pathways (LPP and MPP, respectively), depending on whether the fibers arise from the lateral or medial entorhinal cortex (LEC and MEC, respectively) (Amaral and Witter, 1989). The second pathway is the Mossy Fiber Pathway (MF). The mossy fibers are the axons of DG granule cells. They extend from the dentate gyrus to CA3 pyramidal cells. MF synapses are large and have multiple active zones (Henze et al., 2000). Multiple granule cells can synapse onto a single CA3 pyramidal cell. These synapses show NMDA receptor-independent LTP and it has been shown that LTP is expressed by an enhancement of neurotransmitter release (Yamamoto et al., 1980; Harris and Cotman, 1986). CA3 pyramidal cells send Schaffer collaterals to the apical dendrites of CA1 pyramids, and also extensive collaterals that terminate within CA3.

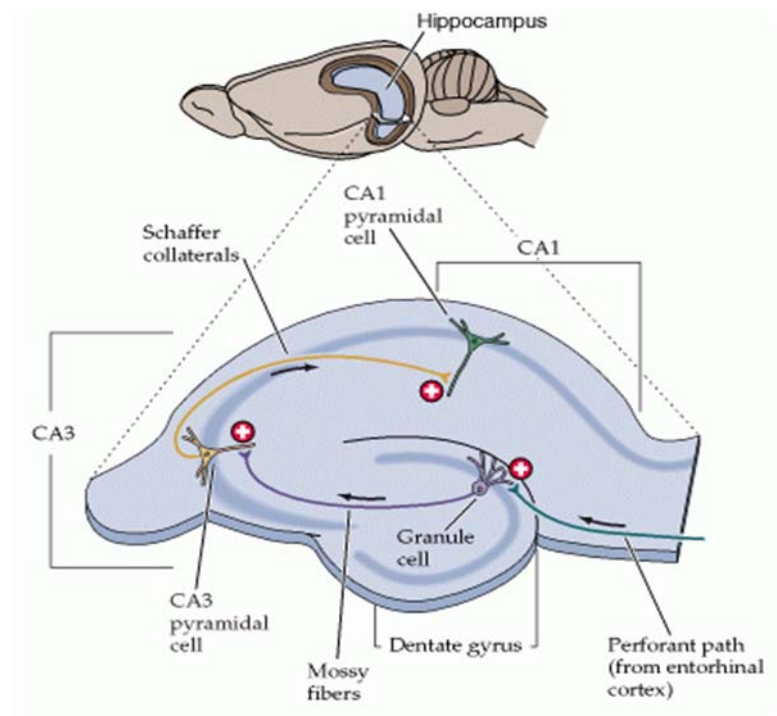


Figure 3- The position of the hippocampal formation in the rat brain. The slice pictured at the bottom is a representation of the major neuronal elements and intrinsic connections of the hippocampal proper. Adapted from (Purves et al; 2001).

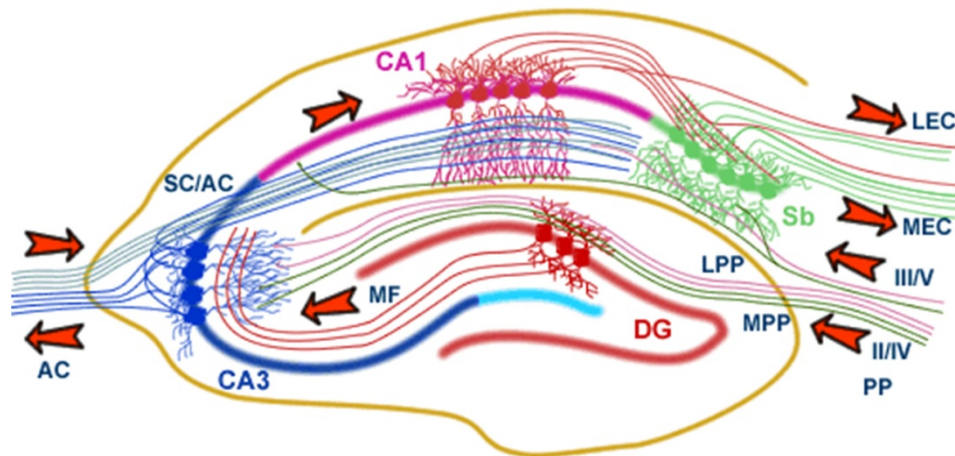


Figure 4- Hippocampal network. Abbreviations: DG, dentate gyrus; Sb, subiculum; MF, mossy fibers; SC/AC, Schaffer collaterals/association commissural path ; PP, perforant path; LPP, lateral perforant path; MPP, medial perforant path; LEC, lateral entorhinal cortex; MEC, medial entorhinal cortex. Adapted from the University of Bristol Centre for Synaptic Plasticity.

The third pathway is the Schaffer Collateral/Associational Commissural Pathway, which is extensively used to study NMDA receptor-dependent LTP and LTD. This pathway comprises the axons, which are projected from CA3 to CA1 area of the hippocampus. These axons either come from CA3 neurons in the same hippocampus (ipsilateral) or from CA3 neurons in the opposite hemisphere (contra lateral). These latter fibers are termed commissural fibers, as they cross from one hemisphere of the brain to the other. Hippocampal CA3-CA1 synapses have been a major model system for understanding basal synaptic transmission and synaptic plasticity. Besides these three main pathways, there is another pathway from CA1 to Subiculum (Sb) and on to the entorhinal cortex. This pathway forms the principal output from the hippocampus.

1.5 Synaptic plasticity

The ability of the brain to change in response to the new experiences is called plasticity. Plasticity is not restricted to a specific part of the brain or in a limited period of life. It is present throughout the lifetime and in most parts of the brain especially in the neurons. Long-lasting changes in the efficacy of synaptic transmission or the strength of synapses between neurons is defined as synaptic plasticity (Bliss and Collingridge, 1993; Martin et al., 2000; Kandel, 2001). Synaptic plasticity is commonly accepted to be a mechanism for memory formation in the central nervous system. The plastic changes that underlie memory are thought to occur at the same synapse that is being strengthened. Donald Hebb has described this rule in his book (Hebb, 1949) in 1949 as following:

“When an axon of cell A is near enough to excite cell B and repeatedly or persistently takes part in firing it, some growth process or metabolic change takes place in one or both cells such that A’s efficacy, as one of the cells firing B, is increased” (Hebb, 1949; Sejnowski, 1999).

Synaptic plasticity has been observed in virtually all types of synapses and is regulated by a variety of short-term or long-term processes. Synaptic plasticity sometimes results in a decrease of synaptic strength and sometimes leads to an increased synaptic efficacy. Two forms of synaptic plasticity will be briefly described in the next part.

1.5.1 Short-term synaptic plasticity

Short-term plasticity is a rapid change in synaptic strength that occurs within several hundred millisecond of the onset of activity. It can be observed in the most synapses of the central nervous system. Several forms of short-term plasticity have been described, such as facilitation, augmentation, depression and post-tetanic potentiation (PTP). Each of these forms is induced by repetitive stimulation of the neurons at different time scales. Most evidence suggest that the origin of short-term plasticity is largely presynaptic (Zucker, 1989); however, postsynaptic mechanisms have also

been suggested (Schneggenburger et al., 2002; Zucker and Regehr, 2002). Short-term plasticity of excitatory synapses in the central nervous system is critical for information processing (Varela et al., 1997; Maass and Zador, 1999).

Facilitation, augmentation and PTP are all generated by the continuing action of residual presynaptic calcium ions. After the tetanus, Ca^{2+} concentration remains elevated and increases the number of transmitter quanta released by each presynaptic action potential (Delaney et al., 1989). The main evidence for this is the ability of Ca^{2+} chelators to reduce both residual Ca^{2+} and facilitation (Zucker and Regehr, 2002). Augmentation is the increased response obtained a few to ten seconds after the tetanus (Zucker and Regehr, 2002). Facilitation, or sometimes-called paired pulse facilitation (PPF), can be observed when synapses are stimulated twice within a short time interval. Facilitation typically persist several hundreds of milliseconds following presynaptic activity. Depending on the time intervals between two stimuli (10 to 400 ms, for example), the second postsynaptic potential (PSP) response can be up to several times bigger than the first PSP size. It has been shown that mutant mice with deficits in paired pulse facilitation show impairment in learning and memory (Silva et al., 1996; Matilla et al., 1998), suggesting that short-term facilitation in hippocampus may play a role in learning.

Rather than facilitation, some synapses show synaptic depression. Repetitive nerve stimulation in certain situations leads to a decrease in postsynaptic potentials called depression. Facilitation and depression probably both occur in most synapses, but which one dominates at a given synapse depends on the release probability. Facilitation is most clearly apparent when the release probability is relatively low and when probability is high synapses show depression (Thomson, 2000).

What are the functions of short-term synaptic enhancement in the neural processing of information? It might be that facilitation, augmentation, or PTP act as effective high-pass allowing the cell to respond only to sustained high frequencies. Evidence for this frequency filter will be shown in chapter 2, where we show that the activation of the Ras pathway selectively promotes release during high frequency stimulation.

Molecular mechanisms modulating short-term plasticity

Synaptic vesicles can be functionally organized in two distinct pools. The first pool is the readily releasable pool or docked vesicle pool, which is near to the pre-synaptic membrane. This pool contains those synaptic vesicles that are docked to the presynaptic membrane and are released at the start of prolonged high frequency stimulation (Rosenmund and Stevens, 1996; Schikorski and Stevens, 2001). The second pool is called the reserve pool, which is farther from the pre-synaptic membrane. From this pool vesicles are mobilized to the docked pool. The vesicles in the reserve pool are anchored to the cytoskeleton by the synapsin proteins, but the docked pool is devoid of Synapsins. It has been shown that presynaptic injection of

synapsin I antibodies leads to the loss of the reserve pool, without any apparent effect on the readily-releasable pool (Pieribone et al., 1995).

The Synapsins are a family of several proteins that are localized at presynaptic nerve terminals. The Synapsins were the first synaptic vesicle-associated proteins to be discovered (Greengard et al., 1993), but their functions still are not clearly known. They are excellent substrates for a variety of protein kinases including protein kinase A (PKA), Ca^{2+} /calmodulin-dependent protein kinases (CaMK) I, II and IV and mitogen-activate protein (MAP) kinase, that phosphorylate them on distinct serine residues. For instance, Synapsin I can be phosphorylated at its Ser-9 (P-site I) by PKA and CaMKI, at its Ser-62 (P-sites 4), Ser-67 (P-site 5) and Ser-549 (P-site 6) by MAPK, and at Ser-566 (P-site 2) and Ser-603 (P-site 3) by CaMKII. Synapsins interact with synaptic vesicles and various cytoskeletal proteins including actin. They control synaptogenesis, regulate synaptic vesicles trafficking and can modulate short-term synaptic plasticity. The critical roles of synapsins make them ideal targets to be involved in presynaptic changes required for learning and memory formation. In chapter 2, we provide evidence for this hypothesis.

1.5.2 Long-term synaptic plasticity

One of the most significant challenges in neuroscience is to identify the cellular and molecular processes that underlie learning and memory. To that end, many researchers have focused on two major forms of long-term synaptic plasticity, which are easily observed *in vitro*; Long-term potentiation (LTP) and Long-term depression (LTD).

LTP

Long-term potentiation (LTP) is a long-lasting activity dependent enhancement of synaptic responses and has been repeatedly proposed to be a molecular mechanism for certain forms of learning and memory (Bliss and Collingridge, 1993; Maren et al., 1993; Izquierdo and Medina, 1995). Although LTP has been described more than 30 years ago and huge number of studies has focused on this long-lasting form of plasticity, there are still many unanswered questions regarding the role of LTP as a cellular mechanism of memory storage. LTP can be induced in all main pathways of the hippocampus (Bliss and Lomo, 1973; Alger and Teyler, 1976; Amaral and Witter, 1989), because the anatomy of hippocampus allows us to stimulate an individual hippocampal pathway and to record simultaneously from an individual or a population of the cell bodies of the postsynaptic targets in another region of the hippocampus. LTP is not restricted to the hippocampus, but is a property of excitatory synapses throughout the brain. Indeed, it is difficult to find an excitatory pathway that does not express one or more forms of LTP (Malenka, 2003).

Basic properties of hippocampal long-term potentiation

LTP of the Schaffer collateral synapse exhibits several properties that make it an attractive neural mechanism for information storage (Purves et al, 2001). These properties of LTP can be explained mechanistically by the biological properties of the NMDA receptors, which are described in the next part.

The first property of LTP is **Cooperativity**, which means that to induce LTP, both pre- and postsynaptic cell need to cooperate and be active. To trigger LTP, a critical number of presynaptic fibers must be activated and simultaneously the postsynaptic cell must be sufficiently depolarized to allow Ca^{2+} influx through the NMDA receptor channel. By increasing the number of stimulated afferents, cooperativity between pre- and post synaptic neurons increases and reaches to the threshold level for induction of LTP. Weak stimulations activate few afferents and do not trigger LTP (Bliss and Collingridge, 1993), but if a single stimulus to the Schaffer collaterals (which would not normally elicit LTP) is paired with strong depolarization of the postsynaptic CA1 cell, LTP is induced.

The second property of LTP is **input specificity**, that is, the enhancement of synaptic efficacy in a synapse does not occur on other synapses of the same neuron. LTP is elicited at one set of synapses on a postsynaptic cell and adjacent synapses that were not activated during the induction protocol do not show LTP.

Finally, LTP is **associative**, which means that induction of LTP at a given synapse can facilitate LTP induction at an independent adjacent synapse on the same neuron if both synapses are activated in a determined time window (Bliss and Collingridge, 1993; Malenka and Nicoll, 1999). As noted, while weak stimulation of a pathway does not by itself trigger LTP, but if this weak stimulation occurs simultaneously with a strong stimulation on a neighboring pathway onto the same cell, both synaptic pathways undergo LTP (Purves, et al, 2001).

There are numerous protocols that can be used for LTP induction. A commonly used protocol is a single train of high frequency stimulation (tetanus, 100 Hz, 1s). This tetanus induces an increase in the responses of the synapses that lasts for 1-2 hour. This form of plasticity that is called early-phase LTP (E-LTP), is protein synthesis-independent. Early-LTP is activated by Ca^{2+} influx through NMDA receptors and subsequent protein phosphorylation events (Bliss and Collingridge, 1993; Malenka and Nicoll, 1999). In contrast, repeated high frequency stimulation at certain time intervals (e.g. four trains of tetanus, at 5- 10 min. interval) results in long-lasting late-phase LTP (L-LTP) that lasts for 6-10 hours. (Frey et al., 1988). Late-LTP begins gradually during the first 2-3 h and can last for 6-10 h in hippocampal slices *in vitro* and for days to months *in vivo* (Reymann et al., 1985; Krug et al., 1989; Otani and Abraham, 1989; Frey et al., 1995; Kandel, 2001).

Molecular mechanisms underlying LTP

For a long time from the discovery of LTP, neuroscientists have been trying to answer this question that LTP has pre-synaptic or postsynaptic mechanism. Both presynaptic and postsynaptic mechanisms have been suggested. Regarding the presynaptic mechanisms, an increased probability of neurotransmitter release has been reported (Bekkers and Stevens, 1990; Malinow and Tsien, 1990). It has been suggested that upon receiving the LTP-inducing stimulation, a retrograde messenger is released from the postsynaptic neurons and is diffused to the pre-synaptic cell. Arachidonic acid and nitric oxide have been suggested as candidate retrograde signals (Bliss and Collingridge, 1993). Recently endocannabinoids have been accepted as a retrograde messenger in the brain (Wilson and Nicoll, 2001; Alger, 2002). Although it seems plausible that long-term synaptic changes require presynaptic changes, most attention has been devoted to the large postsynaptic changes that are induced by LTP. The major molecules involved in these postsynaptic processes are described below.

NMDA receptor

NMDA receptors are composed of assemblies of NR1 and NR2 subunits, which can be one of four separate gene products (NR2A-D). Expression of both subunits is required to form functional channels. At resting membrane potential, NMDA receptors are inactivated by Mg^{2+} ions. To activate the NMDA receptor, and to initiate LTP, two events need to occur simultaneously. First of all glutamate, which is released from pre-synaptic cells has to bind to the postsynaptic NMDA receptor. Second, magnesium block should be released from its binding site within the NMDA receptor during the tetanus. This allows Ca^{2+} to enter the postsynaptic dendritic spine. NMDA receptor, because of its dual requirement for presynaptic glutamate release and postsynaptic depolarization, acts as a molecular coincidence detector.

CaMKII

Calcium-calmodulin dependent Kinase type II (CaMKII) is an abundant protein in the brain and consists of 10-12 subunits (Gaertner et al., 2004). It is clearly shown that Ca^{2+} entry through the NMDA receptor activates CaMKII. Several lines of evidence indicate that activation of CaMKII is both necessary and sufficient to induce long-term potentiation (Pettit et al., 1994; Lledo et al., 1995). For example, inhibition of CaMKII activity blocks the induction of LTP (Malenka et al., 1989; Malinow et al., 1989; Silva et al., 1992; Lisman, 1994). In addition, mutations that prevent persistent activation of CaMKII also block LTP and behavioral memory (Silva et al., 1992; Giese et al., 1998). Following its activation, CaMKII can phosphorylate many other proteins in the cell and is known as a molecular switch that is capable of long-term memory storage (Lisman and McIntyre, 2001). CaMKII has four distinct isoforms, α , β , γ , and δ each encoded by a separate gene. Neuronal CaMKII consists primarily of α and β subunits (Miller and Kennedy, 1985), with the ratio of α to β subunits at 3:1 in the hippocampus (Goldenring et al., 1984). CaMKII isozymes are differently

expressed during and after development. For example, β subunits are expressed during embryonic development (Brocke et al., 1995), but α subunits are expressed solely postnatally. (Burgin et al., 1990). On the other hands, in the forebrain the α CaMKII is main isozyme, whereas in the cerebellum β is the primary isozyme (Miller and Kennedy, 1985). In the postsynaptic densities (PSD) of neurons α isoform has been shown to be the ‘major postsynaptic density protein’ (Kennedy et al., 1983).

The ratio of α CaMKII over β CaMKII is regulated by neuronal activity. In hippocampal cultures, bidirectional modulation of α - and β CaMKII has been demonstrated. For example, suppressing neuronal activity by application of TTX leads to rapid decrease in α CaMKII levels and slower increase in β CaMKII levels (Thiagarajan et al., 2002). In contrast, treatment of the cultures with bicuculline, which increases overall activity by inhibiting GABA release, causes changes in the opposite direction. This modulation of the α/β ratio may serve as a homeostatic mechanism to adjust the sensitivity of the CaMKII to calcium by altering the proportion of β CaMKII. α CaMKII is sensitive to higher levels of Ca^{2+} , while β CaMKII has better sensitivity to lower levels of Ca^{2+} . When the two isoforms are combined in a heteromer, the response to Ca^{2+} signals has been found to depend on the ratio of α to β subunits (Brocke et al., 1999).

Neuronal CaMKII has been shown to be important for several neuronal functions, including neurotransmitter synthesis, neurotransmitter release, modulation of ion channel activity, cellular transport, cell morphology and neurite extension, synaptic plasticity, gene expression, learning and memory (Yamauchi, 2005). Figure 5 shows a schematic representation of CaMKII activation and role of CaMKII in neuronal cells. Each CaMKII subunit contains a catalytic domain, a regulatory domain (containing the auto-inhibitory region and a Ca^{2+} /calmodulin binding site), and an association domain (Figure 6). The catalytic domain has specific binding sites for ATP, substrate, and for interaction with anchoring proteins. This domain is largely responsible for phosphorylation of the substrates. The phosphorylation will occur whenever the catalytic domain is enzymatically active (Colbran, 1992). In the inactive state, an auto-inhibitory domain is bound to the catalytic site, therefore catalytic domain cannot bind to its substrates (Rich et al., 1989; Mukherji et al., 1994). The association domain is the site by which the subunits bind to each other and form the holoenzyme. As shown in the figure 6, most of the structural differences between CaMKII isoforms are related to this domain. This domain enables the kinase to find its specific intracellular sites and modify the sensitivity to Ca^{2+} /CaM. As shown in figure 7, in the absence of Ca^{2+} /CaM, CaMKII is thought to be inactive because the autoinhibitory domain binds to the catalytic domain, preventing access to substrate (Rongo, 2002).

When Ca^{2+} enters the cell, it binds to CaM and makes a Ca^{2+} /CaM complex. Then, this complex binds to the Ca^{2+} /CaM binding site on the CaMKII regulatory subunit and activates it. Activation of Ca^{2+} /CaM binding site disrupts the interaction between the autoinhibitory domain and catalytic domain. The catalytic subunit is then

released and allows the kinase to phosphorylate itself on threonine (T286) site, which is located in the CaMKII autoinhibitory domain and becomes active (Miller and Kennedy, 1986; Meyer et al., 1992). T286 autophosphorylation between adjacent subunits enhances the affinity for Ca^{2+} /calmodulin (Meyer et al., 1992).

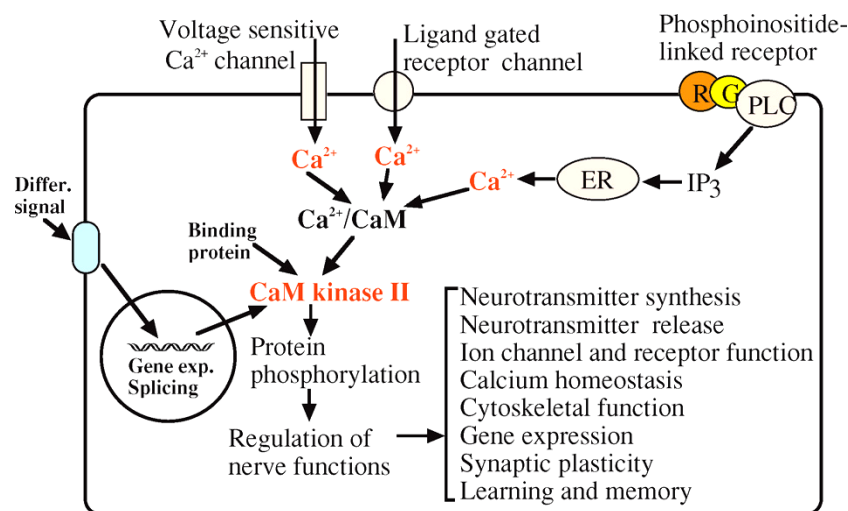


Figure 5- Schematic Representation of Activation and Role of CaM Kinase II in Neuronal Cells. Intracellular Ca^{2+} is increased by extracellular stimuli, binds to calmodulin, and activates CaM kinase II. CaM kinase II phosphorylates various kinds of proteins and regulates physiological processes. Adapted from (Yamauchi, 2005).

Autophosphorylation at T286 allows the kinase to be constitutively active even after Ca^{2+} /CaM dissociation and the absence of calcium (Lisman et al., 2002). Using mutant mice lacking T286 phosphorylation, it has been shown that this phosphorylation is necessary for hippocampal learning and LTP (Giese et al., 1998). In addition, T286 phosphorylation promotes CaMKII association with postsynaptic density (PSD) by binding to the NMDA receptor (Strack et al., 1997; Strack and Colbran, 1998; Shen and Meyer, 1999; Shen et al., 2000). The PSD is a specialization of the cytoskeleton at the synaptic junction, which allows for the assembly and clustering of proteins necessary for proper synaptic function.

Following autophosphorylation at T286, another CaMKII autophosphorylation, called inhibitory autophosphorylation occurs. Upon dissociation of Ca^{2+} /CaM from the activated kinase, the CaM-binding domain becomes exposed, allowing inhibitory phosphorylation at T305 and T306 sites (Colbran and Soderling, 1990; Patton et al., 1990; Mukherji and Soderling, 1994). This causes a dramatic loss of ability of CaMKII to bind Ca^{2+} /CaM, (Kuret and Schulman, 1985; Hashimoto et al., 1987; Mukherji and Soderling, 1994). Phosphorylation at T305/T306 reduces the CaMKII activity.

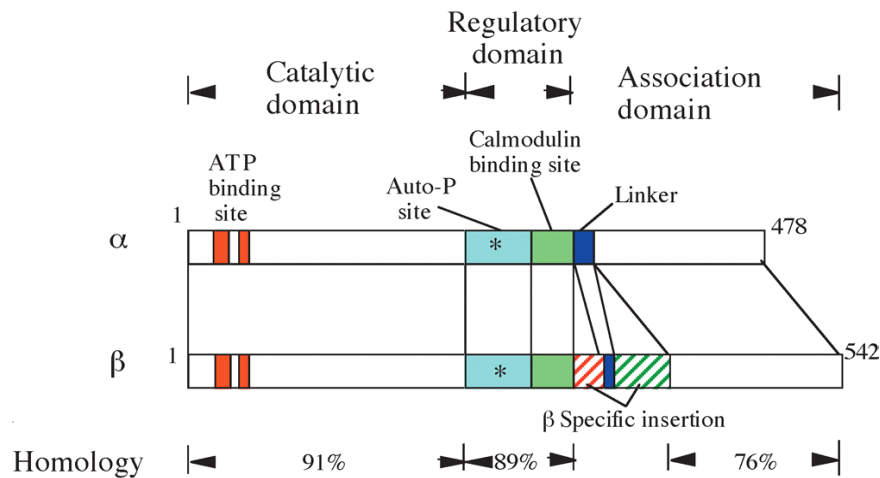


Figure 6- Domain structure of α and β CaM kinase II. Adapted from (Yamauchi, 2005).

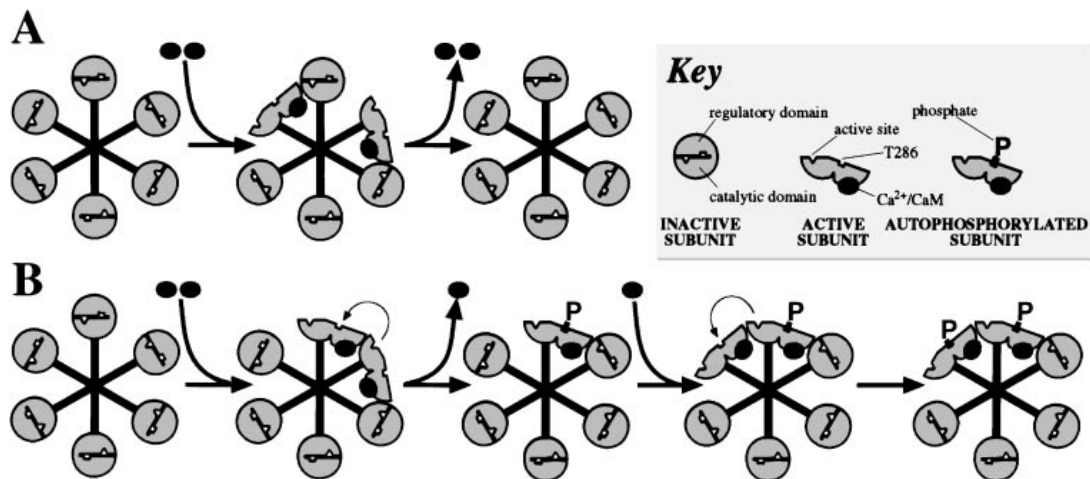


Figure 7- CaMKII autophosphorylation (See text). Adapted from (Rongo, 2002).

AMPA receptor

The α -amino-3-hydroxy-5-methyisoxazole-4-propionic acid (AMPA) receptors mediate fast synaptic transmission in the CNS in response to presynaptic glutamate release. AMPA receptors are found throughout the brain, with particularly high expression levels in cerebral cortex, basal ganglia, thalamus, hippocampus, cerebellum and spinal cord (Blackstone et al., 1992). The presence of AMPA receptors at synaptic sites has been shown by different techniques, including electron microscopy (Baude et al., 1995; Nusser et al., 1998), light microscopy and electrophysiological recordings (Cottrell et al., 2000). The number of AMPA

receptors at synapses are dynamically regulated between synaptic, extrasynaptic, and intracellular pool of receptors (Triller and Choquet, 2003). AMPA receptors can exchange between synaptic and extrasynaptic compartments by lateral diffusion in the neuronal membrane (Borgdorff and Choquet, 2002; Ashby et al., 2006).

Four different AMPA receptor subunits have been identified: GluR1 to GluR4 (Seeburg, 1993; Hollmann and Heinemann, 1994), but the precise function of AMPA receptors is poorly understood. AMPA receptors are phosphorylated at different sites by PKA, CaMKII and PKC and these phosphorylations are important in synaptic plasticity (Song and Huganir, 2002). Electrophysiological studies in the CA1 region of the hippocampus were the first to suggest that synaptic levels of AMPA receptors are rapidly regulated (Isaac et al., 1995; Liao et al., 1995). These studies showed that AMPA receptors are absent in silent synapses. These synapses contain only functional NMDA receptors (Liao et al., 1999; Pickard et al., 2000). Although silent synapses normally lack functional AMPA receptors, synaptic activity that induces LTP can elicit postsynaptic responses mediated by AMPA receptors. AMPA receptors can undergo rapid internalization and reinsertion into the postsynaptic membrane within a few minutes. These studies suggest that AMPA receptors could be recruited rapidly to the silent synapse by either spontaneous or stimulated NMDA receptor activation (Liao et al., 2001; Pickard et al., 2001).

LTD

Long-term depression (LTD) is another major form of long term synaptic plasticity in the brain. It is a well-known form of synaptic plasticity of principal neurons in the mammalian brain. Whereas LTP is proposed to be a cellular model for memory formation, LTD has been suggested to be a mechanism of forgetting (Dudek and Bear, 1992). In contrast to LTP, LTD comprises a persistent reduction of synaptic strength. The phases and mechanisms of LTD are less extensively studied as compared to LTP. Recently, it was reported that within the hippocampal CA1 region, LTD shares similar properties as LTP (Sajikumar and Frey, 2003, 2004). It was shown that different forms of LTD could be induced depending on the induction protocol, as is the case for LTP.

LTD is also segregated to early LTD, a transient form of LTD lasting 2-3 h, and late LTD, which last up to 8h. Early LTD is normally induced using weak low-frequency stimulation (WLFS) consisting of 900 pulses, whereas a strong low-frequency stimulation (SLFS) consisting of 2700 pulses can induce a long-lasting late LTD. Like in LTP, early-LTD is protein synthesis-independent while late-LTD is dependent on protein synthesis (Sajikumar and Frey, 2003).

In the hippocampal CA1 region and the cerebral cortex, both long-term potentiation (LTP) and long-term depression (LTD) are dependent on the activation of NMDA receptors, because both can be blocked by the NMDA receptor antagonist (D/L-AP5) (Collingridge et al., 1983; Harris et al., 1984; Dudek and Bear, 1992; Mulkey and Malenka, 1992; Cummings et al., 1996). High-frequency stimulation

causes strong activation of NMDA receptors and therefore, a large amount of Ca^{2+} enter into postsynaptic neurons to trigger potentiation. Low-frequency stimulation results in a moderate activation of NMDA receptors and a moderate influx of Ca^{2+} , leading to depression. An additional mechanism suggests that high- and low-frequency stimulation activate distinct subpopulations of NMDA receptors (Hrabetova and Sacktor, 1997; Hrabetova et al., 2000). Selectively blocking NMDA receptors that contain the NR2B subunit abolishes the induction of LTD, but not LTP; however, preferential inhibition of NR2A-containing NMDA receptors prevents the induction of LTP without affecting LTD production (Liu et al., 2004). These results demonstrate that distinct NMDA receptor subunits are critical factors that determine the polarity of synaptic plasticity, although the other possibilities such as Ca^{2+} sources and internalization of AMPA receptor are still under discussion.

1.6 Hippocampal impairment in human diseases

Several lines of evidences have shown that the hippocampal structure can be affected by some diseases, resulting in cognitive impairments like learning disability or memory loss. For instance, the first target of Alzheimer's disease is the entorhinal cortex, the input region to the hippocampus, and CA1 region of the hippocampus (Squire and Kandel, 1999). In the following part, two genetic disorders that affect hippocampal function are described briefly.

1.6.1 Angelman syndrome (AS)

Angelman's mental retardation syndrome is a severe neurological disorder in human, affecting one of every 15,000 births (Clayton-Smith, 1993). This syndrome is commonly accompanied by severe mental retardation, motor dysfunction and epilepsy (Fryburg et al., 1991; Williams et al., 1995; Buoni et al., 1999; Laan et al., 1999). The Ube3a gene is identified as the genetic locus for Angelman syndrome (Albrecht et al., 1997). The Ube3a gene encodes for a 100kD protein, called E6-associated protein, (E6-AP) that functions as an ubiquitin ligase enzyme (Huibregtse et al., 1991, 1993; Kishino et al., 1997; Matsuura et al., 1997). The exact function of E6-AP protein is not clearly known, but it has been suggested that this enzyme is involved in protein degradation. Jiang and colleagues generated a mouse model of Angelman syndrome. Electrophysiological recording in Schaffer collateral pathway showed that these mice have normal synaptic transmission (Jiang et al., 1998), however high frequency stimulation leads to a severe deficit in LTP induction that appears to be caused by faulty signal transduction downstream of Ca^{2+} influx (Weeber et al., 2003). Extensive analysis of the known kinase pathways that influence generation of LTP revealed that levels and phosphorylation of PKC isoforms, PKA subunits and ERKs were all normal. The levels of total CaMKII were also normal, but T286 and T305 autophosphorylation were significantly increased (Weeber et al., 2003). Phosphorylation at T305 reduces the CaMKII activity and its affinity for the PSD. The amount of CaMKII associated with the PSD in AS mice was about 50% of

normal, consistent with the T305D knock-in study that indicated that phosphorylation of T305 dominantly decreased PSD binding (Elgersma et al., 2002). These data indicate that in AS mice, CaMKII exhibits numerous alterations in phosphorylation state and therefore could result changes in the activity, regulation and the cellular location of the enzyme. How the loss of Ube3a can result in changes in CaMKII phosphorylation remains to be investigated.

1.6.2 Neurofibromatosis (NF1)

Neurofibromatosis 1 (NF1) is a common, inherited, autosomal dominant disorder in humans that affects approximately 1 in 3500 individuals, with no ethnic or gender-related variability (Huson et al., 1988; Poyhonen et al., 2000). It is caused by a heterozygous loss of function mutation within the NF1 gene located on chromosome 17. The highest level of NF1 gene expression is seen in neural tissues (Daston et al., 1992). There are several isoforms of NF1, which arise by alternative splicing. The most commonly expressed isoform includes exon 23a, which has been shown to have decreased Ras-GAP activity (NF1 type II) (Danglot et al., 1995; Gutmann et al., 1995a; Geist and Gutmann, 1996). Two other common alternatively spliced exons are 9a and 48a. The isoform containing exon 48a is highly expressed in muscle tissues (Gutmann et al., 1995b) and expression of the 9a-containing isoform is seen after development of the brain and in adult mice restricted to the neurons only (Gutmann et al., 1999).

Affected individuals present with pigmentation abnormalities and an increased risk of developing both benign and malignant tumors (Gutmann et al., 1997). In addition, 40 to 60% of children with NF1 have learning disabilities ranging from mild cognitive impairment to attention deficit disorder (North et al., 1997). The NF1 gene encodes a protein called neurofibromin. Neurofibromin has several known properties and function (Figure 8), including Ras GTPase-activating protein activity (Xu et al., 1990), adenylyl cyclase modulation (Guo et al., 1997), microtubule binding (Xu and Gutmann, 1997), and regulation of actin filament reorganization (Ozawa et al., 2005). A mouse model for the Neurofibromatosis type 1 was first developed in 1994 and has been utilized in the investigation and characterization of the disease (Jacks et al., 1994; Cichowski et al., 1996). Studies have shown that *NFI*^{+/-} mice have abnormal spatial learning when tested in the hidden version of Morris water maze (Silva et al., 1997).

Increased Ras activity is the cause for the learning deficits observed in NF1, because spatial learning impairments in *NFI*^{+/-} mutants can be rescued by two different genetic manipulations that decrease Ras levels (Costa et al., 2002). Ras is a low molecular weight protein, regulating many signalling cascades such as the Ras-Raf-MEK pathway, leading to activation of MAPK/extracellular signal-regulated kinase (ERK) and the Ras-phosphoinositide-3-kinase (PI3K) pathway leading to activation of Akt/PKB. Electrophysiological studies in the CA1 region of the hippocampus of *NFI*^{+/-} mice showed that LTP is impaired when induced using a

theta-burst stimulation (TBS) protocol (Costa et al., 2002; Guilding et al., 2007; Guilding and Piggins, 2007), which mimics the *in vivo* activity of hippocampal neurons during exploratory behaviour (Larson et al., 1986). In addition, the *NF1*^{+/-} mice have increased GABA inhibition in the hippocampus, and it has been suggested that this increased inhibition is the cause of the LTP deficits (Costa et al., 2002). Decreasing Ras activity reversed the learning deficits, the increased GABA inhibition and the LTP deficits of the *NF1*^{+/-} mice (Costa et al., 2002).

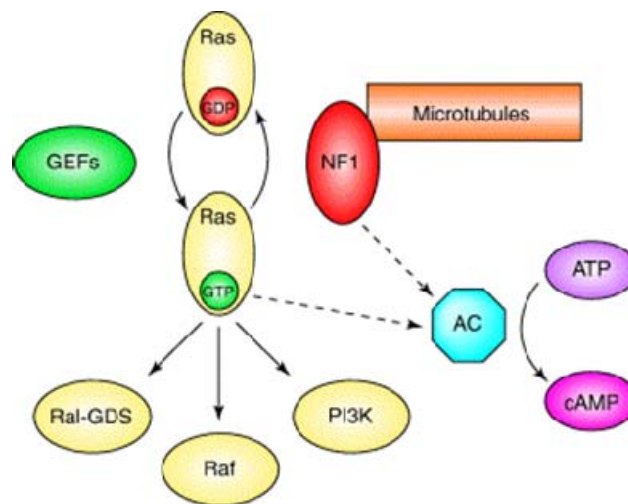


Figure 8- The interactions of neurofibromin (NF1) with different signaling pathways. NF1 has several known biochemical functions, including activation of the Ras GTPase, modulation of adenylyl cyclase (AC), and microtubule association. Ras activates several effector molecules, including the Ral GDP-dissociation stimulator (Ral-GDS), Raf and phosphatidyl inositol 3-kinase (PI3K). Abbreviation: GEF, guanine-nucleotide exchange factor. Adapted from (Costa and Silva, 2003).

1.7 Scope of this thesis

One of the major challenges that many animals have to solve is how to find their way around their world. For example they should know where a particular resource is and how to get to it from their present location, or what is a safe route home to avoid a predator. Many experiments have demonstrated that the hippocampus plays a role in the learning and processing of spatial and contextual information. On the other hand, experiments in mutant mice with cerebellar degeneration suggest that the cerebellum also plays a role in spatial learning. Since the primary aim of this research is to investigate the molecular and cellular mechanisms underlying spatial learning, we have conducted our experiments on these two brain structures, and tested how molecular deficits in these brain areas affect spatial learning. We focused in particular on the role of the ERK and CaMKII signaling pathway on neuronal plasticity and spatial learning. These pathways are not only known to be critical for cellular plasticity, but are also affected in the human disorders Neurofibromatosis 1 and Angelman syndrome, respectively.

This thesis has been organized in seven chapters. Chapter 1 gives a general introduction about hippocampal anatomy and function, hippocampal plasticity, extra-hippocampal structures implicated in spatial learning and a short description of two diseases related to the hippocampus. **Chapter 2** describes how the H-Ras/ERK/Syn I pathway affects presynaptic plasticity. Although extensive evidence supports the involvement of postsynaptic plasticity in mammalian learning and memory, this chapter reveals an experience-dependent presynaptic mechanism that modulates learning and synaptic plasticity.

As explained in this introduction CaMKII can be phosphorylated at different sites and this autophosphorylation and inhibitory phosphorylation play an important role in plasticity and learning. **Chapter 3** using targeted genetic mutations and pharmacologic inhibition, demonstrates that CaMKII plays a non-enzymatic role as well. A structural role for α CaMKII protein in short-term presynaptic plasticity at CA3-CA1 synapses is shown. **Chapter 4** describes a mouse model of Angelman syndrome, in which CaMKII activity is reduced and phosphorylation of the inhibitory T305 and T306 site is increased, to investigate whether the increased inhibitory phosphorylation at T305/6 site is directly responsible for the major deficits seen in AS. **Chapter 5** describes a mouse model of the most common single gene genetic disorder associated with learning disabilities, *i.e.* neurofibromatosis type 1 (NF1). Specifically, the importance of the alternatively spliced exon 9a in NF1 function is investigated. **Chapter 6** is focused on the cellular mechanisms underlying the contribution of the cerebellum in spatial learning. Using a L7-PKCI transgenic mice model, which results in a specific inactivation of Parallel fiber-Purkinje cell LTD, the potential role of this cellular mechanism during spatial navigation is investigated. The final chapter of this thesis (**chapter 7**) provides a summary and discussion of the main findings and results of the present thesis.

1.8 References

- Albrecht U, Sutcliffe JS, Cattanaach BM, Beechey CV, Armstrong D, Eichele G, Beaudet AL (1997) Imprinted expression of the murine Angelman syndrome gene, Ube3a, in hippocampal and Purkinje neurons. *Nat Genet* 17:75-78.
- Alger BE (2002) Retrograde signaling in the regulation of synaptic transmission: focus on endocannabinoids. *Prog Neurobiol* 68:247-286.
- Alger BE, Teyler TJ (1976) Long-term and short-term plasticity in the CA1, CA3, and dentate regions of the rat hippocampal slice. *Brain Res* 110:463-480.
- Amaral DG, Witter MP (1989) The three-dimensional organization of the hippocampal formation: a review of anatomical data. *Neuroscience* 31:571-591.
- Ashby MC, Maier SR, Nishimune A, Henley JM (2006) Lateral diffusion drives constitutive exchange of AMPA receptors at dendritic spines and is regulated by spine morphology. *J Neurosci* 26:7046-7055.
- Baude A, Nusser Z, Molnar E, McIlhinney RA, Somogyi P (1995) High-resolution immunogold localization of AMPA type glutamate receptor subunits at synaptic and non-synaptic sites in rat hippocampus. *Neuroscience* 69:1031-1055.
- Bekkers JM, Stevens CF (1990) Presynaptic mechanism for long-term potentiation in the hippocampus. *Nature* 346:724-729.

- Blackstone CD, Moss SJ, Martin LJ, Levey AI, Price DL, Huganir RL (1992) Biochemical characterization and localization of a non-N-methyl-D-aspartate glutamate receptor in rat brain. *J Neurochem* 58:1118-1126.
- Bliss TV, Lomo T (1973) Long-lasting potentiation of synaptic transmission in the dentate area of the anaesthetized rabbit following stimulation of the perforant path. *J Physiol* 232:331-356.
- Bliss TV, Collingridge GL (1993) A synaptic model of memory: long-term potentiation in the hippocampus. *Nature* 361:31-39.
- Bohbot VD, Kalina M, Stepankova K, Spackova N, Petrides M, Nadel L (1998) Spatial memory deficits in patients with lesions to the right hippocampus and to the right parahippocampal cortex. *Neuropsychologia* 36:1217-1238.
- Borgdorff AJ, Choquet D (2002) Regulation of AMPA receptor lateral movements. *Nature* 417:649-653.
- Brocke L, Srinivasan M, Schulman H (1995) Developmental and regional expression of multifunctional Ca²⁺/calmodulin-dependent protein kinase isoforms in rat brain. *J Neurosci* 15:6797-6808.
- Brocke L, Chiang LW, Wagner PD, Schulman H (1999) Functional implications of the subunit composition of neuronal CaM kinase II. *J Biol Chem* 274:22713-22722.
- Buoni S, Grosso S, Pucci L, Fois A (1999) Diagnosis of Angelman syndrome: clinical and EEG criteria. *Brain Dev* 21:296-302.
- Burgin KE, Waxham MN, Rickling S, Westgate SA, Mobley WC, Kelly PT (1990) In situ hybridization histochemistry of Ca²⁺/calmodulin-dependent protein kinase in developing rat brain. *J Neurosci* 10:1788-1798.
- Burguiere E, Arleo A, Hojjati M, Elgersma Y, De Zeeuw CI, Berthoz A, Rondi-Reig L (2005) Spatial navigation impairment in mice lacking cerebellar LTD: a motor adaptation deficit? *Nat Neurosci* 8:1292-1294.
- Cain DP, Boon F, Corcoran ME (2006) Thalamic and hippocampal mechanisms in spatial navigation: a dissociation between brain mechanisms for learning how versus learning where to navigate. *Behav Brain Res* 170:241-256.
- Cichowski K, Shih TS, Jacks T (1996) Nf1 gene targeting: toward models and mechanisms. *Semin Cancer Biol* 7:291-298.
- Clayton-Smith J (1993) Clinical research on Angelman syndrome in the United Kingdom: observations on 82 affected individuals. *Am J Med Genet* 46:12-15.
- Colbran RJ (1992) Regulation and role of brain calcium/calmodulin-dependent protein kinase II. *Neurochem Int* 21:469-497.
- Colbran RJ, Soderling TR (1990) Calcium/calmodulin-independent autophosphorylation sites of calcium/calmodulin-dependent protein kinase II. Studies on the effect of phosphorylation of threonine 305/306 and serine 314 on calmodulin binding using synthetic peptides. *J Biol Chem* 265:11213-11219.
- Collingridge GL, Kehl SJ, McLennan H (1983) Excitatory amino acids in synaptic transmission in the Schaffer collateral-commissural pathway of the rat hippocampus. *J Physiol* 334:33-46.
- Costa RM, Silva AJ (2003) Mouse models of neurofibromatosis type I: bridging the GAP. *Trends Mol Med* 9:19-23.
- Costa RM, Federov NB, Kogan JH, Murphy GG, Stern J, Ohno M, Kucherlapati R, Jacks T, Silva AJ (2002) Mechanism for the learning deficits in a mouse model of neurofibromatosis type I. *Nature* 415:526-530.
- Cottrell JR, Dube GR, Egles C, Liu G (2000) Distribution, density, and clustering of functional glutamate receptors before and after synaptogenesis in hippocampal neurons. *J Neurophysiol* 84:1573-1587.
- Cummings JA, Mulkey RM, Nicoll RA, Malenka RC (1996) Ca²⁺ signaling requirements for long-term depression in the hippocampus. *Neuron* 16:825-833.
- Danglot G, Regnier V, Fauvet D, Vassal G, Kujas M, Bernheim A (1995) Neurofibromatosis 1 (NF1) mRNAs expressed in the central nervous system are differentially spliced in the 5' part of the gene. *Hum Mol Genet* 4:915-920.

- Danysz W, Zajackowski W, Parsons CG (1995) Modulation of learning processes by ionotropic glutamate receptor ligands. *Behav Pharmacol* 6:455-474.
- Daston MM, Scrable H, Nordlund M, Sturbaum AK, Nissen LM, Ratner N (1992) The protein product of the neurofibromatosis type 1 gene is expressed at highest abundance in neurons, Schwann cells, and oligodendrocytes. *Neuron* 8:415-428.
- De Zeeuw CI, Hansel C, Bian F, Koekkoek SK, van Alphen AM, Linden DJ, Oberdick J (1998) Expression of a protein kinase C inhibitor in Purkinje cells blocks cerebellar LTD and adaptation of the vestibulo-ocular reflex. *Neuron* 20:495-508.
- Delaney KR, Zucker RS, Tank DW (1989) Calcium in motor nerve terminals associated with posttetanic potentiation. *J Neurosci* 9:3558-3567.
- Devan BD, Goad EH, Petri HL (1996) Dissociation of hippocampal and striatal contributions to spatial navigation in the water maze. *Neurobiol Learn Mem* 66:305-323.
- Dudek SM, Bear MF (1992) Homosynaptic long-term depression in area CA1 of hippocampus and effects of N-methyl-D-aspartate receptor blockade. *Proc Natl Acad Sci U S A* 89:4363-4367.
- Eichenbaum H, Otto T, Cohen NJ (1992) The hippocampus--what does it do? *Behav Neural Biol* 57:2-36.
- Eichenbaum H, Schoenbaum G, Young B, Bunsey M (1996) Functional organization of the hippocampal memory system. *Proc Natl Acad Sci U S A* 93:13500-13507.
- Elgersma Y, Fedorov NB, Ikonen S, Choi ES, Elgersma M, Carvalho OM, Giese KP, Silva AJ (2002) Inhibitory autophosphorylation of CaMKII controls PSD association, plasticity, and learning. *Neuron* 36:493-505.
- Fanselow MS (1980) Conditioned and unconditional components of post-shock freezing. *Pavlov J Biol Sci* 15:177-182.
- Fanselow MS, Tighe TJ (1988) Contextual conditioning with massed versus distributed unconditional stimuli in the absence of explicit conditional stimuli. *J Exp Psychol Anim Behav Process* 14:187-199.
- Frey U, Krug M, Reymann KG, Matthies H (1988) Anisomycin, an inhibitor of protein synthesis, blocks late phases of LTP phenomena in the hippocampal CA1 region in vitro. *Brain Res* 452:57-65.
- Frey U, Schollmeier K, Reymann KG, Seidenbecher T (1995) Asymptotic hippocampal long-term potentiation in rats does not preclude additional potentiation at later phases. *Neuroscience* 67:799-807.
- Fryburg JS, Breg WR, Lindgren V (1991) Diagnosis of Angelman syndrome in infants. *Am J Med Genet* 38:58-64.
- Gaertner TR, Kolodziej SJ, Wang D, Kobayashi R, Koomen JM, Stoops JK, Waxham MN (2004) Comparative analyses of the three-dimensional structures and enzymatic properties of alpha, beta, gamma and delta isoforms of Ca²⁺-calmodulin-dependent protein kinase II. *J Biol Chem* 279:12484-12494.
- Geist RT, Gutmann DH (1996) Expression of a developmentally-regulated neuron-specific isoform of the neurofibromatosis 1 (NF1) gene. *Neurosci Lett* 211:85-88.
- Giese KP, Fedorov NB, Filipkowski RK, Silva AJ (1998) Autophosphorylation at Thr286 of the alpha calcium-calmodulin kinase II in LTP and learning. *Science* 279:870-873.
- Goldenring JR, McGuire JS, Jr., DeLorenzo RJ (1984) Identification of the major postsynaptic density protein as homologous with the major calmodulin-binding subunit of a calmodulin-dependent protein kinase. *J Neurochem* 42:1077-1084.
- Greengard P, Valtorta F, Czernik AJ, Benfenati F (1993) Synaptic vesicle phosphoproteins and regulation of synaptic function. *Science* 259:780-785.
- Guilting C, Piggins HD (2007) Challenging the omnipotence of the suprachiasmatic timekeeper: are circadian oscillators present throughout the mammalian brain? *Eur J Neurosci* 25:3195-3216.
- Guilting C, McNair K, Stone TW, Morris BJ (2007) Restored plasticity in a mouse model of neurofibromatosis type 1 via inhibition of hyperactive ERK and CREB. *Eur J Neurosci* 25:99-105.

- Guo HF, The I, Hannan F, Bernards A, Zhong Y (1997) Requirement of *Drosophila* NF1 for activation of adenylyl cyclase by PACAP38-like neuropeptides. *Science* 276:795-798.
- Gutmann DH, Zhang Y, Hirbe A (1999) Developmental regulation of a neuron-specific neurofibromatosis 1 isoform. *Ann Neurol* 46:777-782.
- Gutmann DH, Geist RT, Wright DE, Snider WD (1995a) Expression of the neurofibromatosis 1 (NF1) isoforms in developing and adult rat tissues. *Cell Growth Differ* 6:315-323.
- Gutmann DH, Geist RT, Rose K, Wright DE (1995b) Expression of two new protein isoforms of the neurofibromatosis type 1 gene product, neurofibromin, in muscle tissues. *Dev Dyn* 202:302-311.
- Gutmann DH, Aylsworth A, Carey JC, Korf B, Marks J, Pyeritz RE, Rubenstein A, Viskochil D (1997) The diagnostic evaluation and multidisciplinary management of neurofibromatosis 1 and neurofibromatosis 2. *Jama* 278:51-57.
- Handelmann GE, Olton DS (1981) Spatial memory following damage to hippocampal CA3 pyramidal cells with kainic acid: impairment and recovery with preoperative training. *Brain Res* 217:41-58.
- Harris EW, Cotman CW (1986) Long-term potentiation of guinea pig mossy fiber responses is not blocked by N-methyl D-aspartate antagonists. *Neurosci Lett* 70:132-137.
- Harris EW, Ganong AH, Cotman CW (1984) Long-term potentiation in the hippocampus involves activation of N-methyl-D-aspartate receptors. *Brain Res* 323:132-137.
- Hashimoto Y, Schworer CM, Colbran RJ, Soderling TR (1987) Autophosphorylation of Ca²⁺/calmodulin-dependent protein kinase II. Effects on total and Ca²⁺-independent activities and kinetic parameters. *J Biol Chem* 262:8051-8055.
- Hebb DO (1949) *Organization of behaviour: A Neuropsychological Theory*. New York: John Wiley and Sons.
- Henze DA, Urban NN, Barrionuevo G (2000) The multifarious hippocampal mossy fiber pathway: a review. *Neuroscience* 98:407-427.
- Hollmann M, Heinemann S (1994) Cloned glutamate receptors. *Annu Rev Neurosci* 17:31-108.
- Hrabetova S, Sacktor TC (1997) Long-term potentiation and long-term depression are induced through pharmacologically distinct NMDA receptors. *Neurosci Lett* 226:107-110.
- Hrabetova S, Serrano P, Blace N, Tse HW, Skifter DA, Jane DE, Monaghan DT, Sacktor TC (2000) Distinct NMDA receptor subpopulations contribute to long-term potentiation and long-term depression induction. *J Neurosci* 20:RC81.
- Huibregtse JM, Scheffner M, Howley PM (1991) A cellular protein mediates association of p53 with the E6 oncoprotein of human papillomavirus types 16 or 18. *Embo J* 10:4129-4135.
- Huibregtse JM, Scheffner M, Howley PM (1993) Localization of the E6-AP regions that direct human papillomavirus E6 binding, association with p53, and ubiquitination of associated proteins. *Mol Cell Biol* 13:4918-4927.
- Huson SM, Harper PS, Compston DA (1988) Von Recklinghausen neurofibromatosis. A clinical and population study in south-east Wales. *Brain* 111 (Pt 6):1355-1381.
- Isaac JT, Nicoll RA, Malenka RC (1995) Evidence for silent synapses: implications for the expression of LTP. *Neuron* 15:427-434.
- Izquierdo I, Medina JH (1995) Correlation between the pharmacology of long-term potentiation and the pharmacology of memory. *Neurobiol Learn Mem* 63:19-32.
- Jacks T, Shih TS, Schmitt EM, Bronson RT, Bernards A, Weinberg RA (1994) Tumour predisposition in mice heterozygous for a targeted mutation in Nf1. *Nat Genet* 7:353-361.
- Jiang YH, Armstrong D, Albrecht U, Atkins CM, Noebels JL, Eichele G, Sweatt JD, Beaudet AL (1998) Mutation of the Angelman ubiquitin ligase in mice causes increased cytoplasmic p53 and deficits of contextual learning and long-term potentiation. *Neuron* 21:799-811.

- Kandel ER (2001) The molecular biology of memory storage: a dialogue between genes and synapses. *Science* 294:1030-1038.
- Kennedy MB, Bennett MK, Erongdu NE (1983) Biochemical and immunochemical evidence that the "major postsynaptic density protein" is a subunit of a calmodulin-dependent protein kinase. *Proc Natl Acad Sci U S A* 80:7357-7361.
- Kishino T, Lalande M, Wagstaff J (1997) UBE3A/E6-AP mutations cause Angelman syndrome. *Nat Genet* 15:70-73.
- Krug M, Wagner M, Brodemann R, Matthies H (1989) Habituation of monosynaptic field potentials in the dentate gyrus of freely moving rats interferes with LTP. *Brain Res* 476:163-166.
- Kuret J, Schulman H (1985) Mechanism of autophosphorylation of the multifunctional Ca^{2+} /calmodulin-dependent protein kinase. *J Biol Chem* 260:6427-6433.
- Kushner SA, Elgersma Y, Murphy GG, Jaarsma D, van Woerden GM, Hojjati MR, Cui Y, LeBoutillier JC, Marrone DF, Choi ES, De Zeeuw CI, Petit TL, Pozzo-Miller L, Silva AJ (2005) Modulation of presynaptic plasticity and learning by the H-ras/extracellular signal-regulated kinase/synapsin I signaling pathway. *J Neurosci* 25:9721-9734.
- Laan LA, v Haeringen A, Brouwer OF (1999) Angelman syndrome: a review of clinical and genetic aspects. *Clin Neurol Neurosurg* 101:161-170.
- Lalonde R (1987) Exploration and spatial learning in staggerer mutant mice. *J Neurogenet* 4:285-291.
- Lalonde R, Botez MI (1986) Navigational deficits in weaver mutant mice. *Brain Res* 398:175-177.
- Lalonde R, Manseau M, Botez MI (1988) Spontaneous alternation and exploration in staggerer mutant mice. *Behav Brain Res* 27:273-276.
- Larson J, Wong D, Lynch G (1986) Patterned stimulation at the theta frequency is optimal for the induction of hippocampal long-term potentiation. *Brain Res* 368:347-350.
- LeDoux JE (1995) Emotion: clues from the brain. *Annu Rev Psychol* 46:209-235.
- LeDoux JE (2000) Emotion circuits in the brain. *Annu Rev Neurosci* 23:155-184.
- Lee I, Kesner RP (2002) Differential contribution of NMDA receptors in hippocampal subregions to spatial working memory. *Nat Neurosci* 5:162-168.
- Liao D, Hessler NA, Malinow R (1995) Activation of postsynaptically silent synapses during pairing-induced LTP in CA1 region of hippocampal slice. *Nature* 375:400-404.
- Liao D, Scannevin RH, Hugarir R (2001) Activation of silent synapses by rapid activity-dependent synaptic recruitment of AMPA receptors. *J Neurosci* 21:6008-6017.
- Liao D, Zhang X, O'Brien R, Ehlers MD, Hugarir RL (1999) Regulation of morphological postsynaptic silent synapses in developing hippocampal neurons. *Nat Neurosci* 2:37-43.
- Lisman J (1994) The CaM kinase II hypothesis for the storage of synaptic memory. *Trends Neurosci* 17:406-412.
- Lisman J, Schulman H, Cline H (2002) The molecular basis of CaMKII function in synaptic and behavioural memory. *Nat Rev Neurosci* 3:175-190.
- Lisman JE, McIntyre CC (2001) Synaptic plasticity: a molecular memory switch. *Curr Biol* 11:R788-791.
- Liu L, Wong TP, Pozza MF, Lingenhoehl K, Wang Y, Sheng M, Auberson YP, Wang YT (2004) Role of NMDA receptor subtypes in governing the direction of hippocampal synaptic plasticity. *Science* 304:1021-1024.
- Lledo PM, Hjelmstad GO, Mukherji S, Soderling TR, Malenka RC, Nicoll RA (1995) Calcium/calmodulin-dependent kinase II and long-term potentiation enhance synaptic transmission by the same mechanism. *Proc Natl Acad Sci U S A* 92:11175-11179.
- Logue SF, Paylor R, Wehner JM (1997) Hippocampal lesions cause learning deficits in inbred mice in the Morris water maze and conditioned-fear task. *Behav Neurosci* 111:104-113.
- Lynch MA (2004) Long-term potentiation and memory. *Physiol Rev* 84:87-136.
- Maass W, Zador AM (1999) Dynamic stochastic synapses as computational units. *Neural Comput* 11:903-917.

- Malenka RC (2003) The long-term potential of LTP. *Nat Rev Neurosci* 4:923-926.
- Malenka RC, Nicoll RA (1999) Long-term potentiation--a decade of progress? *Science* 285:1870-1874.
- Malenka RC, Kauer JA, Perkel DJ, Mauk MD, Kelly PT, Nicoll RA, Waxham MN (1989) An essential role for postsynaptic calmodulin and protein kinase activity in long-term potentiation. *Nature* 340:554-557.
- Malinow R, Tsien RW (1990) Presynaptic enhancement shown by whole-cell recordings of long-term potentiation in hippocampal slices. *Nature* 346:177-180.
- Malinow R, Schulman H, Tsien RW (1989) Inhibition of postsynaptic PKC or CaMKII blocks induction but not expression of LTP. *Science* 245:862-866.
- Maren S, Tocco G, Standley S, Baudry M, Thompson RF (1993) Postsynaptic factors in the expression of long-term potentiation (LTP): increased glutamate receptor binding following LTP induction in vivo. *Proc Natl Acad Sci U S A* 90:9654-9658.
- Martin SJ, Clark RE (2007) The rodent hippocampus and spatial memory: from synapses to systems. *Cell Mol Life Sci* 64:401-431.
- Martin SJ, Grimwood PD, Morris RG (2000) Synaptic plasticity and memory: an evaluation of the hypothesis. *Annu Rev Neurosci* 23:649-711.
- Matilla A, Roberson ED, Banfi S, Morales J, Armstrong DL, Burright EN, Orr HT, Sweatt JD, Zoghbi HY, Matzuk MM (1998) Mice lacking ataxin-1 display learning deficits and decreased hippocampal paired-pulse facilitation. *J Neurosci* 18:5508-5516.
- Matsuura T, Sutcliffe JS, Fang P, Galjaard RJ, Jiang YH, Benton CS, Rommens JM, Beaudet AL (1997) De novo truncating mutations in E6-AP ubiquitin-protein ligase gene (UBE3A) in Angelman syndrome. *Nat Genet* 15:74-77.
- McDevitt MA, Shivdasani RA, Fujiwara Y, Yang H, Orkin SH (1997) A "knockdown" mutation created by cis-element gene targeting reveals the dependence of erythroid cell maturation on the level of transcription factor GATA-1. *Proc Natl Acad Sci U S A* 94:6781-6785.
- McDonald RJ, White NM (1994) Parallel information processing in the water maze: evidence for independent memory systems involving dorsal striatum and hippocampus. *Behav Neural Biol* 61:260-270.
- McGaugh JL, Cahill L, Roozendaal B (1996) Involvement of the amygdala in memory storage: interaction with other brain systems. *Proc Natl Acad Sci U S A* 93:13508-13514.
- Meyer T, Hanson PI, Stryer L, Schulman H (1992) Calmodulin trapping by calcium-calmodulin-dependent protein kinase. *Science* 256:1199-1202.
- Miller SG, Kennedy MB (1985) Distinct forebrain and cerebellar isozymes of type II Ca^{2+} /calmodulin-dependent protein kinase associate differently with the postsynaptic density fraction. *J Biol Chem* 260:9039-9046.
- Miller SG, Kennedy MB (1986) Regulation of brain type II Ca^{2+} /calmodulin-dependent protein kinase by autophosphorylation: a Ca^{2+} -triggered molecular switch. *Cell* 44:861-870.
- Milner B, Squire LR, Kandel ER (1998) Cognitive neuroscience and the study of memory. *Neuron* 20:445-468.
- Morris RG, Davis S, Butcher SP (1990a) Hippocampal synaptic plasticity and NMDA receptors: a role in information storage? *Philos Trans R Soc Lond B Biol Sci* 329:187-204.
- Morris RG, Garrud P, Rawlins JN, O'Keefe J (1982) Place navigation impaired in rats with hippocampal lesions. *Nature* 297:681-683.
- Morris RG, Anderson E, Lynch GS, Baudry M (1986) Selective impairment of learning and blockade of long-term potentiation by an N-methyl-D-aspartate receptor antagonist, AP5. *Nature* 319:774-776.
- Morris RG, Schenk F, Tweedie F, Jarrard LE (1990b) Ibotenate Lesions of Hippocampus and/or Subiculum: Dissociating Components of Allocentric Spatial Learning. *Eur J Neurosci* 2:1016-1028.

- Mukherji S, Soderling TR (1994) Regulation of Ca²⁺/calmodulin-dependent protein kinase II by inter- and intrasubunit-catalyzed autophosphorylations. *J Biol Chem* 269:13744-13747.
- Mukherji S, Brickey DA, Soderling TR (1994) Mutational analysis of secondary structure in the autoinhibitory and autophosphorylation domains of calmodulin kinase II. *J Biol Chem* 269:20733-20738.
- Mulkey RM, Malenka RC (1992) Mechanisms underlying induction of homosynaptic long-term depression in area CA1 of the hippocampus. *Neuron* 9:967-975.
- Nakajima A, Tang YP (2005) Genetic approaches to the molecular/neuronal mechanisms underlying learning and memory in the mouse. *J Pharmacol Sci* 99:1-5.
- North KN, Riccardi V, Samango-Sprouse C, Ferner R, Moore B, Legius E, Ratner N, Denckla MB (1997) Cognitive function and academic performance in neurofibromatosis. 1: consensus statement from the NF1 Cognitive Disorders Task Force. *Neurology* 48:1121-1127.
- Nusser Z, Lujan R, Laube G, Roberts JD, Molnar E, Somogyi P (1998) Cell type and pathway dependence of synaptic AMPA receptor number and variability in the hippocampus. *Neuron* 21:545-559.
- O'Keefe J (1979) A review of the hippocampal place cells. *Prog Neurobiol* 13:419-439.
- Otani S, Abraham WC (1989) Inhibition of protein synthesis in the dentate gyrus, but not the entorhinal cortex, blocks maintenance of long-term potentiation in rats. *Neurosci Lett* 106:175-180.
- Ozawa T, Araki N, Yunoue S, Tokuo H, Feng L, Patrakitkomjorn S, Hara T, Ichikawa Y, Matsumoto K, Fujii K, Saya H (2005) The neurofibromatosis type 1 gene product neurofibromin enhances cell motility by regulating actin filament dynamics via the Rho-ROCK-LIMK2-cofilin pathway. *J Biol Chem* 280:39524-39533.
- Patton BL, Miller SG, Kennedy MB (1990) Activation of type II calcium/calmodulin-dependent protein kinase by Ca²⁺/calmodulin is inhibited by autophosphorylation of threonine within the calmodulin-binding domain. *J Biol Chem* 265:11204-11212.
- Penfield W, Mathieson G (1974) Memory. Autopsy findings and comments on the role of hippocampus in experiential recall. *Arch Neurol* 31:145-154.
- Pettit DL, Perlman S, Malinow R (1994) Potentiated transmission and prevention of further LTP by increased CaMKII activity in postsynaptic hippocampal slice neurons. *Science* 266:1881-1885.
- Phillips RG, LeDoux JE (1992) Differential contribution of amygdala and hippocampus to cued and contextual fear conditioning. *Behav Neurosci* 106:274-285.
- Pickard L, Noel J, Henley JM, Collingridge GL, Molnar E (2000) Developmental changes in synaptic AMPA and NMDA receptor distribution and AMPA receptor subunit composition in living hippocampal neurons. *J Neurosci* 20:7922-7931.
- Pickard L, Noel J, Duckworth JK, Fitzjohn SM, Henley JM, Collingridge GL, Molnar E (2001) Transient synaptic activation of NMDA receptors leads to the insertion of native AMPA receptors at hippocampal neuronal plasma membranes. *Neuropharmacology* 41:700-713.
- Pieribone VA, Shupliakov O, Brodin L, Hilfiker-Rothenfluh S, Czernik AJ, Greengard P (1995) Distinct pools of synaptic vesicles in neurotransmitter release. *Nature* 375:493-497.
- Poyhonen M, Kytola S, Leisti J (2000) Epidemiology of neurofibromatosis type 1 (NF1) in northern Finland. *J Med Genet* 37:632-636.
- Purves D et al (2001) Neuroscience, 2 Edition: SINAUER.
- Reymann KG, Malisch R, Schulzeck K, Brodemann R, Ott T, Matthies H (1985) The duration of long-term potentiation in the CA1 region of the hippocampal slice preparation. *Brain Res Bull* 15:249-255.
- Rich DP, Colbran RJ, Schworer CM, Soderling TR (1989) Regulatory properties of calcium/calmodulin-dependent protein kinase II in rat brain postsynaptic densities. *J Neurochem* 53:807-816.

- Rongo C (2002) A fresh look at the role of CaMKII in hippocampal synaptic plasticity and memory. *Bioessays* 24:223-233.
- Rosenmund C, Stevens CF (1996) Definition of the readily releasable pool of vesicles at hippocampal synapses. *Neuron* 16:1197-1207.
- Sajikumar S, Frey JU (2003) Anisomycin inhibits the late maintenance of long-term depression in rat hippocampal slices in vitro. *Neurosci Lett* 338:147-150.
- Sajikumar S, Frey JU (2004) Late-associativity, synaptic tagging, and the role of dopamine during LTP and LTD. *Neurobiol Learn Mem* 82:12-25.
- Save E, Poucet B, Foreman N, Buhot MC (1992) Object exploration and reactions to spatial and nonspatial changes in hooded rats following damage to parietal cortex or hippocampal formation. *Behav Neurosci* 106:447-456.
- Schenk F, Morris RG (1985) Dissociation between components of spatial memory in rats after recovery from the effects of retrohippocampal lesions. *Exp Brain Res* 58:11-28.
- Schikorski T, Stevens CF (2001) Morphological correlates of functionally defined synaptic vesicle populations. *Nat Neurosci* 4:391-395.
- Schneggenburger R, Sakaba T, Neher E (2002) Vesicle pools and short-term synaptic depression: lessons from a large synapse. *Trends Neurosci* 25:206-212.
- Scoville WB, Milner B (1957) Loss of recent memory after bilateral hippocampal lesions. *J Neurol Neurosurg Psychiatry* 20:11-21.
- Seeburg PH (1993) The TINS/TiPS Lecture. The molecular biology of mammalian glutamate receptor channels. *Trends Neurosci* 16:359-365.
- Sejnowski TJ (1999) The book of Hebb. *Neuron* 24:773-776.
- Shen K, Meyer T (1999) Dynamic control of CaMKII translocation and localization in hippocampal neurons by NMDA receptor stimulation. *Science* 284:162-166.
- Shen K, Teruel MN, Connor JH, Shenolikar S, Meyer T (2000) Molecular memory by reversible translocation of calcium/calmodulin-dependent protein kinase II. *Nat Neurosci* 3:881-886.
- Silva AJ, Stevens CF, Tonegawa S, Wang Y (1992) Deficient hippocampal long-term potentiation in alpha-calcium-calmodulin kinase II mutant mice. *Science* 257:201-206.
- Silva AJ, Frankland PW, Marowitz Z, Friedman E, Laszlo GS, Cioffi D, Jacks T, Bourchouladze R (1997) A mouse model for the learning and memory deficits associated with neurofibromatosis type I. *Nat Genet* 15:281-284.
- Silva AJ, Rosahl TW, Chapman PF, Marowitz Z, Friedman E, Frankland PW, Cestari V, Cioffi D, Sudhof TC, Bourchouladze R (1996) Impaired learning in mice with abnormal short-lived plasticity. *Curr Biol* 6:1509-1518.
- Smith ML, Milner B (1989) Right hippocampal impairment in the recall of spatial location: encoding deficit or rapid forgetting? *Neuropsychologia* 27:71-81.
- Song I, Huganir RL (2002) Regulation of AMPA receptors during synaptic plasticity. *Trends Neurosci* 25:578-588.
- Squire LR (1994) Memory and forgetting: long-term and gradual changes in memory storage. *Int Rev Neurobiol* 37:243-269; discussion 285-248.
- Squire LR, Zola SM (1996) Ischemic brain damage and memory impairment: a commentary. *Hippocampus* 6:546-552.
- Squire LR, Kandel ER (1999) *Memory: From Mind to Molecules*. New York: Scientific American Library.
- Strack S, Colbran RJ (1998) Autophosphorylation-dependent targeting of calcium/calmodulin-dependent protein kinase II by the NR2B subunit of the N-methyl-D-aspartate receptor. *J Biol Chem* 273:20689-20692.
- Strack S, Choi S, Lovinger DM, Colbran RJ (1997) Translocation of autophosphorylated calcium/calmodulin-dependent protein kinase II to the postsynaptic density. *J Biol Chem* 272:13467-13470.
- Sutherland RJ, Rodriguez AJ (1989) The role of the fornix/fimbria and some related subcortical structures in place learning and memory. *Behav Brain Res* 32:265-277.

- Sutherland RJ, Whishaw IQ, Kolb B (1983) A behavioural analysis of spatial localization following electrolytic, kainate- or colchicine-induced damage to the hippocampal formation in the rat. *Behav Brain Res* 7:133-153.
- Tang YP, Shimizu E, Dube GR, Rampon C, Kerchner GA, Zhuo M, Liu G, Tsien JZ (1999) Genetic enhancement of learning and memory in mice. *Nature* 401:63-69.
- Thiagarajan TC, Piedras-Renteria ES, Tsien RW (2002) α - and β -CaMKII. Inverse regulation by neuronal activity and opposing effects on synaptic strength. *Neuron* 36:1103-1114.
- Thomson AM (2000) Facilitation, augmentation and potentiation at central synapses. *Trends Neurosci* 23:305-312.
- Triller A, Choquet D (2003) Synaptic structure and diffusion dynamics of synaptic receptors. *Biol Cell* 95:465-476.
- Tsien JZ, Huerta PT, Tonegawa S (1996) The essential role of hippocampal CA1 NMDA receptor-dependent synaptic plasticity in spatial memory. *Cell* 87:1327-1338.
- Varela JA, Sen K, Gibson J, Fost J, Abbott LF, Nelson SB (1997) A quantitative description of short-term plasticity at excitatory synapses in layer 2/3 of rat primary visual cortex. *J Neurosci* 17:7926-7940.
- Weeber EJ, Jiang YH, Elgersma Y, Varga AW, Carrasquillo Y, Brown SE, Christian JM, Mirmikjoo B, Silva A, Beaudet AL, Sweatt JD (2003) Derangements of hippocampal calcium/calmodulin-dependent protein kinase II in a mouse model for Angelman mental retardation syndrome. *J Neurosci* 23:2634-2644.
- Whishaw IQ (1987) Hippocampal, granule cell and CA3-4 lesions impair formation of a place learning-set in the rat and induce reflex epilepsy. *Behav Brain Res* 24:59-72.
- Whishaw IQ, Mittleman G, Bunch ST, Dunnett SB (1987) Impairments in the acquisition, retention and selection of spatial navigation strategies after medial caudate-putamen lesions in rats. *Behav Brain Res* 24:125-138.
- Williams CA, Angelman H, Clayton-Smith J, Driscoll DJ, Hendrickson JE, Knoll JH, Magenis RE, Schinzel A, Wagstaff J, Whidden EM, et al. (1995) Angelman syndrome: consensus for diagnostic criteria. Angelman Syndrome Foundation. *Am J Med Genet* 56:237-238.
- Wilson RI, Nicoll RA (2001) Endogenous cannabinoids mediate retrograde signalling at hippocampal synapses. *Nature* 410:588-592.
- Xavier GF, Oliveira-Filho FJ, Santos AM (1999) Dentate gyrus-selective colchicine lesion and disruption of performance in spatial tasks: difficulties in "place strategy" because of a lack of flexibility in the use of environmental cues? *Hippocampus* 9:668-681.
- Xu GF, Lin B, Tanaka K, Dunn D, Wood D, Gesteland R, White R, Weiss R, Tamanoi F (1990) The catalytic domain of the neurofibromatosis type 1 gene product stimulates ras GTPase and complements ira mutants of *S. cerevisiae*. *Cell* 63:835-841.
- Xu H, Gutmann DH (1997) Mutations in the GAP-related domain impair the ability of neurofibromin to associate with microtubules. *Brain Res* 759:149-152.
- Yamamoto C, Matsumoto K, Takagi M (1980) Potentiation of excitatory postsynaptic potentials during and after repetitive stimulation in thin hippocampal sections. *Exp Brain Res* 38:469-477.
- Yamauchi T (2005) Neuronal Ca^{2+} /calmodulin-dependent protein kinase II--discovery, progress in a quarter of a century, and perspective: implication for learning and memory. *Biol Pharm Bull* 28:1342-1354.
- Zucker RS (1989) Short-term synaptic plasticity. *Annu Rev Neurosci* 12:13-31.
- Zucker RS, Regehr WG (2002) Short-term synaptic plasticity. *Annu Rev Physiol* 64:355-405.

Chapter 2

Modulation of presynaptic plasticity and learning by the H-ras/extracellular signal-regulated kinase/synapsin I signaling pathway

Published in

The Journal of Neuroscience 2005 October 25(42): 9721-9734

Modulation of Presynaptic Plasticity and Learning by the H-ras/Extracellular Signal-Regulated Kinase/Synapsin I Signaling Pathway

Steven A. Kushner,^{1*} Ype Elgersma,^{1,2*} Geoffrey G. Murphy,¹ Dick Jaarsma,² Geeske M. van Woerden,² Mohammad Reza Hojjati,² Yijun Cui,¹ Janelle C. LeBoutillier,³ Diano F. Marrone,³ Esther S. Choi,¹ Chris I. De Zeeuw,² Ted L. Petit,³ Lucas Pozzo-Miller,⁴ and Alcino J. Silva¹

¹Departments of Neurobiology, Psychiatry, and Psychology, Brain Research Institute, University of California, Los Angeles, California 90095-1761,

²Department of Neuroscience, Erasmus Medical Center Rotterdam, 3000 DR Rotterdam, The Netherlands, ³Department of Psychology and Program in Neuroscience, University of Toronto, Scarborough, Ontario, Canada M1C 1A4, and ⁴Department of Neurobiology, University of Alabama at Birmingham, Birmingham, Alabama 35294-0021

Molecular and cellular studies of the mechanisms underlying mammalian learning and memory have focused almost exclusively on postsynaptic function. We now reveal an experience-dependent presynaptic mechanism that modulates learning and synaptic plasticity in mice. Consistent with a presynaptic function for endogenous H-ras/extracellular signal-regulated kinase (ERK) signaling, we observed that, under normal physiologic conditions in wild-type mice, hippocampus-dependent learning stimulated the ERK-dependent phosphorylation of synapsin I, and MEK (MAP kinase kinase)/ERK inhibition selectively decreased the frequency of miniature EPSCs. By generating transgenic mice expressing a constitutively active form of H-ras (H-ras^{G12V}), which is abundantly localized in axon terminals, we were able to increase the ERK-dependent phosphorylation of synapsin I. This resulted in several presynaptic changes, including a higher density of docked neurotransmitter vesicles in glutamatergic terminals, an increased frequency of miniature EPSCs, and increased paired-pulse facilitation. In addition, we observed facilitated neurotransmitter release selectively during high-frequency activity with consequent increases in long-term potentiation. Moreover, these mice showed dramatic enhancements in hippocampus-dependent learning. Importantly, deletion of synapsin I, an exclusively presynaptic protein, blocked the enhancements of learning, presynaptic plasticity, and long-term potentiation. Together with previous invertebrate studies, these results demonstrate that presynaptic plasticity represents an important evolutionarily conserved mechanism for modulating learning and memory.

Key words: Ras; ERK; synapsin; LTP; miniature excitatory postsynaptic currents; mEPSCs; learning; presynaptic

Introduction

Although extensive evidence supports the involvement of postsynaptic plasticity in mammalian learning and memory (Malenka and Nicoll, 1999; Martin et al., 2000), there is little direct experimental evidence that the complex mechanisms reg-

ulating presynaptic plasticity also participate in the acquisition and storage of information in mammals (Powell et al., 2004). Studies using a variety of invertebrate systems have provided compelling evidence for the involvement of presynaptic plasticity in invertebrate learning and memory (Burrell and Sahley, 2001). Additionally, computational models have suggested that short-term presynaptic plasticity is an important mechanism for cortical processing in mammals (Tsodyks and Markram, 1997; Varela et al., 1997; Dobrunz and Stevens, 1999).

By regulating the probability of neurotransmitter release, short-term presynaptic plasticity could affect the induction of long-term changes in synaptic strength thought to underlie learning. In *Aplysia*, presynaptic neurons require mitogen-activated protein (MAP) kinase/extracellular signal-regulated kinase (ERK) signaling to modulate short- and long-term forms of synaptic plasticity (Martin et al., 1997; Sharma et al., 2003). Furthermore, studies in both *Aplysia* and mammals have identified a presynaptic mechanism by which ERK-dependent phosphorylation of synapsin I (SynI) modulates neurotransmitter release in neuronal culture (Jovanovic et al., 2000; Humeau et al., 2001; Chin et al., 2002; Chi et al., 2003).

Received July 10, 2005; revised September 1, 2005; accepted September 7, 2005.

S.A.K. received support from National Institute of Mental Health—National Research Service Award Grant MH063541, National Institutes of Health (NIH)—National Institute of General Medical Sciences Grant GM08042, the Medical Scientist Training Program, the Aesculapian Fund of the University of California Los Angeles School of Medicine, and the Tennenbaum Family Creativity Initiative. Y.E. was supported by grants from Nederlandse Organisatie voor Wetenschappelijk Onderzoek-Zorgonderzoek Nederland Medische Wetenschappen (VIDI and TOP). This work was also supported by a generous donation from C. M. Spivak and by grants from the Michael Tennenbaum Creativity Initiative, NIH (Grant R01 NS038480), Neurofibromatosis (National, Illinois, Massachusetts Bay Area, Minnesota, Arizona, Kansas and Central Plains, Mid-Atlantic, and Texas chapters), and the Merck and Neuroscience Nursing Foundations (A.J.S.). We thank L. van Aelst for the human *H-ras*^{G12V} cDNA, M. Mayford for the pMM403 plasmids, and P. Greengard and J. N. Jovanovic for the phospho-SynI antibodies. We also thank M. Elgersma for help with *in situ* hybridization and immunohistochemistry. We are grateful to J. G. Borst, D. V. Buonamano, P. W. Frankland, S. A. Josselyn, J. N. Jovanovic, K. C. Martin, T. J. O'Dell, and F. E. Schweizer for fruitful discussions.

*S.A.K. and Y.E. contributed equally to this work.

Correspondence should be addressed to Alcino Silva, Departments of Neurobiology, Psychiatry, and Psychology, Brain Research Institute, University of California, Los Angeles, CA 90095-1761. E-mail: silvaa@mednet.ucla.edu.

DOI:10.1523/JNEUROSCI.2836-05.2005

Copyright © 2005 Society for Neuroscience 0270-6474/05/259721-14\$15.00/0

Synapsin I is localized to presynaptic terminals and tethers synaptic vesicles to the actin cytoskeleton located in the distal reserve pool (Pieribone et al., 1995). Phosphorylation of synapsin I has been shown to regulate its affinity for both actin and synaptic vesicles (Schiebler et al., 1986; Bahler and Greengard, 1987; Benfenati et al., 1989, 1992; Jovanovic et al., 1996). Together, these results suggest a model in which presynaptic ERK signaling acts via synapsin I to modulate neurotransmitter release during the induction of activity-dependent changes in synaptic strength by trafficking synaptic vesicles between the reserve and readily-releasable pools (Pieribone et al., 1995; Jovanovic et al., 2000, 2001; Chi et al., 2003).

The present study demonstrates that, within the hippocampus, the endogenous H-ras isoform of p21^{Ras}, a potent upstream activator of ERK, is abundantly localized to axon terminals. Consistent with a presynaptic function for downstream endogenous H-ras signaling, we observe that, under normal physiologic conditions in wild-type (WT) mice, hippocampus-dependent learning stimulates the phosphorylation of synapsin I, whereas MAP kinase kinase (MEK)/ERK inhibition decreases the frequency of miniature EPSCs (mEPSCs). Furthermore, we took advantage of the subcellular localization of H-ras to manipulate the H-ras/ERK/synapsin I signaling pathway presynaptically. Our results demonstrate that transgenic expression of active H-ras^{G12V} in mouse glutamatergic forebrain neurons results in an increased frequency of mEPSCs, the facilitation of neurotransmitter release during high-frequency stimulation, consequent increases in long-term potentiation (LTP), and dramatic enhancements in both spatial learning and contextual fear conditioning.

Materials and Methods

Transgene construction and generation of transgenic mice. The transgene used in these studies is the human *H-ras* cDNA, which carries the G12V mutation. The cDNA is under the control of the 8.5 kb promoter region of α calcium/calmodulin-dependent kinase II (α CaMKII) and flanked by 5' and 3' artificial splice sites. Using PCR, a sequence encoding the hemagglutinin (HA) epitope was fused 5' to the *H-ras*^{G12V} cDNA (kindly provided by L. van Aelst, Cold Spring Harbor Laboratory, Cold Spring Harbor, NY), as well as a 5' *Bam*HI and 3' *Fse*I restriction sites. This PCR product was cloned in the *Bam*HI-*Fse*I sites of pNN265 (kindly provided by M. Mayford, The Scripps Research Institute, La Jolla, CA), resulting in the addition of a 5'-intron and a 3'-intron plus poly(A) signal from simian virus 40. The 2100 bp *Not*I fragment obtained from this plasmid was cloned in the *Not*I site downstream of the α CaMKII promoter in the pMM403 vector (kindly provided by M. Mayford). The resulting plasmid (pYE356) was digested with *Sfi*I, and the purified DNA fragment was injected into pronuclei of C57BL/6 zygotes to generate transgenic mice. Transgenic mice were maintained in the background of C57BL/6N (Taconic Farms, Germantown, NY) and crossed with 129/SvEmsJ mice (The Jackson Laboratory, Bar Harbor, ME) to generate F1 animals used for experiments. *Synapsin I* knock-out mice (Rosahl et al., 1993) were maintained in the background of C57BL/6N (Taconic Farms) and crossed with 129/SvEmsJ mice (The Jackson Laboratory) to generate F1 animals. *H-ras*^{G12V}/*synapsin I* mice were F2 offspring of F1 *H-ras*^{G12V} mice crossed with F1 *synapsin I* knock-out mice, except 100 Hz LTP was performed in *H-ras*^{G12V}/*synapsin I* mice of a C57BL/6N genetic background. Consistent with previous reports (Li et al., 1995; Rosahl et al., 1995), *synapsin I* knock-out mice showing any signs of seizure activity were immediately excluded from experiments. All experiments were performed on adult mice aged 3–6 months old. All experiments were conducted with the experimenter blind to the genotype of the mice and conducted with the approval of the University of California, Los Angeles Animal Research Committee of the Chancellor's Office of Protection of Research Subjects, under continuous supervision of the campus veterinarian.

Expression analysis. *In situ* hybridization was performed essentially as

described by Wisden et al. (1990). The probe used was antisense to the HA sequence: 5' CTC GAC CTA GAA GGT CCT CCC AGG CTG GCA TAG TCA GGC ACG TC 3'. Immunoblot analyses were performed as described previously (Elgersma et al., 2002). In Figures 1 and 4, tissue was collected 30 min after behavioral training. The primary antibodies used for immunoblot analyses were against pan-Ras (F132, #32; Santa Cruz Biotechnology, Santa Cruz, CA), phospho-ERK1/2 (New England Biolabs, Beverly, MA), phospho-Akt (New England Biolabs), and synapsin I (Sigma, St. Louis, MO). Phospho-site 3, phospho-site 4/5, and phospho-site 6 antibodies against synapsin I were kindly provided by J. N. Jovanovic (University College, London, UK) and P. Greengard (Rockefeller University, New York, NY). Blots were quantitated using ECL+ and the Storm 860 phosphorimager system (Molecular Dynamics, Sunnyvale, CA).

Immunohistochemistry. Immunohistochemistry was performed using confocal microscopy as described previously (Jaarsma et al., 2001). The primary antibodies used were against H-ras (C20; Santa Cruz Biotechnology), HA-11 (clone 16812; Babco, Richmond, CA), vesicular glutamate transporter 1 (VGLUT1) (Chemicon, Temecula, CA), phospho-ERK1/2 (New England Biolabs), phospho-cAMP response element-binding protein (CREB) (New England Biolabs), and MAP2 [Chemicon (clone AP20; Sigma)]. For triple-labeling confocal immunofluorescence, FITC donkey anti-rabbit, cyanine 3 (Cy3) donkey anti-mouse, and Cy5 donkey anti-guinea pig from Jackson ImmunoResearch (West Grove, PA) were used as secondary antibodies. Sections were analyzed with a Zeiss (Oberkochen, Germany) LSM 510 confocal laser-scanning microscope using a 63 \times /1.4 numerical aperture oil immersion objective.

Immunogold. For EM immunogold immunohistochemistry, 50 μ m vibratome sections of 4% paraformaldehyde, 0.1% glutaraldehyde, transcardially perfused mice were processed for osmium-free embedment (Phend et al., 1995). Ultrathin sections were cut, mounted on Formvar-coated nickel grids, and processed for immunogold labeling using the procedure described by Phend et al. (1995). HA-11 diluted at 1:750 and 10 nm gold-conjugated goat anti-mouse (Aurion, Wageningen, The Netherlands) diluted 1:30 were used as primary and secondary antibodies, respectively. Gold-labeled sections were analyzed in a Phillips CM10 electron microscope at 80 kV.

Golgi analysis. Whole hippocampi from WT and *H-ras*^{G12V} mice were dissected and processed by a rapid Golgi procedure (5 d in osmium dichromate and 1 d in silver nitrate), embedded in low-viscosity nitrocellulose, cut at 100–120 μ m on a sliding microtome, and mounted on glass slides. In each animal, qualitative light microscopic analysis was performed on 10 fully impregnated cells with minimal background artifact. In these cells, dendritic spines were analyzed at 1000 \times under oil immersion along random 25 μ m segments of midapical, apical tuft, and basilar dendrites.

Behavioral analysis. The basic protocol for the water maze experiments has been described previously (Costa et al., 2001). Mice were trained with two trials per day for 9 d (1 min intertrial interval). Probe trials were administered after 6 and 9 d, as well as 14 d after the completion of training.

The basic protocol for the contextual fear conditioning experiments has been described previously (Frankland et al., 2001). For experiments using standard delay conditioning, mice were placed in the conditioning chamber for 120 s before the onset of the unconditioned stimulus (US) (0.4 mA, 1 s scrambled footshock). Experiments involving three footshocks used a 20 s intershock interval. For experiments using immediate shock, mice were placed in the conditioning chamber for 2 s before the onset of the US (0.75 mA, 2 s continuous footshock). During the testing phase, conditioning was assessed by measuring freezing and activity for 5 consecutive minutes in the training chamber using a computerized automated scoring system (Anagnostaras et al., 2000). Freezing is operationally defined as a lack of any movement other than that caused by respiration for 2 continuous seconds. Suppression of activity was used as an independent measure of conditioned fear and was calculated as activity_{test}/(activity_{training} + activity_{test}). All values are reported as mean \pm SEM. Statistical comparisons were made using ANOVA with Fisher's protected least significant difference (PLSD) for *post hoc* comparisons.

Electrophysiology. Sagittal hippocampal slices (400 μ m) were placed in

a submerged recording chamber and perfused continuously at a rate of 1.5 ml/min with artificial CSF (ACSF) equilibrated with 95% O₂, 5% CO₂ at 30°C. ACSF contained the following (in mM): 120 NaCl, 3.5 KCl, 2.5 CaCl₂, 1.3 MgSO₄, 1.25 NaH₂PO₄, 26 NaHCO₃, and 10 D-glucose. Extracellular recording of field EPSP (fEPSPs) were made in CA1 stratum radiatum with platinum/iridium electrodes (Frederick Haer Company, Bowdoinham, ME). In all experiments, one bipolar platinum/iridium electrode was used to stimulate Schaffer collateral/commissural afferents orthodromically. During LTP studies, a second electrode was used to monitor an independent control pathway. Experiments to observe responses during theta-burst stimulation (TBS) and 5 and 10 Hz stimulation were performed in the presence of 50 μ M D-2-amino-5-phosphonopentanoate (APV) and 100 μ M picrotoxin with CA3 removed to prevent epileptic discharges. Paired-pulse facilitation (PPF) experiments were conducted in the presence of 50 μ M APV. All stimulus pulses were 100 μ s in duration and one-third to two-thirds of the maximum fEPSP. Average stimulation strength and baseline fEPSP was similar between genotypes for all of the experiments conducted. For LTP studies, short-term potentiation (STP) was defined as the first posttetanic measurement, made 30 s after LTP induction.

Whole-cell current-clamp recordings were used to study the induction of LTP by low-frequency presynaptic fiber stimulation paired with postsynaptic depolarization. In these experiments, slices with the CA3 region removed were bathed in normal ACSF containing 100 μ M picrotoxin. EPSPs evoked by 0.05 Hz presynaptic fiber stimulation were recorded from CA1 pyramidal neurons using an Axoclamp 2B amplifier (Axon Instruments, Union City, CA) in bridge mode. Patch electrodes had resistances of 5–7 M Ω and contained a K⁺-based solution (in mM): 120 potassium methyl-sulfate, 20 KCl, 0.2 EGTA, HEPES, 2 MgCl₂, 4 Na₂-ATP, 0.3 Tris-GTP, and 7 phosphocreatine. LTP was induced by pairing each of 100 presynaptic fiber stimuli delivered at 0.5 Hz, with a 200 ms, 0.8 nA square-pulse current injection through the whole-cell patch electrode beginning +5 ms after presynaptic fiber stimulation.

Whole-cell voltage-clamp recordings using a 3900A Integrating Patch Clamp Amplifier (Dagan, Minneapolis, MN) were performed to measure spontaneous mEPSCs. In this experiment, we used ACSF (in mM): 126 NaCl, 2.5 KCl, 2 CaCl₂, 2 MgCl₂, 1.25 NaH₂PO₄, 26 NaHCO₃, 10 D-glucose, 0.001 TTX, 0.025 CGP-35348 [3-amino-propyl-(diethoxymethyl)phosphonic acid], 0.05 picrotoxin, and 0.05 APV. The recording protocol involved a baseline mEPSC recording in ACSF, changing to bath perfusion with ACSF containing U0126 [1,4-diamino-2,3-dicyano-1,4-bis(*o*-aminophenylmercapto) butadiene] (10 μ M) for 15 min, followed by another mEPSC recording. Intracellular pipette solution contained the following (in mM): 135 CsCl, 4 NaCl, 2 MgCl₂, 10 HEPES, 0.05 EGTA, 5 QX-314 [N-(2,6-dimethylphenyl) carbonylmethyl triethylammonium bromide], 2 Mg-ATP, and 0.5 Na₂-GTP. Voltage-clamp recordings were made at a holding potential of –70 mV. The direct current resistances of the electrodes were 4–6 M Ω . Series resistance was compensated by 70–90% using lag values of 7–10 μ s. Before compensation, series resistance was <15 M Ω . All recordings were acquired and low-pass filtered (eight-pole Bessel; Brownlee Precision 200, Brownlee Precision, Santa Clara, CA) at 10 kHz and digitized on-line at 20 kHz using a PCI-MIO-1GE data acquisition board (National Instruments, Austin, TX).

Average LTP was assessed during the final 10 min of each protocol. Statistical comparisons were made using the number of mice as the sample size. ANOVA was used with Fisher's PLSD for *post hoc* comparisons. The Kolmogorov–Smirnov test was used to compare cumulative probability distributions of LTP. All values are reported as mean \pm SEM. Statistical comparisons of mEPSC data were performed using paired and unpaired *t* tests. mEPSC data were analyzed using custom-written software. Synaptic plasticity data were acquired and analyzed using pClamp 7.0 (Axon Instruments).

Analysis of presynaptic vesicle distribution. Electron microscopy using random sampling of synapses was performed as described previously (Pozzo-Miller et al., 1999). Only complete profiles of nonperforated asymmetric synapses on dendritic spines in stratum radiatum of area CA1 were photographed. The parameters measured in each synapse were length of the active zone, thickness of the postsynaptic density (PSD),

total number of small (~50 nm) synaptic vesicles per terminal, and number of docked vesicles. The docked vesicles are defined as those up to one-vesicle-diameter (~50 nm) distance from the active zone, according to criteria developed by Dickinson-Nelson and Reese (1983), because these vesicles have been shown to be depleted during sustained, repetitive activity.

Electron microscopy using three-dimensional terminal reconstruction was performed as described previously (Schikorski and Stevens, 1997, 2001). Briefly, for each animal, a series of electron micrographs were obtained at a final magnification of 30,000 \times from a ribbon of 28–36 serial sections in stratum radiatum of area CA1. Only complete terminals containing a single nonperforated asymmetric synapse on a dendritic spine were analyzed. The parameters measured in each terminal were total terminal volume, area of the PSD, total number of synaptic vesicles per terminal, and number of docked vesicles. The docked vesicles are defined as those in which no visible gap existed between the vesicle and the membrane wall opposite the PSD (Schikorski and Stevens, 1997).

Results

Enhanced phosphorylation of synapsin I during learning

Although previous studies have demonstrated a robust increase in ERK activation after experience-dependent plasticity (English and Sweatt, 1996; Atkins et al., 1998), few downstream effectors have been identified that contribute to learning and synaptic plasticity (Adams et al., 2000; Yuan et al., 2002). Synapsin I has been identified previously as a prominent downstream effector of ERK (Jovanovic et al., 1996), but phosphorylation-dependent regulation has never been evaluated during learning. Using contextual fear conditioning, we evaluated the dynamics of ERK-dependent synapsin I phosphorylation. During contextual fear conditioning, an association is formed between a distinct context and an aversive footshock delivered in that context. However, significantly decreasing the interval between placement into the conditioning context and delivery of the footshock limits hippocampus-dependent processing of the context. Administering the footshock immediately after introducing animals to the training context (immediate shock) prevents the formation of the contextual representation necessary for fear conditioning (Fanselow, 1990; Rudy et al., 2002). Consistent with a robust and specific function in presynaptic signaling during learning, wild-type C57BL/6N mice showed increased ERK-dependent synapsin I phosphorylation during contextual conditioning compared with the immediate shock condition (Fig. 1*A,B*) ($F_{(1,6)} = 10.18$; $p < 0.05$). Phosphorylation of ERK2 was also increased with a similar specificity (Fig. 1*A,B*) ($F_{(1,6)} = 8.29$; $p < 0.05$).

H-ras localizes to axon terminals and signals through ERK

We sought to explore the function of ERK-dependent synapsin I phosphorylation in learning and synaptic plasticity by engineering transgenic mice to express HA-tagged H-ras containing a substitution of glycine-12 for valine (H-ras^{G12V}) under the control of the α CaMKII promoter (Mayford et al., 1995). The H-ras^{G12V} transgene is a potent upstream activator of ERK in postmitotic neurons (Rosen et al., 1994; Heumann et al., 2000; Koh et al., 2002). In addition, the late postnatal onset of the α CaMKII promoter restricts transgene expression to postmitotic neurons, thereby minimizing putative developmental effects caused by the oncogenic properties of the transgene.

The transgenic allele (H-ras^{G12V}) was inherited in the expected Mendelian frequency, and H-ras^{G12V} mice appeared healthy with no gross behavioral or anatomical abnormalities. Nissl-stained brain sections appeared normal with no gross morphological changes (Fig. 2*A*). To study the expression pattern of the transgene, *in situ* hybridization was performed on coronal sections

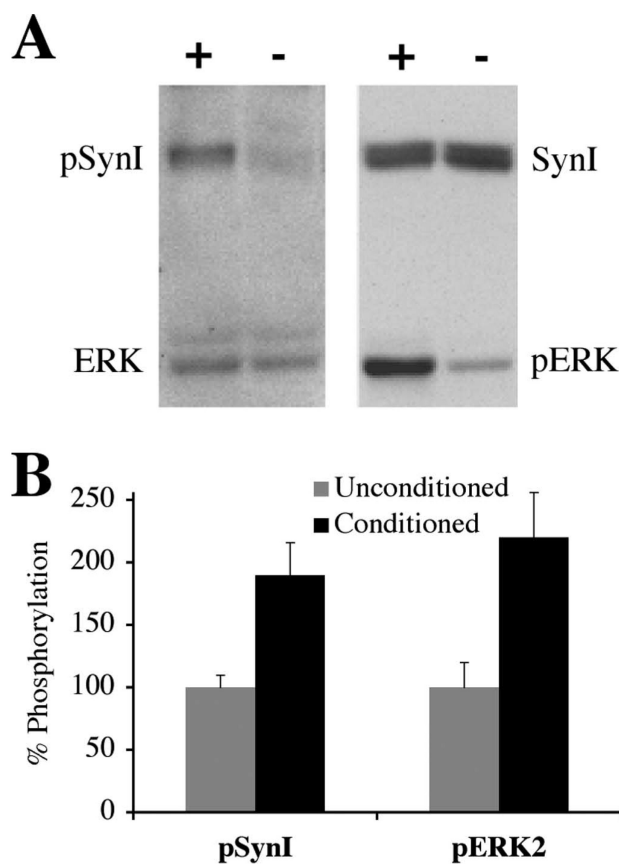


Figure 1. ERK and synapsin I sites 4/5 are phosphorylated in C57BL/6N mice during contextual conditioning. **A**, Immunoblot of hippocampal lysates using a phospho-synapsin I antibody against sites 4/5 (pSynI), phospho-ERK1/2 antibody (pERK), and antibodies against total synapsin I (SynI) and total ERK1/2 (ERK). The second blot was obtained after stripping the first blot and reprobing with the antibodies indicated. + symbols denote normal contextual conditioning with a 3 min delay before the footshock was given. — symbols denote that the shock was delivered immediately after placement in the chamber. **B**, Quantification of synapsin I phosphorylation at sites 4/5 and ERK2 phosphorylation shows a significant increase in conditioned mice [+, $n = 3$] compared with the mice that received a shock immediately after placement in the chamber [—, $n = 3$].

from adult *H-ras*^{G12V} and WT mice using a probe specific for the transgene. mRNA expression was evident throughout the forebrain, including cortex, striatum, and amygdala, with particularly high concentration in the hippocampus, in which staining was restricted to the pyramidal cell layer in CA regions and to the granule cell layer in the dentate gyrus (Fig. 2B).

Previous studies have suggested that fourfold to fivefold overexpression of *H-ras*^{G12V} results in significant cytoarchitectural changes in pyramidal neurons (Gartner et al., 2004). However, in our mice, we observed a normal dendritic spine density, quantified by stereologic analysis of Golgi-stained pyramidal neurons in CA1 stratum radiatum (WT, 1.55 ± 0.05 spines/ μm^3 ; *H-ras*^{G12V}, 1.58 ± 0.06 spines/ μm^3 ; $F_{(1,223)} = 0.04$; $p = 0.84$). The absence of morphological changes in the *H-ras*^{G12V} mice likely reflects the moderate level of transgene overexpression compared with endogenous *H-ras* (Fig. 2C) ($110 \pm 16\%$ of endogenous *H-ras*). No significant change in endogenous *H-ras* expression was observed in *H-ras*^{G12V} mice compared with WT littermates (Fig. 2C) ($p = 0.44$).

Although previous studies have implicated p21^{Ras} in neuronal function, isoform-specific subcellular localization in neurons has

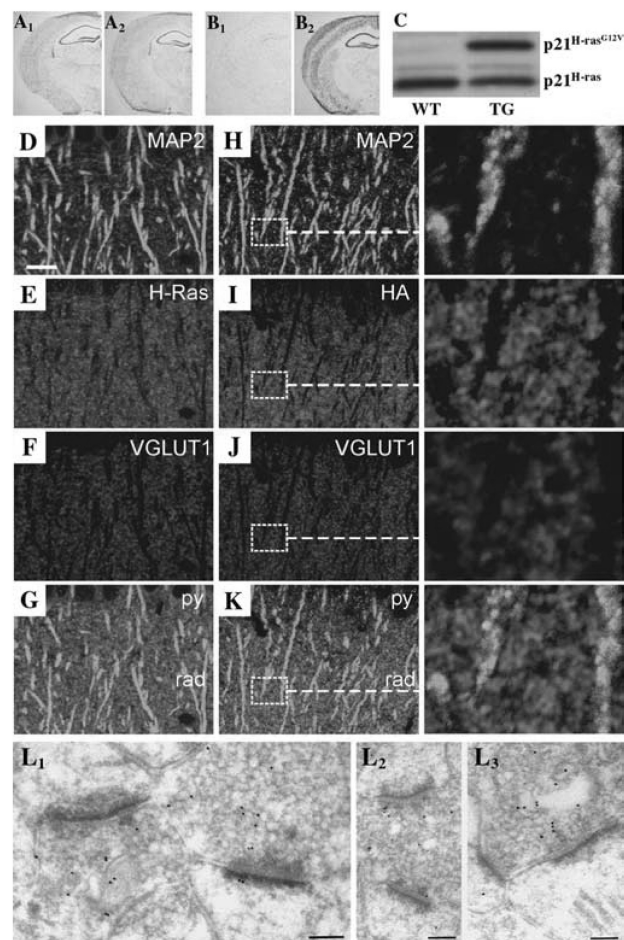


Figure 2. *H-ras* is predominantly localized to axon terminals in the hippocampus of adult animals. **A**, WT (**A**₁) and *H-ras*^{G12V} (**A**₂) Nissl staining demonstrated normal gross anatomical morphology. **B**, *In situ* hybridization of adult coronal sections showed no detectable *H-ras*^{G12V} expression in WT slices (**B**₁), whereas in transgenic mice, strong expression was evident throughout the cerebral cortex and hippocampus with less staining in the striatum and amygdala (**B**₂). **C**, Immunoblot of hippocampal lysates obtained from WT and transgenic *H-ras*^{G12V} mice (TG) using an *H-ras* antibody. Expression of transgenic HA-tagged *H-ras*^{G12V} (top band in TG lane) is comparable with endogenous *H-ras* (bottom bands). **D–K**, Confocal microscopy images of the hippocampus obtained after triple labeling with α -MAP2 (**D**, **H**; green), α -*H-ras* (**E**) or α -HA (**I**) (red), and α -VGLUT1 (**F**, **J**; blue). **D–G** were obtained from adult WT mice, and **H–K** were obtained from adult transgenic mice. Overlay images (**G**, **K**) demonstrate that, in WT mice (**G**), endogenous *H-ras* is excluded from the MAP2 compartment but shows extensive colocalization (purple) with the excitatory presynaptic marker VGLUT1. In transgenic mice (**K**), *H-ras*^{G12V} shows a similar subcellular distribution as endogenous *H-ras*. py, CA1 pyramidal cell layer; rad, stratum radiatum. Scale bar (in **D**), 4 μm . **L**, Immunogold electron microscopy demonstrates that *H-ras*^{G12V} is located predominantly in axon terminals in stratum radiatum of the CA1 region with significantly less labeling in postsynaptic spines. Note that the postsynaptic profile in **L**₃ contains a spine apparatus. Scale bars: **L**₁, 170 nm; **L**₂, 130 nm; **L**₃, 190 nm.

not been well characterized. Therefore, we examined the subcellular localization of endogenous *H-ras* and transgenic *H-ras*^{G12V}. Confocal microscopy in the hippocampal CA1 region of WT mice demonstrated extensive colocalization between endogenous *H-ras* and the excitatory presynaptic marker VGLUT1. In contrast, there was no significant overlap between *H-ras* and the dendritic marker MAP2 (Fig. 2D–G). In transgenic mice, the subcellular distribution of *H-ras*^{G12V} was similar to endogenous *H-ras* and highly localized with the presynaptic marker VGLUT1 (Fig. 2H–K). Analogous to endogenous *H-ras*, the distribution of

transgenic H-ras^{G12V} showed little overlap with MAP2 (Fig. 2*G,K*), consistent with a predominantly axonal localization of H-ras.

Because confocal immunofluorescence microscopy does not provide adequate resolution to independently evaluate expression in presynaptic axon terminals and postsynaptic dendritic spines, we performed immunogold analysis using electron microscopy to examine the synaptic distribution of H-ras^{G12V}. Gold particles were highly abundant in presynaptic axon terminals (Fig. 2*L₁–L₃*). In contrast, substantially less labeling was present in postsynaptic dendritic spines. The ratio of the number of gold particles in presynaptic terminals to that in postsynaptic spines was 3.5 ± 0.19 (paired $t_{(41)} = 9.8$; $p < 0.001$).

Importantly, although we observed a predominantly presynaptic localization of H-ras in the hippocampus of mature animals, we observed abundant H-ras^{G12V} localization at presynaptic as well as postsynaptic sites in primary hippocampal cultures (Y. Elgersma and D. Jaarsma, unpublished data), consistent with previous reports (Zhu et al., 2002), suggesting that the localization of p21^{Ras} isoforms *in vivo* may be developmentally regulated.

We next sought to examine the effects of H-ras^{G12V} expression on downstream signaling pathways. Consistent with many previous studies demonstrating p21^{Ras}-mediated activation of neuronal ERK (Rosen et al., 1994; Heumann et al., 2000; Iida et al., 2001; Adams and Sweatt, 2002; Koh et al., 2002; Komiyama et al., 2002), H-ras^{G12V} mice had increased levels of phosphorylated ERK1 and ERK2 without a change in total ERK1/2 expression (Fig. 3*A,B*) (pERK1, $F_{(1,9)} = 24.9$, $p < 0.001$; pERK2, $F_{(1,9)} = 10.2$, $p < 0.01$; total ERK1, $F_{(1,9)} = 0.26$, $p = 0.62$; total ERK2, $F_{(1,9)} = 0.16$, $p = 0.74$). In contrast, phosphorylated and total levels of Akt, a downstream effector of phosphoinositide-3 kinase, were both unchanged (Fig. 3*A,B*) (pAkt, $F_{(1,9)} = 0.002$, $p = 0.96$; total Akt, $F_{(1,9)} = 0.97$, $p = 0.35$). These results are consistent with a biochemical specificity of downstream H-ras effector activation observed in previous studies using neuronal H-ras^{G12V} *in vivo* (Heumann et al., 2000; Koh et al., 2002). Immunohistochemical analysis in the hippocampal CA1 region demonstrated that areas containing increased pERK1/2 corresponded closely to those expressing H-ras^{G12V} (Fig. 3*C–F*). In contrast, no change in the number of pERK1/2- or pCREB-positive (+) nuclei were observed (Fig. 3*E–H*), consistent with the absence of H-ras^{G12V} in the pyramidal cell-body layer (Fig. 3*D*). Therefore, these data suggest that H-ras expression is highly abundant in axon terminals and functions to regulate local ERK activation.

Synapsin I phosphorylation is increased in H-ras^{G12V} mice

We next sought to characterize ERK activation and ERK-dependent phosphorylation of synapsin I in H-ras^{G12V} mice. Hippocampal lysates were prepared from H-ras^{G12V} and WT littermates after contextual fear conditioning with either an immediate shock or delayed shock. There was a significant interaction of genotype with conditioning on ERK activation and on phosphorylation of synapsin I at the ERK-dependent sites 4/5 (Fig. 4*A,B*) (pERK2, $F_{(1,9)} = 4.56$, $p = 0.077$; pSynI, $F_{(1,9)} = 4.75$, $p = 0.072$). Consistent with the experiment in Figure 1 conducted with mice from a C57BL/6N genetic background, contextual conditioning in WT mice (C57BL/6N \times 129SvEms) F1 hybrid) significantly increased phosphorylation of both synapsin I and ERK2 (Fisher's PLSD; pSynI, $p < 0.05$; pERK2, $p < 0.05$). In contrast, synapsin I and ERK2 phosphorylation were equivalent between H-ras^{G12V} mice receiving contextual conditioning and immediate shock and were similar to conditioned WT mice (pSynI, $p = 0.94$; pERK2, $p = 0.75$). Importantly, phosphoryla-

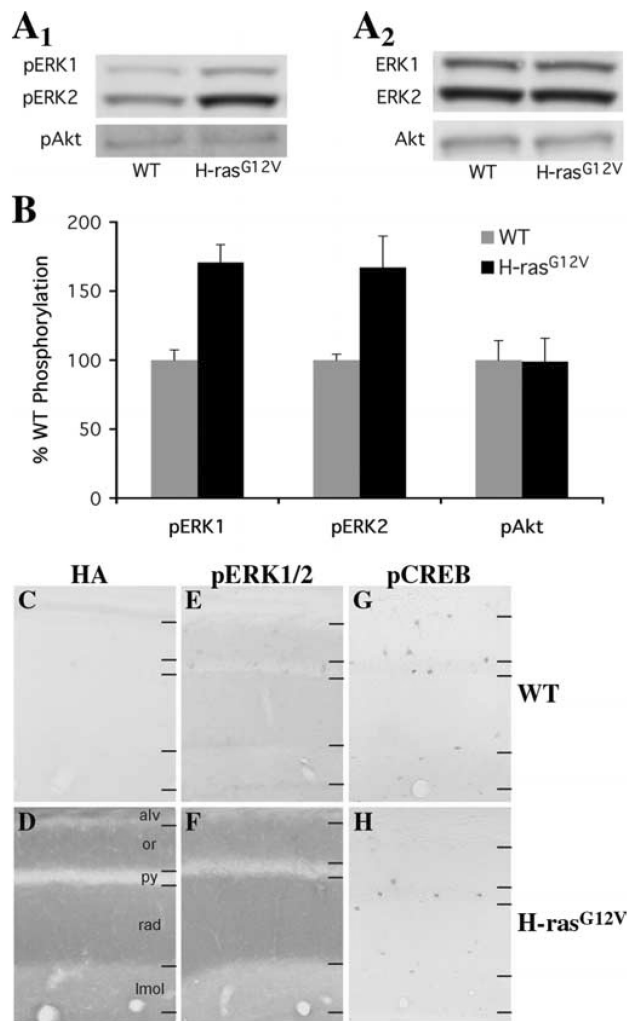


Figure 3. Increased ERK signaling in H-ras^{G12V} mice. **A**, Immunoblots of phosphorylated (**A₁**) and total (**A₂**) forms of the downstream H-ras effectors ERK1, ERK2, and Akt from hippocampal lysates. Blots shown in **A₂** were obtained after stripping the blots shown in **A₁**. **B**, Quantification of changes in the phosphorylation of downstream H-ras effectors demonstrated a significant increase of pERK1 and pERK2 in H-ras^{G12V} mice without any observable changes in pAkt (WT, $n = 6$; H-ras^{G12V}, $n = 5$). **C–H**, Within the CA1 hippocampal region, areas of increased pERK1/2 (**E, F**) correspond closely with H-ras^{G12V} expression (**C, D**). Note that the nuclear localization of both pERK1/2 and pCREB was normal in H-ras^{G12V} mice (**F, H**) compared with control mice (**E, G**), consistent with the absence of transgene expression in the somatodendritic compartment. alv, Alveolus; or, stratum oriens; py, pyramidal cell layer; rad, stratum radiatum; Imol, stratum lacunosum moleculare.

tion of synapsin I and ERK2 after hippocampus-dependent learning was equivalent between WT and H-ras^{G12V} mice, arguing that the transgenic manipulation produces biochemical changes that are observed physiologically during learning in WT mice (pSynI, $p = 0.84$; pERK2, $p = 0.43$).

In contrast to the differences observed at the ERK-dependent sites 4/5, synapsin I phosphorylation at the CaMKII-dependent site 3 (Bahler and Greengard, 1987) was equivalent in WT and H-ras^{G12V} mice (WT, $100 \pm 11.7\%$; H-ras^{G12V}, $89.5 \pm 10.3\%$; $F_{(1,9)} = 0.44$; $p = 0.52$), demonstrating the specificity of the transgenic manipulation. Together, these data suggest that learning-related presynaptic biochemical changes in H-ras/ERK/synapsin I signaling are potentiated in H-ras^{G12V} mice.

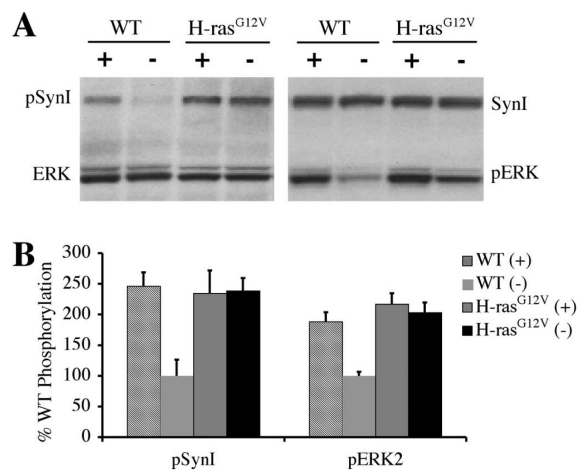


Figure 4. Phosphorylation of ERK and synapsin I sites 4/5 in *H-ras*^{G12V} mice receiving unconditioned shock is comparable with pERK and pSynI levels in conditioned WT mice. **A**, Immunoblot of hippocampal lysates obtained from conditioned and immediately shocked WT and *H-ras*^{G12V} mice using phospho-synapsin I antibodies against sites 4/5, pERK antibodies, and antibodies against total synapsin I and ERK. The second blot was obtained after stripping the first blot and reprobing with the antibodies indicated. + symbols denote normal contextual conditioning with a 3 min delay before the footshock was delivered. — symbols denote that the shock was given immediately after placement in the chamber. **B**, Quantification of ERK2 phosphorylation and synapsin I phosphorylation at sites 4/5 shows a significant increase in WT conditioned mice that received a delayed shock compared with WT mice that received a shock immediately after placement in the chamber. Note that pERK and pSynI levels of immediately shocked *H-ras*^{G12V} mice are comparable with the levels observed in WT conditioned (delay shocked) animals ($n = 3$, for each condition).

Enhanced presynaptic plasticity in *H-ras*^{G12V} mice

Together, the predominantly presynaptic localization of H-ras and enhanced phosphorylation of synapsin I suggest that presynaptic function may be altered in *H-ras*^{G12V} mice. To explore the frequency-dependent impact of the *H-ras*^{G12V} mutation on short-term plasticity, we examined PPF, which is thought to depend primarily on presynaptic mechanisms (Dobrunz et al., 1997; Zucker and Regehr, 2002). Indeed, *H-ras*^{G12V} mice showed a frequency-dependent enhancement of PPF (Fig. 5A) ($F_{(8,88)} = 3.4$; $p < 0.01$), performed in the presence of APV to block postsynaptic plasticity. At interpulse intervals ≤ 100 ms, PPF was significantly larger in *H-ras*^{G12V} mice than WT littermates (PLSD, $p < 0.001$). However, at longer intervals, PPF was equivalent in *H-ras*^{G12V} and WT mice (PLSD, $p > 0.42$). Together, these data suggest a model in which synaptic transmission is enhanced in *H-ras*^{G12V} mice during high-frequency stimulation although low-frequency responses are normal. Consistent with this model, baseline synaptic transmission was normal in *H-ras*^{G12V} mice (Fig. 5B–D) ($F_{(4,76)} = 0.07$; $p = 0.99$).

During high-frequency stimulation of the hippocampal Schaffer collateral pathway, depletion of presynaptic neurotransmitter vesicles from the readily-releasable pool occurs rapidly. This is a key mechanism regulating the rate of short-term synaptic depression and serves to limit postsynaptic depolarization (Dobrunz and Stevens, 1997; Brager et al., 2002). To probe the trafficking of reserve pool vesicles to the readily-releasable pool after depletion, we measured responses during a prolonged 10 Hz tetanus in the presence of APV and picrotoxin, which has been used in previous studies to examine vesicle trafficking (Rosahl et al., 1995; Dobrunz and Stevens, 1997; Schnell and Nicoll, 2001; Chi et al., 2003). Responses to

stimulation at this frequency reveal the competing processes of facilitation, depression, vesicle depletion, and vesicle mobilization (Dobrunz and Stevens, 1997). *H-ras*^{G12V} mice showed significantly larger responses at the end of the tetanus, suggesting an increased rate for mobilization of reserve pool vesicles into the readily-releasable pool (Fig. 5E) ($F_{(1,12)} = 5.2$; $p < 0.05$). These data further support a model in which ERK-dependent synapsin I phosphorylation enhances neurotransmitter release selectively during patterns of stimulation that significantly deplete the readily-releasable pool of presynaptic neurotransmitter vesicles.

Presynaptic plasticity enhancement requires synapsin I

The data presented above suggest that increased trafficking of synaptic vesicles to the readily-releasable pool by ERK-phosphorylated synapsin I may underlie the increased responses to high-frequency stimulation in *H-ras*^{G12V} mice. To examine whether synapsin I is required for mediating the effects of the *H-ras*^{G12V} transgene, we crossed *synapsin I* knock-out mice (Rosahl et al., 1993) with the *H-ras*^{G12V} transgenics. Next, we examined whether synapsin I mediates the presynaptic facilitation of release during high-frequency stimulation in *H-ras*^{G12V} mice. Indeed, there was a significant interaction of genotype on fEPSP responses during the 10 Hz tetanus measured in the presence of APV and picrotoxin (Fig. 5F) ($F_{(3,24)} = 4.8$; $p < 0.01$). As expected in mice carrying the wild-type *synapsin I* allele, *H-ras*^{G12V}(+) mice showed significantly larger responses during the tetanus than *H-ras*^{G12V}-negative (–) littermates (Fig. 5F) (PLSD, $p < 0.05$). However, in the background of the *synapsin I* knock-out allele, *H-ras*^{G12V}(+) and *H-ras*^{G12V}(–) mice showed equivalent responses throughout the tetanus (Fig. 5F) (PLSD, $p = 0.90$). These results strongly argue that synapsin I is necessary to mediate the enhanced presynaptic plasticity observed in *H-ras*^{G12V} mice.

Increased density of docked vesicles in *H-ras*^{G12V} mice

Synapsin I plays a critical role in establishing the distribution of synaptic vesicles within axon terminals (Hilfiker et al., 1999; Humeau et al., 2001). The finding of a synapsin I-mediated increase in neurotransmitter release during high-frequency stimulation led us to hypothesize that *H-ras*^{G12V} mice may have an altered distribution of vesicles in presynaptic terminals. Using electron microscopy, we directly addressed this possibility by quantifying the number of morphologically docked vesicles at presynaptic active zones of Schaffer collateral–CA1 synapses, the anatomical correlate of the readily-releasable pool (Dickinson-Nelson and Reese, 1983; Pozzo-Miller et al., 1999; Schikorski and Stevens, 2001) (Fig. 6A). Indeed, significantly more docked vesicles were observed in synapses from *H-ras*^{G12V} mice (Fig. 6B) ($F_{(1,118)} = 29.5$; $p < 0.001$). Additional measurements of the total number of vesicles, active zone area, axon terminal volume, postsynaptic density thickness, and synapse density were normal in *H-ras*^{G12V} mice (data not shown).

In an independent group of mice, we also performed three-dimensional reconstruction of synaptic terminals using unbiased serial sectioning (Schikorski and Stevens, 1997, 2001). Again, we found a significant increase in docked vesicle density in *H-ras*^{G12V} terminals (Fig. 6C) ($F_{(1,58)} = 12.6$; $p < 0.001$). Together, these data provide anatomical evidence that H-ras/ERK-dependent phosphorylation of synapsin I regulates the size of the readily-releasable pool of neurotransmitter vesicles.

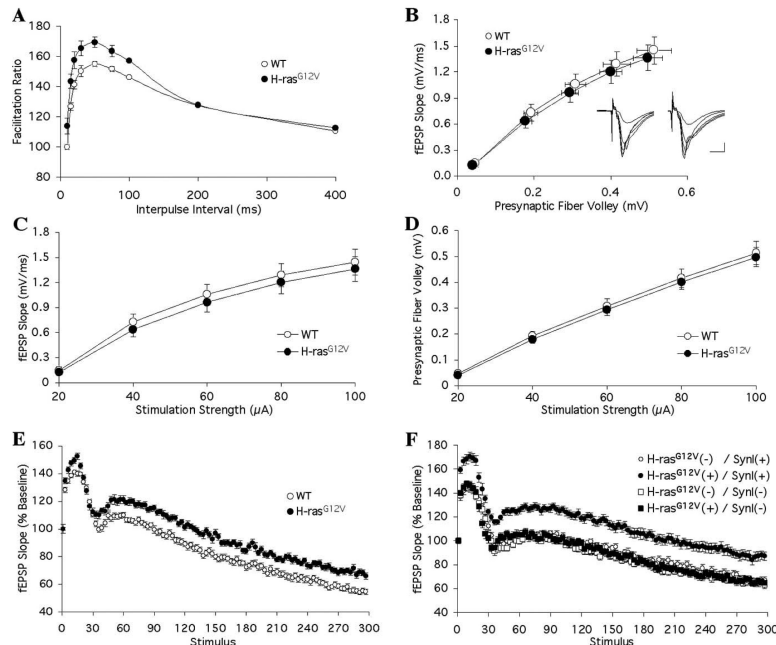


Figure 5. Presynaptic changes in *H-ras*^{G12V} mice are mediated by synapsin I. **A**, Paired-pulse facilitation was enhanced in *H-ras*^{G12V} mice for intervals ≤ 100 ms but normal for longer intervals (WT, 9 slices, 7 mice; *H-ras*^{G12V}, 8 slices, 6 mice). **B–D**, Basal synaptic transmission was normal in WT (10 slices, 10 mice) and *H-ras*^{G12V} (11 slices, 11 mice) littermates. Plots show the fEPSP as a function of the evoked presynaptic fiber volley (**B**), the fEPSP as a function of stimulation strength (**C**), and the presynaptic fiber volley as a function of stimulation strength (**D**). Inset in **B** shows representative traces (left, WT; right, *H-ras*^{G12V}). Calibration: 5 ms, 0.5 mV. **E**, Reserve pool mobilization during high-frequency stimulation in WT and *H-ras*^{G12V} mice was probed by 10 Hz (30 s) tetanization in the presence of APV and picrotoxin. Compared with WT littermates (9 slices, 7 mice), *H-ras*^{G12V} mice (9 slices, 7 mice) showed larger responses throughout the tetanus. **F**, Reserve pool mobilization during high-frequency stimulation in WT and *H-ras*^{G12V} mice with or without the presence of the *synapsin I* gene. The mobilization was probed using 10 Hz (30 s) tetanization in the presence of APV and picrotoxin. *H-ras*^{G12V}(+)/*SynI*(+) mice (7 slices, 7 mice) showed significantly larger fEPSPs than *H-ras*^{G12V}(–)/*SynI*(+) (7 slices, 7 mice) throughout the tetanus. In contrast, deletion of *synapsin I* prevented the increased plasticity because *H-ras*^{G12V}(–)/*SynI*(–) (7 slices, 7 mice) and *H-ras*^{G12V}(+)/*SynI*(–) (7 slices, 7 mice) showed equivalent responses.

ERK activity modulates mEPSC frequency but not amplitude

Our electrophysiologic data suggest that, during patterns of activity that tend to rapidly deplete the readily-releasable pool of neurotransmitter vesicles, *H-ras*^{G12V} mice have an attenuation of homosynaptic depression. The demonstration of an increased size of the morphologically docked pool of vesicles further supports our model of presynaptic H-ras/ERK signaling in which ERK-dependent phosphorylation of synapsin I shifts the distribution of presynaptic vesicles toward the readily-releasable pool. Therefore, we measured spontaneous mEPSCs in CA1 pyramidal neurons to further examine the functional effects of the alteration in synaptic vesicle distribution in *H-ras*^{G12V} mice (Fig. 6D–H). Consistent with a presynaptic locus for the observed alterations in synaptic plasticity of *H-ras*^{G12V} mice, mEPSC frequency was significantly increased without any change in mEPSC amplitude (unpaired *t* test; frequency, $t_{(1,24)} = 9.19$, $p < 0.001$; amplitude, $t_{(1,24)} = 0.43$, $p = 0.67$).

We have hypothesized that ERK-dependent phosphorylation of synapsin I is an important biochemical event that modulates presynaptic plasticity. Our results have demonstrated that robust physiologic ERK-dependent synapsin I phosphorylation occurs during learning in WT mice. We also hypothesized that, through increased downstream ERK activity, transgenic expression of

H-ras^{G12V} requires synapsin I to mediate an enhancement of presynaptic plasticity. Therefore, we perfused the MEK inhibitor U0126 into the extracellular solution immediately after the baseline mEPSC recordings to ask two important questions. First, does presynaptic MEK/ERK activity modulate neurotransmitter release under normal physiologic conditions in WT mice? Second, is the increased mEPSC frequency observed in *H-ras*^{G12V} mice dependent on a high level of downstream MEK/ERK activity?

After introduction of U0126 into the extracellular solution, the frequency of mEPSCs decreased significantly in CA1 pyramidal neurons of WT mice without any observed change in mEPSC amplitude (paired *t* test; frequency, $t_{(1,24)} = 7.15$, $p < 0.001$; amplitude, $t_{(1,24)} = 0.58$, $p = 0.57$), demonstrating that, under normal physiologic conditions, ERK activity modulates presynaptic neurotransmitter release. Additionally, U0126 completely abolished the increase in mEPSC frequency observed in *H-ras*^{G12V} mice without affecting mEPSC amplitude (unpaired *t* test; frequency, $t_{(1,24)} = 0.16$, $p = 0.88$; amplitude, $t_{(1,24)} = 0.28$, $p = 0.78$), confirming that the ERK pathway downstream of H-ras is responsible for the changes in presynaptic function in *H-ras*^{G12V} mice. These data further support our model hypothesizing that presynaptic neurotransmitter release is modulated over a short temporal window by presynaptic H-ras/ERK/synapsin I signaling.

Frequency-dependent enhancement of presynaptic plasticity and LTP

Because *H-ras*^{G12V} mice show anatomical and functional changes at presynaptic sites, we next investigated whether the observed alterations in presynaptic plasticity were relevant during the induction of LTP in *H-ras*^{G12V} mice. To explore this possibility, we examined LTP at the Schaffer collateral–CA1 synapse in acute hippocampal slices. We focused on the Schaffer collateral pathway because many previous studies have demonstrated that LTP at this synapse is crucial for learning contextual and spatial information (Martin et al., 2000). LTP was first induced using five TBS, which mimics the *in vivo* activity of hippocampal neurons during exploratory behavior (Larson et al., 1986; Otto et al., 1991). TBS consisted of four stimuli delivered at 100 Hz with a 200 ms interval between bursts. Significantly more LTP and STP were observed after five TBS in *H-ras*^{G12V} mice (Fig. 7A) (LTP, $F_{(1,12)} = 4.8$, $p < 0.05$; STP, $F_{(1,12)} = 11.2$, $p < 0.01$). In addition, the cumulative probability distribution of LTP was shifted toward significantly larger potentiation after five TBS (Fig. 7B) (Kolmogorov–Smirnov test, $D = 0.71$; $p = 0.056$). Therefore, *H-ras*^{G12V} expression enhanced the induction of both short- and long-term changes in synaptic strength after high-frequency presynaptic stimulation.

The predominantly presynaptic localization of H-ras^{G12V} as well as the larger STP suggests that the enhancement in LTP could

be mediated by increased neurotransmitter release during high-frequency stimulation. To evaluate this possibility, we recorded fEPSPs during five TBS in the presence of APV and picrotoxin to block NMDA receptor-dependent postsynaptic plasticity and GABA-mediated inhibition, respectively. A significant increase in fEPSP amplitude was observed in response to each theta burst in *H-ras*^{G12V} mice (Fig. 7C) ($F_{(19,266)} = 23.5$, $p < 0.001$). In contrast, fEPSPs returned to normal between the bursts ($F_{(4,56)} = 1.0$; $p = 0.40$), suggesting that the enhancement in STP may be frequency dependent.

We next sought to examine the interaction between the observed changes in short-term plasticity and long-term potentiation in *H-ras*^{G12V} mice. If the enhanced LTP after TBS in *H-ras*^{G12V} mice is mediated by increased presynaptic release during induction, then LTP should be normal when induced using lower frequencies of presynaptic stimulation that do not result in substantial homosynaptic depression. Indeed, 5 Hz LTP was indistinguishable between WT and *H-ras*^{G12V} mice (Fig. 7D) ($F_{(1,10)} = 0.002$; $p = 0.97$), and the cumulative probability distribution was normal (Fig. 7E) ($D = 0.25$; $p = 0.96$). Similarly, *H-ras*^{G12V} mice showed normal fEPSPs throughout the equivalent 5 Hz stimulus delivered in the presence of APV and picrotoxin (Fig. 7F) ($F_{(1,12)} = 0.002$; $p = 0.97$). Therefore, our results suggest that the alterations in long-term synaptic plasticity observed in the transgenic mice are a direct consequence of the frequency-dependent modulation of presynaptic neurotransmitter release during LTP induction.

Our model predicts that STP and LTP are enhanced in *H-ras*^{G12V} mice selectively after high-frequency stimulation protocols known to substantially deplete the readily-releasable pool. Therefore, similar to the STP and LTP enhancements observed with TBS, a different high-frequency induction protocol should also produce increased potentiation in *H-ras*^{G12V} mice. Indeed, both STP and LTP induced using a 100 Hz tetanus resulted in significantly more potentiation in *H-ras*^{G12V} mice (Fig. 8A) (LTP, $F_{(1,28)} = 10.1$, $p < 0.01$; STP, $F_{(1,28)} = 23.0$, $p < 0.001$). Additionally, the cumulative probability distribution was shifted toward significantly larger LTP in *H-ras*^{G12V} mice (Fig. 8B) ($D = 0.53$; $p < 0.05$). These data suggest that both short- and long-term synaptic potentiation are enhanced in *H-ras*^{G12V} mice selectively after high-frequency stimulation, consistent with a frequency-dependent increase in presynaptic release.

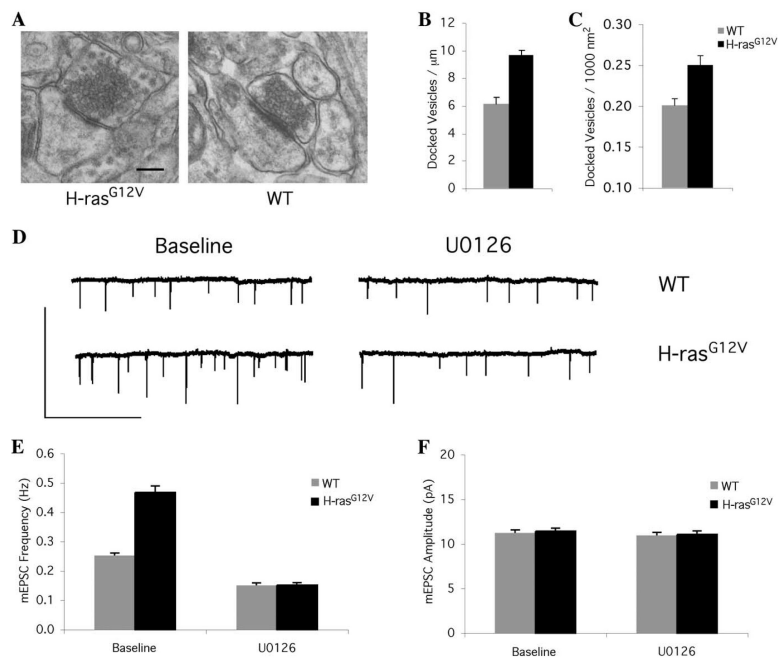


Figure 6. *H-ras*^{G12V} mice have more docked vesicles at presynaptic active zones. **A**, Representative electron micrographs of excitatory synapses onto dendritic spines in CA1 stratum radiatum. Scale bar, 200 nm. **B**, Using random sampling of excitatory synapses, *H-ras*^{G12V} mice had significantly more docked vesicles at presynaptic active zones (WT, 62 synapses, 3 mice; *H-ras*^{G12V}, 58 synapses, 3 mice). **C**, Three-dimensional reconstruction of synaptic terminals confirmed the increased density of docked vesicles (WT, 30 synapses, 3 mice; *H-ras*^{G12V}, 30 synapses, 3 mice). **D**, Representative traces of mEPSC recordings in WT and *H-ras*^{G12V} mice at baseline and after application of the MEK inhibitor U0126. Calibration: 10 s, 40 pA. **E**, mEPSC frequency was significantly increased in *H-ras*^{G12V} neurons and rescued by the application of U0126. Note that WT neurons showed a significant reduction in mEPSC frequency during application of U0126, consistent with a functional presynaptic H-ras/ERK pathway under normal physiologic conditions. **F**, mEPSC amplitude was maintained in *H-ras*^{G12V} neurons and unaltered by application of U0126.

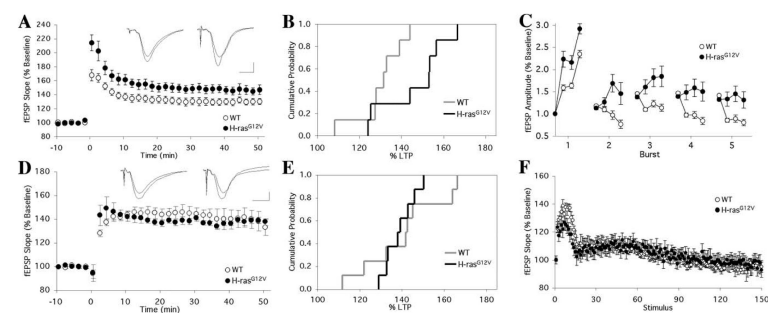


Figure 7. High-frequency stimulation augments neurotransmitter release and enhances long-term potentiation in *H-ras*^{G12V} mice. **A**, LTP induced by a five TBS protocol was increased in *H-ras*^{G12V} mice. Short-term potentiation measured 30 s after the tetanus was also increased (WT, 7 slices, 7 mice; *H-ras*^{G12V}, 7 slices, 7 mice). **B**, Cumulative probability distribution of LTP for the five theta-burst protocol shows significantly larger LTP in *H-ras*^{G12V} mice. **C**, fEPSP amplitude was significantly increased during TBS delivered in the presence of APV and picrotoxin (WT, 8 slices, 8 mice; *H-ras*^{G12V}, 8 slices, 8 mice). **D**, Low-frequency LTP induced using 5 Hz (30 s) stimulation was normal between WT (8 slices, 6 mice) and *H-ras*^{G12V} (8 slices, 6 mice) littermates. **E**, Cumulative probability distribution of 5 Hz LTP shows normal probability distributions between WT and *H-ras*^{G12V} mice. **F**, Responses during 5 Hz (30 s) stimulation in the presence of APV and picrotoxin were also equivalent (WT, 7 slices, 7 mice; *H-ras*^{G12V}, 7 slices, 7 mice). Representative traces (**A**, **D**) are shown at baseline and during LTP (left, WT; right, *H-ras*^{G12V}). Calibration: 5 ms, 0.5 mV.

H-ras^{G12V} mice show normal pairing-induced associative LTP

Our model for the presynaptic frequency-dependent effects of *H-ras*^{G12V} also predicts that NMDA-dependent associative LTP induced by low-frequency presynaptic stimulation, which does not significantly challenge the readily-releasable pool, should be

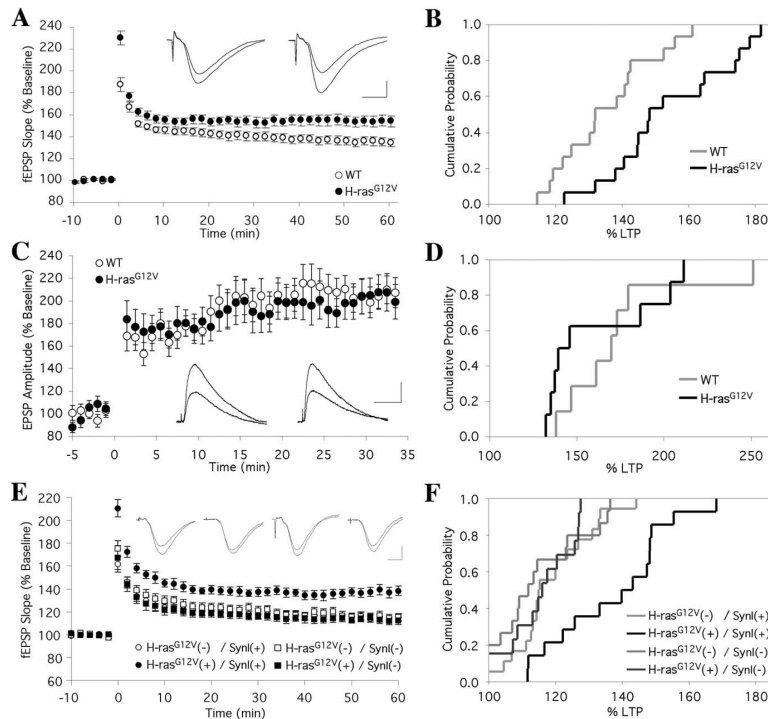


Figure 8. LTP enhancement in *H-ras*^{G12V} mice is mediated by a presynaptic mechanism during induction. **A**, Both STP and LTP induced by 100 Hz (1 s) tetanization were increased in *H-ras*^{G12V} mice (WT, 15 slices, 15 mice; *H-ras*^{G12V}, 15 slices, 15 mice). Representative traces are shown at baseline and during LTP (left, WT; right, *H-ras*^{G12V}). Calibration: 5 ms, 0.5 mV. **B**, Cumulative probability distribution of 100 Hz LTP shows significantly larger LTP in *H-ras*^{G12V} mice. **C**, Pairing LTP induced under whole-cell patch clamp at 0.5 Hz (50 s) using single presynaptic stimuli and 200 ms of 0.8 nA postsynaptic depolarization. WT (9 cells, 7 mice) and *H-ras*^{G12V} (10 cells, 8 mice) showed equivalent LTP. Representative traces are shown at baseline and during LTP (left, WT; right, *H-ras*^{G12V}). Calibration: 30 ms, 3 mV. **D**, Cumulative probability distribution of LTP induced with 0.5 Hz pairing is equivalent between WT and *H-ras*^{G12V} mice. **E**, Both STP and LTP induced by 100 Hz (1 s) tetanization were increased in *H-ras*^{G12V}(+) mice with a wild-type *synapsin I* allele [*H-ras*^{G12V}(+)/*Synl*(+), 19 slices, 9 mice; *H-ras*^{G12V}(-)/*Synl*(+), 14 slices, 7 mice]. However, the plasticity enhancements were abolished in the absence of *synapsin I* [*H-ras*^{G12V}(+)/*Synl*(-), 15 slices, 5 mice; *H-ras*^{G12V}(-)/*Synl*(-), 14 slices, 5 mice]. Representative traces are shown at baseline and during LTP (left to right, *H-ras*^{G12V}(+)/*Synl*(+), *H-ras*^{G12V}(-)/*Synl*(+), *H-ras*^{G12V}(+)/*Synl*(-), *H-ras*^{G12V}(-)/*Synl*(-)). Calibration: 5 ms, 0.2 mV. **F**, Cumulative probability distribution of 100 Hz LTP shows that the LTP enhancement in *H-ras*^{G12V} mice requires the presynaptic protein *synapsin I*.

normal in *H-ras*^{G12V} mice. Using whole-cell patch clamp, LTP was reliably induced by 100 pairings at 0.5 Hz of a single presynaptic stimulus with a 200 ms postsynaptic current injection and train of action potentials (APs). The whole-cell patch-clamp configuration provided an additional opportunity to detect changes in postsynaptic plasticity because many previous studies have demonstrated that associative LTP requires intact postsynaptic ERK signaling (Watanabe et al., 2002; Zhu et al., 2002; Selcher et al., 2003). Therefore, we used potassium methyl-sulfate in the patch pipette solution to avoid blockade of A-type potassium channels that are modulated by postsynaptic ERK and regulate dendritic excitability (Yuan et al., 2002; Frick et al., 2004). Consistent with intact postsynaptic function in *H-ras*^{G12V} mice, LTP was normal (Fig. 8C,D) ($F_{(1,13)} = 0.49$, $p = 0.49$; cumulative probability distribution, $D = 0.48$, $p = 0.35$). Importantly, AP frequency, AP amplitude, AP threshold, membrane potential, and input resistance were also unchanged in *H-ras*^{G12V} mice (data not shown). Together, these data strongly suggest that enhanced LTP in *H-ras*^{G12V} mice results from increased synaptic transmission during high-frequency stimulation. Conversely, because low-frequency stimulation does not significantly challenge the

presynaptic readily-releasable pool, LTP induced under these conditions is normal. These results highlight the specificity of the electrophysiologic changes and suggest that presynaptic plasticity is enhanced in *H-ras*^{G12V} mice although postsynaptic function is normal.

Enhanced long-term potentiation requires *synapsin I*

Consistent with a frequency-dependent facilitation of presynaptic neurotransmitter release, *H-ras*^{G12V} mice demonstrate an enhancement in LTP using induction protocols with high-frequency, but not low-frequency, presynaptic stimulation. Thus far, we have demonstrated that a critical downstream effector of H-ras/ERK in modulating short-term presynaptic plasticity is *synapsin I*. To further examine our hypothesis that *synapsin I* is a necessary downstream target of presynaptic H-ras/ERK signaling for the modulation of synaptic plasticity, we performed 100 Hz LTP in mice carrying the *H-ras*^{G12V} transgene in a C57BL/6 genetic background with a targeted deletion of *synapsin I* (Fig. 8E,F). There was a significant effect of genotype on the magnitude of LTP induced (Fig. 8E) ($F_{(3,59)} = 9.10$; $p < 0.001$). Consistent with our previous experiments using high-frequency LTP induction protocols, in mice carrying the wild-type *synapsin I* allele, *H-ras*^{G12V}(+) mice showed significantly larger LTP (Fig. 8E) (PLSD, $p < 0.001$), with a significant shift in the cumulative probability distribution (Fig. 8F) ($D = 0.64$; $p < 0.01$). However, in the background of the *synapsin I* knock-out allele, *H-ras*^{G12V}(+) and *H-ras*^{G12V}(-) mice showed an equivalent magnitude of LTP (Fig. 8E) ($p = 0.83$) and similar cumulative probability distributions (Fig. 8F) ($D = 0.22$; $p = 0.85$).

Importantly, in the absence of the *H-ras*^{G12V} transgene, we replicated the previously published finding that *synapsin I* knock-out mice have normal 100 Hz LTP (Rosahl et al., 1993) [Fig. 8E ($p = 0.33$), F ($D = 0.31$; $p = 0.41$)]. Therefore, the presynaptic H-ras/ERK signaling pathway requires *synapsin I* as a necessary downstream target for modulation of presynaptic plasticity and LTP.

Enhanced hippocampus-dependent learning

To examine the effects of increased H-ras/ERK/*synapsin I* signaling on spatial learning, we trained *H-ras*^{G12V} mice and WT littermates using the Morris water maze. In this hippocampus-dependent task, mice learn to navigate to a submerged platform by using extra-maze cues (Morris et al., 1982). *H-ras*^{G12V} and WT mice showed equivalent latencies to find the hidden platform during training, with no differences in swimming speed or floating (data not shown). Spatial learning was assessed using probe trials (Brandeis et al., 1989) in which the platform was removed from the pool and the search path was recorded. *H-ras*^{G12V} mice spent significantly more time in the target quadrant than WT mice during the probe trial conducted on day 6 (Fig. 9A)

($F_{(1,23)} = 4.7$; $p < 0.05$). Additionally, the cumulative probability distribution of target quadrant occupancy times revealed that, compared with their WT littermates, *H-ras*^{G12V} mice showed higher selectivity in their probe trial search path (Fig. 9B). The learning enhancement was confirmed using two additional measures to assess spatial learning during the probe trial. First, *H-ras*^{G12V} mice searched significantly closer to the target platform location than WT mice (*H-ras*^{G12V}, 45.1 ± 3.3 cm; WT, 56.3 ± 3.2 cm; $F_{(1,23)} = 6.0$; $p < 0.05$). Second, the number of crossings through the target platform location was significantly higher in *H-ras*^{G12V} (3.0 ± 0.7 crosses) than WT mice (1.2 ± 0.4 crosses) ($F_{(1,23)} = 4.7$; $p < 0.05$).

After 3 additional days of training, WT mice improved the selectivity of their probe trial search to a similar level as *H-ras*^{G12V} littermates (Fig. 9C) ($F_{(1,23)} = 0.40$; $p = 0.53$). These results indicate that, although *H-ras*^{G12V} mice require less training to learn the spatial location of the target platform, additional training allows WT mice to improve their search strategy to a similar asymptotic level.

Although *H-ras*^{G12V} mice demonstrate enhanced spatial learning, an important question is the stability of their memory for the target platform location. Therefore, we tested mice in a probe trial conducted 14 d after the end of training. Importantly, both groups maintained an equivalently high level of target quadrant selectivity (WT, $40.9 \pm 6.3\%$ time; *H-ras*^{G12V}, $49.3 \pm 4.5\%$ time; $F_{(1,23)} = 1.2$; $p = 0.28$), confirming that the long-term stability of spatial memory in *H-ras*^{G12V} mice is intact.

Using contextual fear conditioning, a robust hippocampus-dependent task (Kim and Fanselow, 1992) that relies on stimuli and behavioral outputs distinct from the water maze permitted an independent test of the hypothesis that the enhanced spatial learning in *H-ras*^{G12V} mice results from a change in hippocampal function. After training with three footshocks, mice were returned to the same context 24 h later to assess long-term memory, and freezing behavior was recorded using automated procedures (Anagnostaras et al., 2000). *H-ras*^{G12V} mice showed significantly more contextual learning during the 24 h test compared with their WT littermates ($F_{(1,14)} = 9.4$; $p < 0.01$), whereas baseline freezing before training was normal (Fig. 9D) ($F_{(1,14)} = 0.23$; $p = 0.64$). We also examined the suppression of activity as an additional measure of conditioned fear (Anagnostaras et al., 2000). Indeed, *H-ras*^{G12V} mice also showed an enhanced suppression ratio consistent with increased fear of the context (WT, 0.21 ± 0.02 ; *H-ras*^{G12V}, 0.13 ± 0.01 ; $F_{(1,14)} = 9.9$; $p < 0.01$). Importantly, the enhancement in fear conditioning was not attributable to differences in footshock sensitivity

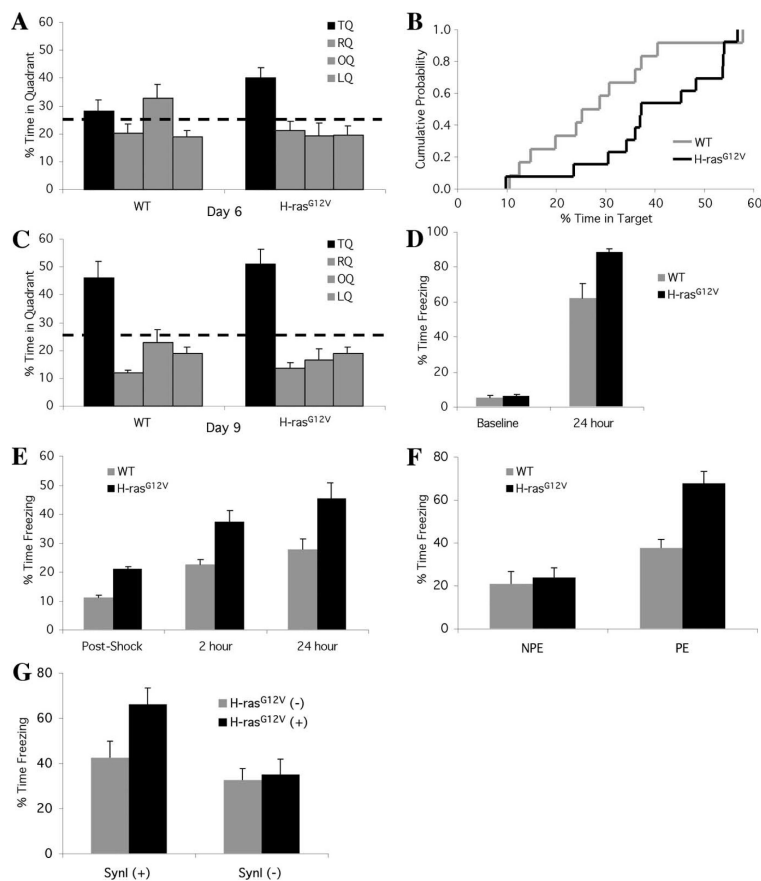


Figure 9. Enhanced learning of hippocampus-dependent tasks in *H-ras*^{G12V} mice is mediated by synapsin I. **A–C**, WT ($n = 12$) and *H-ras*^{G12V} ($n = 13$) littermates were trained in the Morris water maze for 9 d. A probe trial conducted after the sixth day of training revealed that *H-ras*^{G12V} mice searched selectively in the target quadrant, but their WT littermates showed no preference (**A**). Dashed line at 25% time quadrant represents random searching. The cumulative probability distribution of target quadrant occupancy time during the probe trial demonstrates that *H-ras*^{G12V} mice are more highly selective during searching than their WT littermates (**B**). During a probe trial performed after the ninth training day, WT and *H-ras*^{G12V} mice showed similar target quadrant selectivity (**C**). TQ, Target quadrant; RQ, adjacent right quadrant; OQ, opposite quadrant; LQ, adjacent left quadrant. **D**, **E**, Short- and long-term memory of *H-ras*^{G12V} mice were evaluated using contextual fear conditioning. Learning was enhanced in *H-ras*^{G12V} mice during a 24 h long-term memory test for contextual fear conditioning with three footshocks in the absence of any observed changes in baseline freezing (WT, $n = 8$; *H-ras*^{G12V}, $n = 8$) (**D**). Conditional freezing was increased in *H-ras*^{G12V} mice immediately after shock (WT, $n = 23$; *H-ras*^{G12V}, $n = 21$) and 2 h (WT, $n = 8$; *H-ras*^{G12V}, $n = 10$) and 24 h (WT, $n = 15$; *H-ras*^{G12V}, $n = 11$) after training with a single footshock (**E**). **F**, Three minute context preexposure, 24 h before receiving immediate shock training, resulted in enhanced conditional fear for *H-ras*^{G12V} ($n = 10$) compared with WT mice ($n = 13$). There was no difference in conditional freezing between WT ($n = 11$) and *H-ras*^{G12V} ($n = 13$) mice after immediate shock training in the absence of preexposure. **G**, Enhanced learning in *H-ras*^{G12V} mice is dependent on synapsin I. Contextual fear conditioning using three footshocks showed that, in the background of the wild-type *synapsin I* allele, [*Synl*(+)], *H-ras*^{G12V}(+) mice ($n = 10$) showed significantly more conditioned fear than *H-ras*^{G12V}(–) littermates ($n = 11$). In contrast, deletion of *synapsin I* [*Synl*(–)] prevented the learning enhancement [*Synl*(–): *H-ras*^{G12V}(–), $n = 11$; *H-ras*^{G12V}(+), $n = 7$].

because unconditioned responding during footshock was equivalent for *H-ras*^{G12V} (38.4 ± 7.1 cm/s) and WT (40.6 ± 4.9 cm/s) littermates ($F_{(1,14)} = 0.17$; $p = 0.69$). Short-term memory was assessed after training with a single footshock to avoid saturating the conditioned response. Separate groups of mice were used to independently examine freezing at 2 and 24 h after training. *H-ras*^{G12V} mice showed significantly more freezing than their WT littermates immediately after shock ($F_{(1,42)} = 5.1$; $p < 0.05$) as well as 2 h ($F_{(1,16)} = 4.6$; $p < 0.05$) and 24 h ($F_{(1,24)} = 6.6$; $p < 0.05$) after training (Fig. 9E).

The formation of contextual fear memory requires an animal

to create a hippocampus-dependent representation of the training environment (Kim and Fanselow, 1992; Rudy et al., 2002). Significantly decreasing the placement-to-shock interval during contextual conditioning, so that the animal is shocked immediately after entering the training chamber, results in a concomitant decrease in the strength of the resulting fear memory, known as the immediate shock deficit (ISD). This deficit is thought to arise from an inability to form an adequate representation of the training context (Fanselow, 1990; Frankland et al., 2004). Consistent with this interpretation, preexposure (PE) to the training context can rescue the ISD (Fanselow, 1990) and has been shown to require protein synthesis within the hippocampus (Rudy et al., 2002; Frankland et al., 2004). If the learning enhancements seen in *H-ras*^{G12V} mice result from an alteration in the processing of contextual and spatial information in the hippocampus, the amount of PE sufficient to rescue the ISD should be decreased in *H-ras*^{G12V} mice compared with their WT littermates. Therefore, we used a 3 min PE to the training context, which is insufficient to rescue the ISD in WT mice (Frankland et al., 2004). Animals of each genotype received either no preexposure training (NPE) or context PE 24 h before receiving an immediate footshock. Conditioned fear was assessed 24 h after immediate shock training. There was a significant interaction of genotype with preexposure on conditioned fear (Fig. 9F) ($F_{(1,43)} = 7.6; p < 0.01$). In groups receiving PE training, *H-ras*^{G12V} mice showed a significant increase in freezing compared with WT mice (PLSD, $p < 0.001$). Importantly, *H-ras*^{G12V} and WT mice receiving NPE showed similar freezing after immediate shock training, indicating that increased freezing in *H-ras*^{G12V} mice is dependent on an involvement of the hippocampus in the formation of contextual representations during fear conditioning (PLSD, $p = 0.69$).

Learning enhancement is mediated by synapsin I

Our data suggests a model in which presynaptic activation of H-ras/ERK/synapsin I signaling during experience-dependent plasticity functions to modulate learning. Therefore, we hypothesized that, similar to the facilitation in presynaptic plasticity, the hippocampus-dependent learning enhancement displayed by *H-ras*^{G12V} mice should require synapsin I. To examine whether synapsin I is required for the enhancement in learning, we crossed *synapsin I* knock-out mice (Rosahl et al., 1993) with *H-ras*^{G12V} transgenics. Contextual fear conditioning was performed using three footshocks, and long-term memory was assessed in the same context 24 h later in all four genotypic groups. Indeed, there was a significant effect of genotype on conditioned fear (Fig. 9G) ($F_{(3,35)} = 5.3; p < 0.01$). As expected, *H-ras*^{G12V}(+) mice showed significantly more freezing than *H-ras*^{G12V}(-) littermates in the presence of the wild-type *synapsin I* allele (PLSD, $p < 0.05$). However in the background of the *synapsin I* knock-out allele, *H-ras*^{G12V}(+) and *H-ras*^{G12V}(-) mice showed equivalent responses (PLSD, $p = 0.81$), demonstrating that the H-ras^{G12V}-mediated learning enhancement requires synapsin I. Together, these results strongly argue that integrity of the presynaptic H-ras/ERK/synapsin I signaling pathway is necessary for the enhanced synaptic and behavioral plasticity observed in *H-ras*^{G12V} mice.

Discussion

In invertebrate systems, coordinated plasticity between presynaptic and postsynaptic neurons has been shown to contribute directly to learning (Antonov et al., 2003; Roberts and Glanzman, 2003). Genetic and pharmacologic studies in mammalian systems have provided considerable evidence that postsynaptic pro-

cesses required for synaptic plasticity are critical for learning and memory (Martin et al., 2000). However, few studies have identified presynaptic mechanisms necessary for mammalian cognition (Powell et al., 2004). The present study is the first example that targeted manipulation of biochemical signaling in axon terminals can enhance learning and synaptic plasticity in mammals. In addition, our data support the long-standing hypothesis that short-term presynaptic plasticity influences the induction of LTP (Dobrunz and Stevens, 1999). Specifically, our results demonstrate a novel cellular function of H-ras/ERK signaling: by regulating the density of docked vesicles via ERK-dependent phosphorylation of synapsin I, experience-dependent changes in the activity of presynaptic H-ras modulate the induction of long-term synaptic plasticity underlying learning through a frequency-dependent facilitation of neurotransmitter release.

Our confocal and electron microscopy studies demonstrate that H-ras is abundantly localized to axon terminals, with limited expression in postsynaptic spines. Although under certain conditions p21^{Ras} appears to be involved in NMDA-dependent postsynaptic plasticity (Husi et al., 2000; Manabe et al., 2000; Zhu et al., 2002), our transgenic results were not caused by postsynaptic mechanisms. Long-term potentiation induced by both theta-frequency extracellular stimulation and associative whole-cell pairing are dependent on ERK signaling in dendrites downstream of the postsynaptic NMDA receptor (Winder et al., 1999; Watanabe et al., 2002). Consistent with intact postsynaptic ERK signaling, 5 Hz extracellular and 0.5 Hz associative LTP were normal in *H-ras*^{G12V} mice. In contrast, LTP was increased using NMDA-dependent theta-burst and 100 Hz stimulation protocols, which cause significant short-term presynaptic vesicle depletion. Importantly, the increases in LTP induction observed in *H-ras*^{G12V} mice were associated with similar increases in short-term presynaptic plasticity, highlighted by the frequency-dependent enhancement of PPF. In particular, our electrophysiologic analyses of short-term plasticity were conducted in the presence of APV and picrotoxin, ensuring that the observed changes truly reflected a modulation of neurotransmitter release, not attributable to alterations in postsynaptic or inhibitory plasticity. The demonstration of enhanced neurotransmitter release during high-frequency stimulation is further supported by the associated increase in docked neurotransmitter vesicles at presynaptic active zones of *H-ras*^{G12V} mice and an increased frequency but not amplitude of mEPSCs. Interestingly, although PPF, STP, mEPSC frequency, and the density of docked vesicles were all increased, baseline synaptic transmission was maintained, likely mediated through presynaptic homeostatic plasticity (Davis and Goodman, 1998; Jones et al., 1998; Daniels et al., 2004; Piedras-Renteria et al., 2004). Together, these data suggest that the LTP enhancements in *H-ras*^{G12V} mice do not result from changes in postsynaptic plasticity but rather from a frequency-dependent facilitation of short-term presynaptic plasticity leading to increased neurotransmitter release specifically during high-frequency LTP induction.

Furthermore, we have used a genetic approach to evaluate the hypothesis that the ERK-dependent phosphorylation of synapsin I represents a critical presynaptic mechanism responsible for mediating H-ras-dependent changes in behavioral and synaptic plasticity. By crossing *H-ras*^{G12V} and *synapsin I*^{-/-} mice, we have confirmed the requirement for the presynaptic target of ERK1/2, synapsin I, in mediating the enhancements of presynaptic plasticity, LTP, and learning observed in *H-ras*^{G12V} mice. Interestingly, although we show that enhancing synapsin I function leads to LTP and learning enhancements, our present data are consis-

tent with previous studies demonstrating that *synapsin I* knock-out mice have seemingly normal LTP and learning (Rosahl et al., 1993; Silva et al., 1996), reflecting a functional redundancy between synapsin I and II (Rosahl et al., 1995; Silva et al., 1996). Accordingly, *synapsin I/II* double mutants show synaptic and learning deficits absent in either single gene mutant (Rosahl et al., 1995; Silva et al., 1996). Consistent with these findings, both synapsin I and II are required for an ERK-dependent facilitation of synaptosomal neurotransmitter release (Jovanovic et al., 2000).

Under normal physiologic conditions in WT mice, we have performed multiple experiments supporting the presence *in vivo* of a dynamic and experience-dependent endogenous presynaptic H-ras/ERK/synapsin I signaling pathway. In two different genetic backgrounds of WT mice, we demonstrate that ERK-dependent synapsin I phosphorylation occurs specifically during hippocampus-dependent learning but not after unconditioned shock. In addition, the expression level and subcellular localization of H-ras^{G12V} is equivalent to endogenous H-ras, demonstrating that the mechanisms underlying the learning enhancement in *H-ras^{G12V}* mice are physiologically relevant. Consistent with an important endogenous function for ERK-dependent phosphorylation of synapsin I in regulating presynaptic neurotransmitter release dynamics, we also showed that MEK/ERK inhibition selectively decreases mEPSC frequency but not amplitude in normal WT mice and completely abolishes the increased mEPSC frequency in *H-ras^{G12V}* mice. Importantly, the timescale of MEK/ERK inhibition (15–20 min) during the mEPSC recordings makes a transcription/translation mechanism very unlikely, while supporting a posttranslational mechanism such as the inhibition of ERK-dependent synapsin I phosphorylation at presynaptic sites.

How might the facilitation of neurotransmitter release during high-frequency stimulation mediate an enhancement in spatial learning? Salient information in hippocampal CA1 neuronal ensembles is thought to be encoded during synchronous high-frequency spike bursts contrasting against a homeostatic background of low-frequency activity (Otto et al., 1991; Lisman, 1997). The present findings demonstrate that the *H-ras^{G12V}* mutation specifically enhances release during patterns of high-frequency synaptic activity typically observed during hippocampus-dependent learning (Otto et al., 1991; Lisman, 1997), while leaving basal synaptic transmission unchanged. Thus, one parsimonious model for the learning enhancements in *H-ras^{G12V}* mice is an increased fidelity of synaptic transmission during hippocampus-dependent encoding of salient stimuli.

How is the presynaptic H-ras/ERK/synapsin I signaling pathway recruited during learning? A potent presynaptic activator of p21^{Ras} is the brain-derived neurotrophic factor (BDNF) receptor TrkB. Several genetic and pharmacologic studies have shown that BDNF/TrkB signaling can modulate presynaptic function and learning (Xu et al., 2000; Tyler et al., 2002; Zhang and Poo, 2002). Consistent with our results, BDNF has been shown to increase synaptosomal glutamate release through the ERK-dependent phosphorylation of synapsin I (Jovanovic et al., 2000). In addition, treatment of organotypic hippocampal slices with BDNF results in an increase in the density of docked vesicles (Tyler and Pozzo-Miller, 2001). Similar studies performed in neonatal hippocampal slices demonstrated a BDNF-specific and ERK-dependent attenuation of synaptic fatigue selectively during high-frequency stimulation (Gottschalk et al., 1998, 1999). Finally, the LTP enhancements observed in *H-ras^{G12V}* mice are consistent with a recent study demonstrating that BDNF modu-

lates presynaptic plasticity at the hippocampal Schaffer collateral–CA1 synapse *in vivo* (Zakharenko et al., 2003).

The studies presented here represent a first step toward understanding how presynaptic signaling modulates learning and memory in mammals. Together with previous findings in invertebrate models, these results demonstrate that the modulation of presynaptic function is an evolutionarily conserved mechanism for learning and memory.

References

- Adams JP, Sweatt JD (2002) Molecular psychology: roles for the ERK MAP kinase cascade in memory. *Annu Rev Pharmacol Toxicol* 42:135–163.
- Adams JP, Anderson AE, Varga AW, Dineley KT, Cook RG, Pfaffinger PJ, Sweatt JD (2000) The A-type potassium channel Kv4.2 is a substrate for the mitogen-activated protein kinase ERK. *J Neurochem* 75:2277–2287.
- Anagnostaras SG, Josselyn SA, Frankland PW, Silva AJ (2000) Computer-assisted behavioral assessment of Pavlovian fear conditioning in mice. *Learn Mem* 7:58–72.
- Antonov I, Antonova I, Kandel ER, Hawkins RD (2003) Activity-dependent presynaptic facilitation and hebbian LTP are both required and interact during classical conditioning in *Aplysia*. *Neuron* 37:135–147.
- Atkins CM, Selcher JC, Petraitis J, Trzaskos J, Sweatt J (1998) The MAPK cascade is required for mammalian associative learning. *Nat Neurosci* 1:602–609.
- Bahler M, Greengard P (1987) Synapsin I bundles F-actin in a phosphorylation-dependent manner. *Nature* 326:704–707.
- Benfenati F, Bahler M, Jahn R, Greengard P (1989) Interactions of synapsin I with small synaptic vesicles: distinct sites in synapsin I bind to vesicle phospholipids and vesicle proteins. *J Cell Biol* 108:1863–1872.
- Benfenati F, Valtorta F, Rubenstein JL, Gorelick FS, Greengard P, Czernik AJ (1992) Synaptic vesicle-associated Ca²⁺/calmodulin-dependent protein kinase II is a binding protein for synapsin I. *Nature* 359:417–420.
- Brager DH, Capogna M, Thompson SM (2002) Short-term synaptic plasticity, simulation of nerve terminal dynamics, and the effects of protein kinase C activation in rat hippocampus. *J Physiol (Lond)* 541:545–559.
- Brandeis R, Brandys Y, Yehuda S (1989) The use of the Morris water maze in the study of memory and learning. *Int J Neurosci* 48:29–69.
- Burrell BD, Sahley CL (2001) Learning in simple systems. *Curr Opin Neurobiol* 11:757–764.
- Chi P, Greengard P, Ryan TA (2003) Synaptic vesicle mobilization is regulated by distinct synapsin I phosphorylation pathways at different frequencies. *Neuron* 38:69–78.
- Chin J, Angers A, Cleary LJ, Eskin A, Byrne JH (2002) Transforming growth factor β -1 alters synapsin distribution and modulates synaptic depression in *Aplysia*. *J Neurosci* 22:1–6.
- Costa RM, Yang T, Huynh DP, Pulst SM, Viskochil DH, Silva AJ, Brannan CI (2001) Learning deficits, but normal development and tumor predisposition, in mice lacking exon 23a of Nf1. *Nat Genet* 27:399–405.
- Daniels RW, Collins CA, Gelfand MV, Dant J, Brooks ES, Krantz DE, DiAntonio A (2004) Increased expression of the *Drosophila* vesicular glutamate transporter leads to excess glutamate release and a compensatory decrease in quantal content. *J Neurosci* 24:10466–10474.
- Davis GW, Goodman CS (1998) Synapse-specific control of synaptic efficacy at the terminals of a single neuron. *Nature* 392:82–86.
- Dickinson-Nelson A, Reese TS (1983) Structural changes during transmitter release at synapses in the frog sympathetic ganglion. *J Neurosci* 3:42–52.
- Dobrunz LE, Stevens CF (1997) Heterogeneity of release probability, facilitation, and depletion at central synapses. *Neuron* 18:995–1008.
- Dobrunz LE, Stevens CF (1999) Response of hippocampal synapses to natural stimulation patterns. *Neuron* 22:157–166.
- Dobrunz LE, Huang EP, Stevens CF (1997) Very short-term plasticity in hippocampal synapses. *Proc Natl Acad Sci USA* 94:14843–14847.
- Elgersma Y, Fedorov N, Ikonen S, Choi E, Elgersma M, Carvalho O, Giese K, Silva A (2002) Inhibitory autophosphorylation of CaMKII controls PSD association, plasticity and learning. *Neuron* 36:493–505.
- English JD, Sweatt JD (1996) Activation of p42 mitogen-activated protein kinase in hippocampal long term potentiation. *J Biol Chem* 271:24329–24332.
- Fanselow MS (1990) Factors governing one-trial contextual conditioning. *Anim Learn Behav* 18:264–270.

- Frankland P, O'Brien C, Ohno M, Kirkwood A, Silva A (2001) Alpha-CaMKII-dependent plasticity in the cortex is required for permanent memory. *Nature* 411:309–313.
- Frankland PW, Josselyn SA, Anagnostaras SG, Kogan JH, Takahashi E, Silva AJ (2004) Consolidation of CS and US representations in associative fear conditioning. *Hippocampus* 14:557–569.
- Frick A, Magee J, Johnston D (2004) LTP is accompanied by an enhanced local excitability of pyramidal neuron dendrites. *Nat Neurosci* 7:126–135.
- Gartner U, Alpar A, Seeger G, Heumann R, Arendt T (2004) Enhanced Ras activity in pyramidal neurons induces cellular hypertrophy and changes in afferent and intrinsic connectivity in synRas mice. *Int J Dev Neurosci* 22:165–173.
- Gottschalk W, Pozzo-Miller LD, Figuero A, Lu B (1998) Presynaptic modulation of synaptic transmission and plasticity by brain-derived neurotrophic factor in the developing hippocampus. *J Neurosci* 18:6830–6839.
- Gottschalk WA, Jiang H, Tartaglia N, Feng L, Figuero A, Lu B (1999) Signaling mechanisms mediating BDNF modulation of synaptic plasticity in the hippocampus. *Learn Mem* 6:243–256.
- Heumann R, Goemans C, Bartsch D, Lingenhohl K, Waldmeier PC, Hengerer B, Allegrini PR, Schellander K, Wagner EF, Arendt T, Kamdem RH, Obst-Pernberg K, Narz F, Wahle P, Berns H (2000) Transgenic activation of Ras in neurons promotes hypertrophy and protects from lesion-induced degeneration. *J Cell Biol* 151:1537–1548.
- Hilfiker S, Pieribone VA, Czernik AJ, Kao HT, Augustine GJ, Greengard P (1999) Synapsins as regulators of neurotransmitter release. *Philos Trans R Soc Lond B Biol Sci* 354:269–279.
- Humeau Y, Doussau F, Vitiello F, Greengard P, Benfenati F, Poulain B (2001) Synapsin controls both reserve and releasable synaptic vesicle pools during neuronal activity and short-term plasticity in *Aplysia*. *J Neurosci* 21:4195–4206.
- Husi H, Ward MA, Choudhary JS, Blackstock WP, Grant SG (2000) Proteomic analysis of NMDA receptor-adhesion protein signaling complexes. *Nat Neurosci* 3:661–669.
- Iida N, Namikawa K, Kiyama H, Ueno H, Nakamura S, Hattori S (2001) Requirement of Ras for the activation of mitogen-activated protein kinase by calcium influx, cAMP, and neurotrophin in hippocampal neurons. *J Neurosci* 21:6459–6466.
- Jaaarsma D, Rognoni F, van Duijn W, Verspaget HW, Haasdijk ED, Holstege JC (2001) CuZn superoxide dismutase (SOD1) accumulates in vacuolated mitochondria in transgenic mice expressing amyotrophic lateral sclerosis-linked SOD1 mutations. *Acta Neuropathol (Berl)* 102:293–305.
- Jones SR, Gainetdinov RR, Jaber M, Giros B, Wightman RM, Caron MG (1998) Profound neuronal plasticity in response to inactivation of the dopamine transporter. *Proc Natl Acad Sci USA* 95:4029–4034.
- Jovanovic JN, Benfenati F, Siow YL, Sihra TS, Sanghera JS, Pelech SL, Greengard P, Czernik AJ (1996) Neurotrophins stimulate phosphorylation of synapsin I by MAP kinase and regulate synapsin I-actin interactions. *Proc Natl Acad Sci USA* 93:3679–3683.
- Jovanovic JN, Czernik AJ, Fienberg AA, Greengard P, Sihra TS (2000) Synapsins as mediators of BDNF-enhanced neurotransmitter release. *Nat Neurosci* 3:323–329.
- Jovanovic JN, Sihra TS, Nairn AC, Hemmings Jr HC, Greengard P, Czernik AJ (2001) Opposing changes in phosphorylation of specific sites in synapsin I during Ca^{2+} -dependent glutamate release in isolated nerve terminals. *J Neurosci* 21:7944–7953.
- Kim JJ, Fanselow MS (1992) Modality-specific retrograde amnesia of fear. *Science* 256:675–677.
- Koh YH, Ruiz-Canada C, Gorczyca M, Budnik V (2002) The Ras1-mitogen-activated protein kinase signal transduction pathway regulates synaptic plasticity through fasciclin II-mediated cell adhesion. *J Neurosci* 22:2496–2504.
- Komiyama NH, Watabe AM, Carlisle HJ, Porter K, Charlesworth P, Monti J, Strathdee DJ, O'Carroll CM, Martin SJ, Morris RG, O'Dell TJ, Grant SG (2002) SynGAP regulates ERK/MAPK signaling, synaptic plasticity, and learning in the complex with postsynaptic density 95 and NMDA receptor. *J Neurosci* 22:9721–9732.
- Larson J, Wong D, Lynch G (1986) Patterned stimulation at the theta frequency is optimal for the induction of hippocampal long-term potentiation. *Brain Res* 368:347–350.
- Li L, Chin LS, Shupliakov O, Brodin L, Sihra TS, Hvalby O, Jensen V, Zheng D, McNamara JO, Greengard P, Andersen P (1995) Impairment of synaptic vesicle clustering and of synaptic transmission, and increased seizure propensity, in synapsin I-deficient mice. *Proc Natl Acad Sci USA* 92:9235–9239.
- Lisman JE (1997) Bursts as a unit of neural information: making unreliable synapses reliable. *Trends Neurosci* 20:38–43.
- Malenka RC, Nicoll RA (1999) Long-term potentiation—a decade of progress? *Science* 285:1870–1874.
- Manabe T, Aiba A, Yamada A, Ichise T, Sakagami H, Kondo H, Katsuki M (2000) Regulation of long-term potentiation by *H-ras* through NMDA receptor phosphorylation. *J Neurosci* 20:2504–2511.
- Martin KC, Michael D, Rose JC, Barad M, Casadio A, Zhu H, Kandel ER (1997) MAP kinase translocates into the nucleus of the presynaptic cell and is required for long-term facilitation in *Aplysia*. *Neuron* 18:899–912.
- Martin SJ, Grimwood PD, Morris RG (2000) Synaptic plasticity and memory: an evaluation of the hypothesis. *Annu Rev Neurosci* 23:649–711.
- Mayford M, Wang J, Kandel ER, O'Dell TJ (1995) CaMKII regulates the frequency-response function of hippocampal synapses for the production of both LTD and LTP. *Cell* 81:891–904.
- Morris RG, Garrud P, Rawlins JN, O'Keefe J (1982) Place navigation impaired in rats with hippocampal lesions. *Nature* 297:681–683.
- Otto T, Eichenbaum H, Wiener SI, Wible CG (1991) Learning-related patterns of CA1 spike trains parallel stimulation parameters optimal for inducing hippocampal long-term potentiation. *Hippocampus* 1:181–192.
- Phend KD, Rustioni A, Weinberg RJ (1995) An osmium-free method of epon embedding that preserves both ultrastructure and antigenicity for post-embedding immunocytochemistry. *J Histochem Cytochem* 43:283–292.
- Piedras-Renteria ES, Pyle JL, Diehn M, Glickfeld LL, Harata NC, Cao Y, Kavalali ET, Brown PO, Tsien RW (2004) Presynaptic homeostasis at CNS nerve terminals compensates for lack of a key Ca^{2+} entry pathway. *Proc Natl Acad Sci USA* 101:3609–3614.
- Pieribone VA, Shupliakov O, Brodin L, Hilfiker-Rothenfluh S, Czernik AJ, Greengard P (1995) Distinct pools of synaptic vesicles in neurotransmitter release. *Nature* 375:493–497.
- Powell CM, Schoch S, Monteggia L, Barrot M, Matos MF, Feldmann N, Sudhof TC, Nestler EJ (2004) The presynaptic active zone protein RIM1 alpha is critical for normal learning and memory. *Neuron* 42:143–153.
- Pozzo-Miller LD, Gottschalk W, Zhang L, McDermott K, Du J, Gopalakrishnan R, Oho C, Sheng ZH, Lu B (1999) Impairments in high-frequency transmission, synaptic vesicle docking, and synaptic protein distribution in the hippocampus of BDNF knock-out mice. *J Neurosci* 19:4972–4983.
- Roberts AC, Glanzman DL (2003) Learning in *Aplysia*: looking at synaptic plasticity from both sides. *Trends Neurosci* 26:662–670.
- Rosahl TW, Geppert M, Spillane D, Herz J, Hammer RE, Malenka RC, Sudhof TC (1993) Short-term synaptic plasticity is altered in mice lacking synapsin I. *Cell* 75:661–670.
- Rosahl TW, Spillane D, Missler M, Herz J, Selig DK, Wolff JR, Hammer RE, Malenka RC, Sudhof TC (1995) Essential functions of synapsins I and II in synaptic vesicle regulation. *Nature* 375:488–493.
- Rosen LB, Ginty DD, Weber MJ, Greenberg ME (1994) Membrane depolarization and calcium influx stimulate MEK and MAP kinase via activation of Ras. *Neuron* 12:1207–1221.
- Rudy JW, Barrientos RM, O'Reilly RC (2002) Hippocampal formation supports conditioning to memory of a context. *Behav Neurosci* 116:530–538.
- Schiebeler W, Jahn R, Doucet JP, Rothlein J, Greengard P (1986) Characterization of synapsin I binding to small synaptic vesicles. *J Biol Chem* 261:8383–8390.
- Schikorski T, Stevens CF (1997) Quantitative ultrastructural analysis of hippocampal excitatory synapses. *J Neurosci* 17:5858–5867.
- Schikorski T, Stevens CF (2001) Morphological correlates of functionally defined synaptic vesicle populations. *Nat Neurosci* 4:391–395.
- Schnell E, Nicoll RA (2001) Hippocampal synaptic transmission and plasticity are preserved in myosin Va mutant mice. *J Neurophysiol* 85:1498–1501.
- Selcher JC, Weeber EJ, Christian J, Nekrasova T, Landreth GE, Sweatt JD (2003) A role for ERK MAP kinase in physiologic temporal integration in hippocampal area CA1. *Learn Mem* 10:26–39.
- Sharma SK, Sherff CM, Shobe J, Bagnall MW, Sutton MA, Carew TJ (2003) Differential role of mitogen-activated protein kinase in three distinct phases of memory for sensitization in *Aplysia*. *J Neurosci* 23:3899–3907.
- Silva AJ, Rosahl TW, Chapman PF, Marowitz Z, Friedman E, Frankland PW,

- Cestari V, Cioffi D, Sudhof TC, Bourtschuladze R (1996) Impaired learning in mice with abnormal short-lived plasticity. *Curr Biol* 6:1509–1518.
- Tsodyks MV, Markram H (1997) The neural code between neocortical pyramidal neurons depends on neurotransmitter release probability. *Proc Natl Acad Sci USA* 94:719–723.
- Tyler WJ, Pozzo-Miller LD (2001) BDNF enhances quantal neurotransmitter release and increases the number of docked vesicles at the active zones of hippocampal excitatory synapses. *J Neurosci* 21:4249–4258.
- Tyler WJ, Alonso M, Bramham CR, Pozzo-Miller LD (2002) From acquisition to consolidation: on the role of brain-derived neurotrophic factor signaling in hippocampal-dependent learning. *Learn Mem* 9:224–237.
- Varela JA, Sen K, Gibson J, Fost J, Abbott LF, Nelson SB (1997) A quantitative description of short-term plasticity at excitatory synapses in layer 2/3 of rat primary visual cortex. *J Neurosci* 17:7926–7940.
- Watanabe S, Hoffman DA, Migliore M, Johnston D (2002) Dendritic K^+ channels contribute to spike-timing dependent long-term potentiation in hippocampal pyramidal neurons. *Proc Natl Acad Sci USA* 99:8366–8371.
- Winder DG, Martin KC, Muzzio IA, Rohrer D, Chruscinski A, Kobilka B, Kandel ER (1999) ERK plays a regulatory role in induction of LTP by theta frequency stimulation and its modulation by beta-adrenergic receptors. *Neuron* 24:715–726.
- Wisden W, Errington ML, Williams S, Dunnett SB, Waters C, Hitchcock D, Evan G, Bliss TVP, Hunt SP (1990) Differential expression of immediate early genes in the hippocampus and spinal cord. *Neuron* 4:603–614.
- Xu B, Gottschalk W, Chow A, Wilson RI, Schnell E, Zang K, Wang D, Nicoll RA, Lu B, Reichardt LF (2000) The role of brain-derived neurotrophic factor receptors in the mature hippocampus: modulation of long-term potentiation through a presynaptic mechanism involving TrkB. *J Neurosci* 20:6888–6897.
- Yuan LL, Adams JP, Swank M, Sweatt JD, Johnston D (2002) Protein kinase modulation of dendritic K^+ channels in hippocampus involves a mitogen-activated protein kinase pathway. *J Neurosci* 22:4860–4868.
- Zakharenko SS, Patterson SL, Dragatsis I, Zeitlin SO, Siegelbaum SA, Kandel ER, Morozov A (2003) Presynaptic BDNF required for a presynaptic but not postsynaptic component of LTP at hippocampal CA1-CA3 synapses. *Neuron* 39:975–990.
- Zhang X, Poo MM (2002) Localized synaptic potentiation by BDNF requires local protein synthesis in the developing axon. *Neuron* 36:675–688.
- Zhu JJ, Qin Y, Zhao M, Van Aelst L, Malinow R (2002) Ras and Rap control AMPA receptor trafficking during synaptic plasticity. *Cell* 110:443–455.
- Zucker RS, Regehr WG (2002) Short-term synaptic plasticity. *Annu Rev Physiol* 64:355–405.

Chapter 3

Kinase activity is not required for α CaMKII-dependent presynaptic plasticity at hippocampal CA3-CA1 synapses

Published in

Nature Neuroscience 2007 September 10(9): 1125-1127

Kinase activity is not required for α CaMKII-dependent presynaptic plasticity at CA3-CA1 synapses

Mohammad Reza Hojjati^{1,2}, Geeske M van Woerden¹, William J Tyler^{3,6}, Karl Peter Giese⁴, Alcino J Silva⁵, Lucas Pozzo-Miller³ & Ype Elgersma^{1,5}

Using targeted mouse mutants and pharmacologic inhibition of α CaMKII, we demonstrate that the α CaMKII protein, but not its activation, autophosphorylation or its ability to phosphorylate synapsin I, is required for normal short-term presynaptic plasticity. Furthermore, α CaMKII regulates the number of docked vesicles independent of its ability to be activated. These results indicate that α CaMKII has a nonenzymatic role in short-term presynaptic plasticity at hippocampal CA3-CA1 synapses.

The α isoform of Ca^{2+} /calmodulin-dependent protein kinase II (α CaMKII) was originally identified as synapsin I kinase¹. Subsequent studies showed that α CaMKII is abundantly associated with presynaptic vesicles by binding to synapsin I (ref. 2). Together with the observation that α CaMKII is one of the most abundant proteins of the hippocampus³, these results suggest that α CaMKII also has a nonenzymatic function, but such a function has not directly been demonstrated yet. Analysis of α CaMKII knockout (KO) mice confirmed a presynaptic role for α CaMKII in short-term presynaptic plasticity^{4,5}, but these experiments did not address whether this role is mediated by α CaMKII as a kinase, as a structural protein, or as both.

To study the enzymatic requirements of α CaMKII in presynaptic plasticity, we used four different lines of α CaMKII mutants. Autophosphorylation at the threonine 286 (T286) and T305/T306 sites was prevented by using α CaMKII-T286A (T286 is mutated to alanine) mice, which lack α CaMKII autonomous (Ca^{2+} /CaM independent) activity⁶, and α CaMKII-T305V/T306A (T305 and T306 are mutated to valine and alanine, respectively) mice, which lack α CaMKII inhibitory autophosphorylation⁷. Furthermore, we used α CaMKII-T305D (T305 is mutated to an aspartic acid) mice, in which constitutive autophosphorylation at the T305 site in the Ca^{2+} /CaM domain is mimicked, preventing α CaMKII in these mice from becoming activated⁷. The fourth line (α CaMKII-KO) lacks the entire α CaMKII protein⁷ (for an overview of all phenotypes see⁸).

Because these mutants were backcrossed in C57BL/6, we first tested whether the originally reported long-term potentiation (LTP) deficits

(in hybrid 129Sv/C57BL/6 mice) were still present^{6,7,9}. We confirmed that α CaMKII activation and its subsequent autophosphorylation at T286 are absolute requirements for LTP, but that loss of α CaMKII can partially be compensated for (Supplementary Fig. 1 online). In contrast, loss of inhibitory phosphorylation in α CaMKII-T305V/T306A mice reduced the threshold for LTP induction as reported previously⁷ (Supplementary Fig. 1). Western blots of isolated synaptosomes of all the mutants did not reveal changes in the levels of the β , γ and δ CaMKII isoforms, nor was the amount of calmodulin affected in these mutants (Supplementary Fig. 2 online).

We looked at the ability of these mutants to phosphorylate synapsin I at serine 603 (S603, site 3), which is an exclusive CaMKII site. α CaMKII-KO mice showed a marked decrease of synapsin I phosphorylation compared to wild-type mice ($P < 0.001$, ANOVA, Fig. 1), suggesting that none of the other CaMKII isoforms could efficiently compensate for the loss of α CaMKII phosphorylation of synapsin I *in vivo*. Notably, steady-state levels of phosphorylated synapsin I were not affected in α CaMKII-T286A ($P = 0.2$) mice and in α CaMKII-T305V/T306A mice ($P = 0.3$), indicating that loss of autonomous activity or self-inhibition does not have a large effect on synapsin I phosphorylation *in vivo*. In contrast, activation of α CaMKII is an absolute requirement for synapsin I phosphorylation, as S603 phosphorylation in the α CaMKII-T305D mutant was not significantly

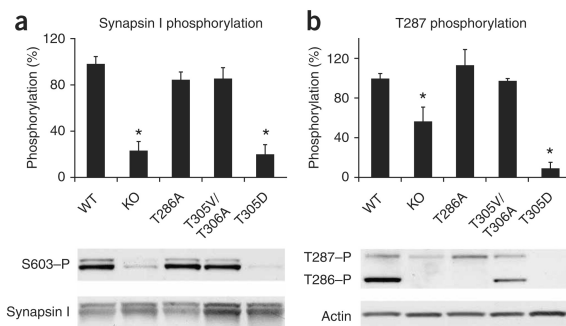


Figure 1 Phosphorylation of synapsin I and CaMKII-T286/T287 in synaptosomes obtained from α CaMKII mutants. (a) Phosphorylation of synapsin I S603 was not affected by impaired α CaMKII autophosphorylation, but required α CaMKII protein and its activation by Ca^{2+} /calmodulin. (b) Phosphorylation of α CaMKII-T286 and β CaMKII-T287 was absent in α CaMKII-T305D mice. Graph represents data from β CaMKII-T287 only. Error bars indicate s.e.m. Each sample contains pooled fractions from four independent isolations.

¹Department of Neuroscience, Erasmus University Medical Center, Dr. Molewaterplein 50, 3015 GE Rotterdam, The Netherlands. ²Department of Physiology, Shahrekord University of Medical Sciences, Kashani Blvd, Shahrekord 88155, Iran. ³Department of Neurobiology, McKnight Brain Institute, Civitan International Research Center, University of Alabama at Birmingham, Birmingham, Alabama 35294-2182, USA. ⁴Institute of Psychiatry, King's College London, 125 Coldharbour Lane, London SE59NU, UK. ⁵Departments of Neurobiology, Psychiatry and Psychology, Brain Research Institute, 695 Charles Young Drive South, University of California, Los Angeles, California 90095-1761, USA. ⁶Present address: Arizona State University, School of Life Sciences, 1711 South Rural Road, Tempe, Arizona 85287, USA. Correspondence should be addressed to Y.E. (y.elgersma@erasmusmc.nl).

above background level ($P = 0.2$; **Fig. 1a**). The dominant-negative nature of the α CaMKII-T305D mutation was further illustrated by the fact that this was also the only mutant in which autophosphorylation at both α CaMKII-T286 and β CaMKII-T287 was indistinguishable from background level (both $P > 0.8$; **Fig. 1b**), further suggesting that α CaMKII is inactive in this mutant. Taken together, these results show that these mutants provide an ideal tool for dissecting the requirements of α CaMKII activation, α CaMKII autophosphorylation and synapsin I S603 phosphorylation in short-term presynaptic plasticity.

Previous studies from multiple laboratories^{4,5,8}, using independently generated targeted deletions of α CaMKII^{5,9}, have demonstrated that the loss of α CaMKII results in enhanced augmentation and decreased synaptic fatigue, which are both measures of presynaptic plasticity. Augmentation is an increase in the evoked postsynaptic response that is observed several seconds after high-frequency afferent stimulation, caused by facilitated exocytosis¹⁰. We measured augmentation at hippocampal CA3-CA1 synapses using extracellular field recording (**Supplementary Methods** online). α CaMKII-KO mice showed a striking increase in synaptic augmentation (during 3–11 s: $F_{4,92} = 13$, $P < 0.0001$, repeated measures ANOVA; **Fig. 2**), confirming that α CaMKII critically regulates this form of presynaptic plasticity⁴. Activation of presynaptic α CaMKII may be important in synaptic augmentation, as transiently elevated presynaptic calcium is thought to be a major factor underlying this process. However, although α CaMKII activity is regulated by autophosphorylation, augmentation was not affected in the T286A and T305V/T306A autophosphorylation-deficient mutants (**Fig. 2c**). The lack of a phenotype in these mutants could reflect the short-term nature of this kind of plasticity, and/or the fact that phosphorylation of synapsin I S603 was unaffected in these mutants (**Fig. 1**). Unexpectedly however, augmenta-

tion was also unaffected in α CaMKII-T305D mutants ($P = 0.5$, ANOVA; **Fig. 2b,c**), where α CaMKII activation was blocked and synapsin I phosphorylation was absent (**Fig. 1**). These results strongly suggest that synaptic augmentation does not depend on the ability of α CaMKII to phosphorylate synapsin I, nor on the activation of α CaMKII.

Because activation of both α CaMKII and β CaMKII seem to be impaired in the α CaMKII-T305D mutant (**Fig. 1b**), we would expect that a similar result should be obtained if the augmentation experiment is carried out in the presence of the membrane-permeable CaMKII inhibitor KN-93 (ref. 11). This inhibitor competes with Ca^{2+} /calmodulin binding and therefore prevents activation of both α CaMKII and β CaMKII. LTP experiments in the presence of this inhibitor showed that KN-93 was indeed able to block LTP (**Supplementary Fig. 1**). In contrast, we observed similar levels of augmentation in the presence of KN-93 or its inactive analog KN-92 ($P = 0.5$, ANOVA; **Fig. 2c**), confirming that CaMKII activation is not required for normal augmentation.

Our biochemical analyses (**Fig. 1**) indicated that CaMKII activity in the α CaMKII-T305D mutant was reduced to such an extent that phosphorylation of CaMKII substrates was undetectable. If CaMKII activity is indeed not required for augmentation, the potent CaMKII inhibitor AIP-II (autocamtide-2-related inhibitory peptide II) should not affect augmentation either. This inhibitor is 500 times more potent than KN-93, and it is noncompetitive for Ca^{2+} /calmodulin and exogenous substrates, thus also blocking basal and autonomously active CaMKII¹². Efficient penetration was achieved by making use of AIP that was fused to the antennapedia transport peptide, and by preincubating slices for 1 h with AIP (see **Supplementary Methods**). Indeed, LTP was fully blocked, indicating that the drug was able to penetrate the slice (**Supplementary Fig. 1**), and notably, Ant-AIP-II showed no

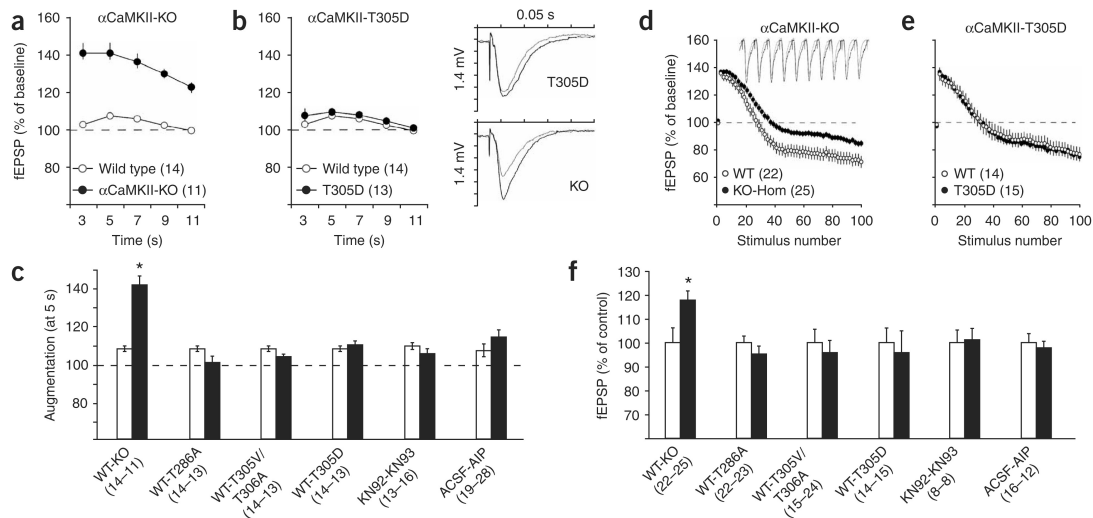


Figure 2 Presynaptic short-term plasticity requires α CaMKII protein, but not its autophosphorylation, activation or activity. (**a–c**) Increased synaptic augmentation in α CaMKII-KO mutant mice was not caused by the lack of CaMKII kinase activity. fEPSP responses (normalized to pretetanus baseline) of CaMKII-KO (**a**) and CaMKII-T305D (**b**) mice were recorded at the indicated time after a 10 theta-burst tetanus. Traces are from baseline response (gray) and the response 5 s post-tetanus (black). Augmentation summary of responses obtained 5 s post-tetanus normalized to baseline is shown in **c**. Black bars represent mutants or drug-treated slices, white bars represent control slices as indicated. (**d–f**) Decreased synaptic fatigue during repetitive stimulation in α CaMKII-KO mice was not caused by the lack of α CaMKII kinase activity. (**d,e**) fEPSP responses (normalized against baseline) of CaMKII-KO (**d**) and CaMKII-T305D (**e**) mice were recorded during a 10-Hz tetanus. Only the first and even numbered stimuli are shown for clarity. Traces are from wild-type (gray) and α CaMKII-KO slices (black) recorded from stimulus number 21–30. Depletion summary of the last (100) stimulus of the 10-Hz train is shown in **f**. Black bars represent mutant or drug-treated slices, normalized against the controls as indicated (white bars, set at 100%). Numbers between brackets indicate the number of slices. Error bars indicate s.e.m.

discernable effect on synaptic transmission (Supplementary Fig. 3 online), which makes it suitable for use in these experiments. However, like KN-93, Ant-AIP-II did not affect augmentation ($P = 0.1$, ANOVA; Fig. 2c). Taken together, these results indicate that α CaMKII protein, but not α CaMKII activity, is required for normal augmentation.

Previous whole-cell patch-clamp recordings in CA3-restricted α CaMKII-KO mice showed a substantial enhancement of the excitatory postsynaptic current amplitude during repetitive stimulation of CA3-CA1 synapses⁵, suggesting that the fatigue rate of neurotransmitter release is regulated by α CaMKII. Likewise, extracellular field recordings from our global α CaMKII-KO mice also demonstrated reduced synaptic fatigue (Fig. 2d). The responses to repetitive 10-Hz stimulation reveal the competing processes of facilitation, vesicle depletion and vesicle mobilization¹⁰. α CaMKII-KO mutants had a similarly shaped curve as wild-type mice; however, there was a significant effect of genotype ($F_{1,45} = 4.5$, $P < 0.05$) and a significant interaction between genotype and stimulus number ($F_{99,4455} = 4.5$, $P < 0.0001$). α CaMKII-KO mutants were only significantly different from wild-type mice after 20 stimuli (first 20: $F_{19,855} = 1.2$, $P = 0.3$; last 80: $F_{79,3555} = 2.6$, $P < 0.001$), suggesting a differential rate of vesicle depletion and/or mobilization, the cellular processes primarily responsible for the maintenance of excitatory postsynaptic potential (EPSP) amplitude during prolonged stimulation¹⁰.

To test the α CaMKII autophosphorylation and synapsin I phosphorylation requirements in this presynaptic measure, we repeated this experiment in the α CaMKII point mutants. No significant effect of genotype was observed in either α CaMKII-T286A or α CaMKII-T305V/T306A autophosphorylation-defective mutants (both $P > 0.3$, ANOVA at stimulus number 100; Fig. 2f). Notably, the depletion rate was also not affected in α CaMKII-T305D mutants ($P > 0.7$; Fig. 2e,f), in which activation of α CaMKII was prevented and phosphorylation of synapsin I was absent. In addition, there was no discernable effect on depression in slices treated with KN-93 or Ant-AIP-II ($P = 0.9$ and $P = 0.7$, respectively; Fig. 2f). Taken together, these data strongly suggest that the α CaMKII protein plays a structural role rather than an enzymatic role, during this form of short-term presynaptic plasticity.

Mechanistically, enhanced synaptic augmentation and reduced synaptic depression could reflect changes in the pool sizes of the synaptic vesicles, in particular the size of the readily releasable pool (RRP). Therefore, we used electron microscopy to measure the number of docked vesicles, a morphological correlate of the RRP^{13,14}. We obtained measurements at the active zone of excitatory synapses on CA1 spines of wild-type, α CaMKII-KO and α CaMKII-T305D mice. Indeed, there was a significant effect of genotype ($F_{2,41} = 4.7$, $P < 0.05$), with synapses in α CaMKII-KO mice showing a 20% increase in the total number of docked vesicles compared with wild-type (Fisher's PLSD, $P < 0.05$) or α CaMKII-T305D mice ($P < 0.01$) (Fig. 3a). In contrast, no significant difference in the number of docked vesicles was observed between the α CaMKII-T305D mutant and wild-type mice (Fisher's PLSD, $P = 0.24$). Additional measurements of the number of reserve pool vesicles, active zone length and presynaptic terminal area were similar between the mutants and wild-type mice (all measures $P > 0.2$; Supplementary Fig. 4 online). Thus, the absence of α CaMKII protein results in an increased number of docked vesicles, whereas the loss of α CaMKII activation and synapsin I S603 phosphorylation does not affect vesicle docking.

Together, these results suggest a model in which α CaMKII functions nonenzymatically to limit the size of the RRP, thereby modulating short-term presynaptic plasticity. If the observed increase in the size of EPSPs during repetitive stimulation in α CaMKII-KO mice is indeed mediated by a larger RRP, then presynaptic function should be normal

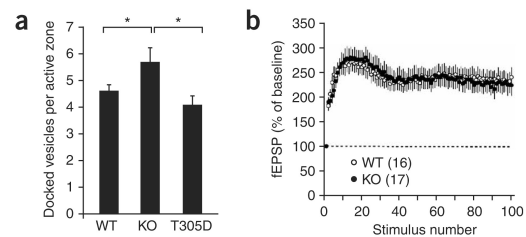


Figure 3 α CaMKII protein regulates the number of docked vesicles. (a) Quantitative electron microscopy of asymmetric synapses on dendritic spines of CA1 pyramidal neurons showed a 20% increase in the number of docked vesicles in α CaMKII-KO mice. (b) Decreasing the depletion rate by lowering extracellular calcium reversed the phenotype of the α CaMKII-KO mice during repetitive stimulation. Error bars indicate s.e.m.

under conditions that minimize depletion of the RRP. Accordingly, we decreased the extracellular calcium concentration, which limits the rate of depletion from the RRP¹⁵. Decreasing the extracellular calcium concentration from 2.5 to 0.8 mM normalized the responses during 10-Hz stimulation in α CaMKII-KO mice ($F_{1,31} < 0.0001$, $P = 1$, Fig. 3b), supporting the idea that α CaMKII limits the available pool of readily-releasable neurotransmitter vesicles.

Taken together, our experiments suggest that synapsin I S603 phosphorylation and α CaMKII activity are not required for short-term presynaptic plasticity measures such as augmentation and synaptic fatigue during repetitive stimulation. Specifically, we have demonstrated that, at hippocampal CA3-CA1 synapses, α CaMKII functions independently of its kinase activity to modulate short-term presynaptic plasticity by limiting the number of presynaptic docked neurotransmitter vesicles.

Note: Supplementary information is available on the Nature Neuroscience website.

ACKNOWLEDGMENTS

We greatly appreciate the help of H. Beck, M. Merckens, R. Anwyl, K. Wang and R. Colbran for their (hands-on) advice on the use of CaMKII inhibitors, and from G. Borst and S. Kushner and members of the Silva and Elgersma lab for stimulating discussions and critically reading the manuscript. We thank M. Elgersma, H. van der Burg and E. Phillips for technical support. This work was supported by grants from NWO-ZonMW (TOP, VIDI) and Neuro-BSIK to Y.E. We also thank the University of Alabama, Birmingham Neuroscience Cores (P30-NS47466, P30-HD38985, P30-NS57098).

COMPETING INTERESTS STATEMENT

The authors declare no competing financial interests.

Published online at <http://www.nature.com/natureneuroscience>

Reprints and permissions information is available online at <http://npg.nature.com/reprintsandpermissions>

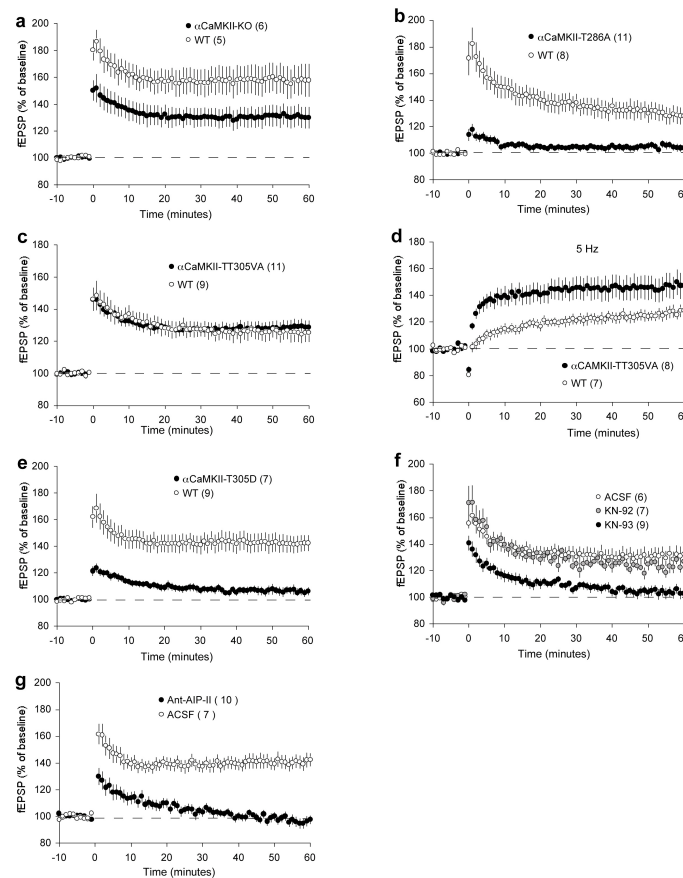
- Bennett, M.K., Erond, N.E. & Kennedy, M.B. *J. Biol. Chem.* **258**, 12735–12744 (1983).
- Benfenati, F. *et al. Nature* **359**, 417–420 (1992).
- Erond, N.E. & Kennedy, M.B. *J. Neurosci.* **5**, 3270–3277 (1985).
- Chapman, P.F., Frenguelli, B.G., Smith, A., Chen, C.M. & Silva, A.J. *Neuron* **14**, 591–597 (1995).
- Hinds, H.L., Goussakov, I., Nakazawa, K., Tonegawa, S. & Bolshakov, V.Y. *Proc. Natl. Acad. Sci. USA* **100**, 4275–4280 (2003).
- Giese, K.P., Fedorov, N.B., Filipkowski, R.K. & Silva, A.J. *Science* **279**, 870–873 (1998).
- Elgersma, Y., Sweatt, J.D. & Giese, K.P. *J. Neurosci.* **24**, 8410–8415 (2004).
- Silva, A.J., Stevens, C.F., Tonegawa, S. & Wang, Y. *Science* **257**, 201–206 (1992).
- Zucker, R.S. & Regehr, W.G. *Annu. Rev. Physiol.* **64**, 355–405 (2002).
- Sumi, M. *et al. Biochem. Biophys. Res. Commun.* **181**, 968–975 (1991).
- Ishida, A., Kameshita, I., Okuno, S., Kitani, T. & Fujisawa, H. *Biochem. Biophys. Res. Commun.* **212**, 806–812 (1995).
- Schikorski, T. & Stevens, C.F. *Nat. Neurosci.* **4**, 391–395 (2001).
- Tyler, W.J. & Pozzo-Miller, L.D. *J. Neurosci.* **21**, 4249–4258 (2001).
- Borst, J.G. & Sakmann, B. *Nature* **383**, 431–434 (1996).

Supplementary Data

Kinase activity is not required for CaMKII-dependent presynaptic plasticity at hippocampal CA3-CA1 synapses

Mohammad Reza Hojjati, Geeske M. van Woerden, William J. Tyler, Karl Peter Giese, Alcino J. Silva, Lucas Pozzo-Miller and Ype Elgersma

Supplementary Figure 1



Supplementary Fig. 1. Long-term potentiation at Schaffer Collateral CA1 synapses in α CaMKII mutant mice after back-crossing in C57BL6 (**a-e**)

and in pharmacologically treated wild-type slices (**f,g**). LTP in all experiments was induced by four bursts of high frequency stimulation (four stimuli at 100 Hz), each burst separated by 200 ms, except in (**d**) in which LTP was induced by 150 stimuli at 5 Hz.

(**a**) LTP is reduced but not absent in α CaMKII-KO mice, as observed previously^(7,9,19).

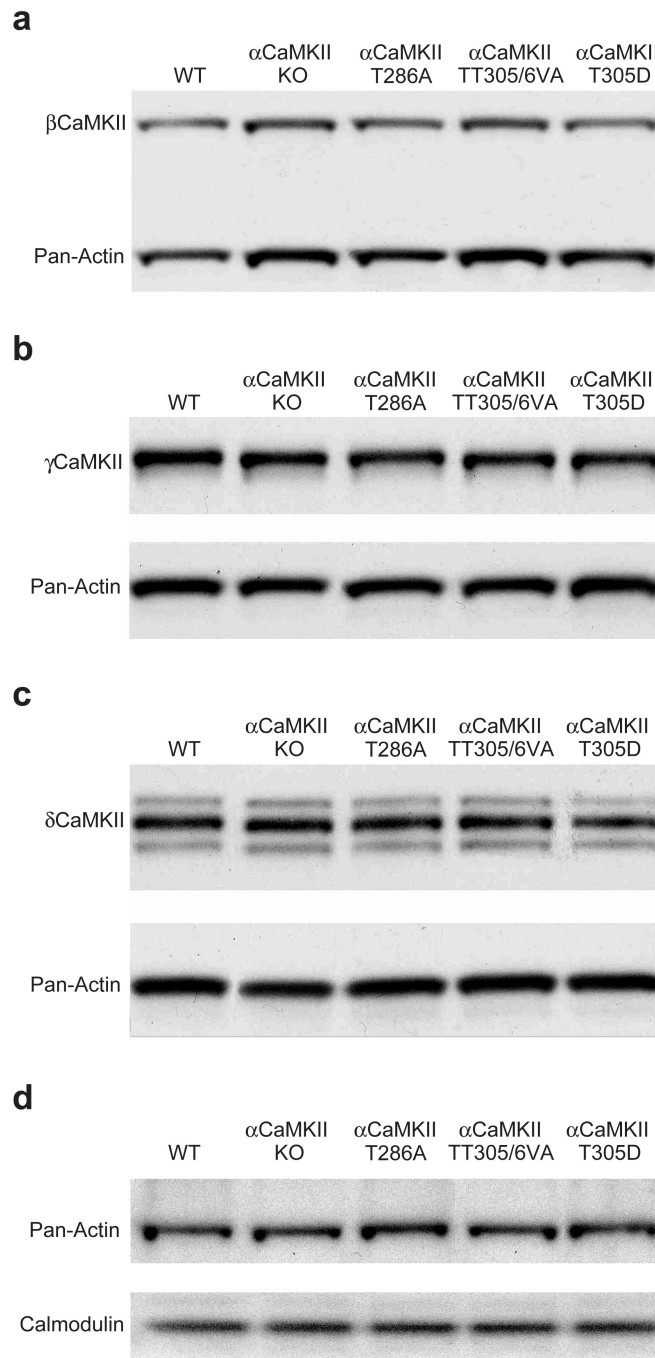
(**b,e**) LTP is absent in α CaMKII-T286A and T305D mice, as reported previously^(6,7).

(**c,d**) LTP in α CaMKII-TT305/6VA mice is normal upon strong stimulation (4 theta burst LTP) but increased upon weak stimulation (5Hz), consistent with previous findings^(7,20).

(**f,g**) LTP is blocked in wild-type slices in presence of CaMKII inhibitor KN93 (**f**) and Ant-AIP-II (**g**).

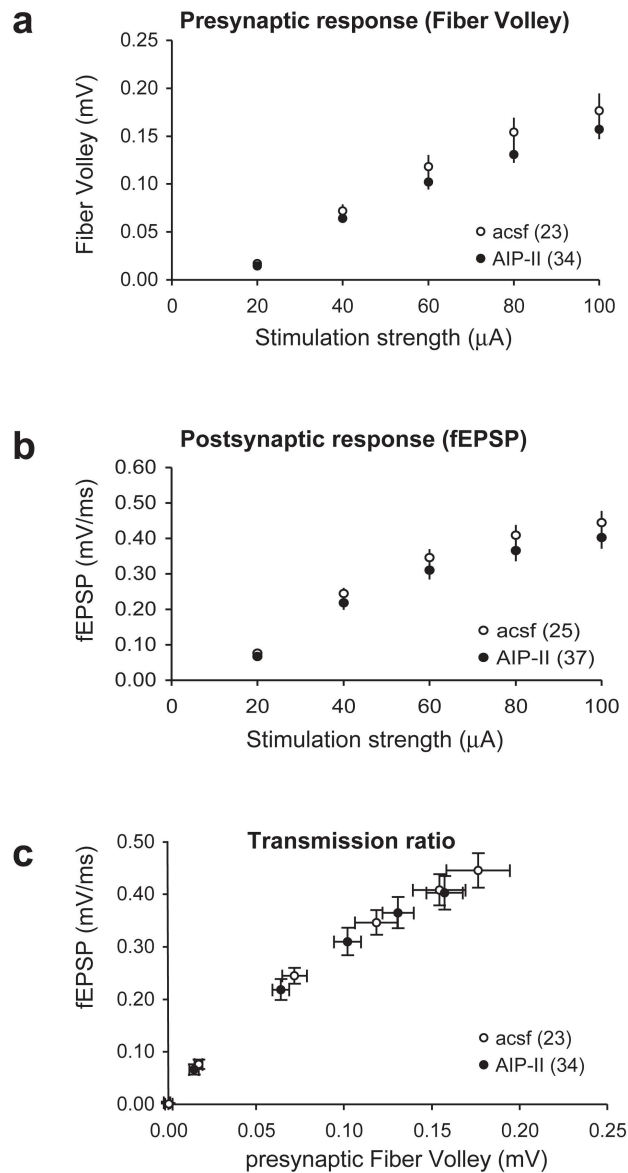
Error bars represent SEM. Numbers between brackets refer to the number of slices used. See **Supplementary methods** for cited references.

Supplementary Figure 2



Supplementary Fig. 2. No changes in synaptic β CaMKII, γ CaMKII, δ CaMKII and Calmodulin in α CaMKII-KO mutants or point mutants. Synaptosomes were isolated as described (**Supplementary methods**), and analyzed by Western blotting. Each sample contains pooled fractions from 4 independent isolations.

Supplementary Figure 3



Supplementary Fig. 3. Synaptic transmission is not affected by Ant-AIP-II.

(a) Presynaptic excitability is not significantly affected by Ant-AIP-II

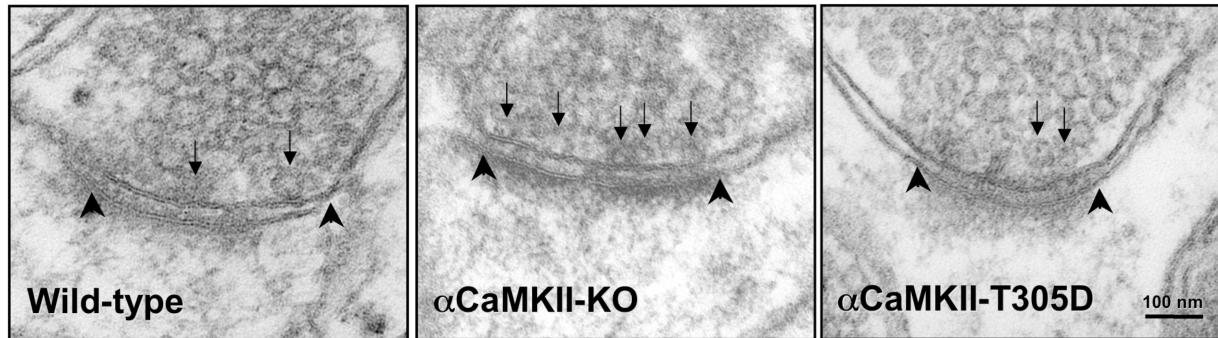
($F_{1,55}=1.4$; $p=0.24$ Repeated Measures ANOVA) .

(b) Postsynaptic fEPSP responses are not affected by Ant-AIP-II ($F_{1,60}=0.9$; $p=0.34$).

(c) Overall synaptic transmission (fEPSP as function of the presynaptic fiber volley) is unaffected by Ant-AIP-II, in agreement with previous findings⁽²¹⁾.

Error bars represent SEM. See **Supplementary methods** for cited references.

Supplementary Figure 4



Measure	Wild-Type	α CaMKII-KO	α CaMKII-T305D
Active zone (AZ) length (nm)	234 \pm 10	242 \pm 26	190 \pm 15
Terminal area	138 \pm 15	158 \pm 18	112 \pm 19
Reserve pool vesicles	40 \pm 4	47 \pm 5	37 \pm 5
Reserve pool vesicles/area	309 \pm 21	306 \pm 15	365 \pm 40
Docked vesicles/AZ	4.6 \pm 0.2	5.6\pm0.5	4.0 \pm 0.3
Docked vesicles μ m	20 \pm 0.7	24\pm1.3	21 \pm 1.2

Supplementary Fig. 4. Quantitative electron microscopy of asymmetric synapses on dendritic spines of CA1 pyramidal neurons. α CaMKII-KO have more docked vesicles at the active zone than wild-type mice and α CaMKII-T305D mice. Arrowheads denote the lateral boundaries of the postsynaptic density, which was used to define the active zone across the synaptic cleft. Arrows show examples of vesicles counted as docked (see Methods for their definition). Statistical differences ($p < 0.05$ compared to wild-type mice) are printed in bold. All values are mean \pm SEM.

Supplementary Materials and Methods

Animals

To study the role of presynaptic α CaMKII, we made use of a α CaMKII mutant, in which α CaMKII exon 2 is deleted⁷. Exon 2 encodes the catalytic site, and deletion of this exon results in a premature translation stop due to a frame shift, thus effectively resulting in a α CaMKII knock-out (KO) line⁷. To study the role of autophosphorylation and activity of α CaMKII, we made use of three different mutants in which the endogenous α CaMKII was mutated using ES cell-mediated gene targeting. In the first mutant (T286A), α CaMKII Thr286 is substituted by alanine⁶. This mutation results in a kinase that is unable to switch to its Ca^{2+} /CaM-independent state. In the α CaMKII TT305/306VA mutant, α CaMKII Thr305 and Thr306 are substituted by non-phosphorylatable amino acids (respectively, Valine and Alanine) to block inhibitory autophosphorylation⁷. In the α CaMKII-T305D mutant, Thr305 is substituted by negative charged Aspartate. This mimics persistent Thr305 phosphorylated α CaMKII, which interferes with Ca^{2+} /CaM binding, thus blocking α CaMKII activation in this mutant⁷. For a review of previous reported phenotypes see⁹.

All mice were obtained by breeding heterozygous parents. Littermate control animals were used for every experiment except for augmentation. For augmentation we combined the littermate wild-type animals of the various genotypes since they were indistinguishable. All mutants described in this paper were homozygous for the mutation unless specified otherwise. To allow for direct comparison with previously published experiments, we made use of hybrid F2, 129SvJ-C57BL/6 animals for augmentation experiments and C57BL/6 (backcrossed at least 8 times) animals for all other experiments. For experiments using CaMKII inhibitors we used wild-type mice in the appropriate (see above) background. All experiments were approved by a Dutch ethical committee (DEC) for animal research.

Slice preparation and electrophysiological recordings

Electrophysiology experiments were performed on mice between the ages of 2 and 5 months and all experiments and analysis were performed blind to genotype. After the animals had been sacrificed, hippocampi were removed in ice-cold artificial cerebrospinal fluid (ACSF), and sagittal hippocampal slices (400 μm) were prepared using a vibratome. Normal hippocampal slices and hippocampal minislices (from which the CA3 area was removed) were maintained in artificial cerebrospinal fluid (ACSF) at room temperature for at least 1.5 hour to recover before experiments were initiated. Then they were transferred to a submerged chamber field recording set-up and perfused continuously at a rate of 2mL/minute with ACSF equilibrated with 95% O_2 , 5% CO_2 at 30°C. ACSF contained (in mM) 120 NaCl, 3.5 KCl, 2.5 CaCl_2 , 1.3 MgSO_4 , 1.25 NaH_2PO_4 , 26 NaHCO_3 and 10 D-glucose. For the low-calcium experiment (**Fig. 3**), the calcium concentration was reduced to 0.8 mM. Extracellular recording of field excitatory postsynaptic potentials (fEPSPs) were started 20 minutes after transfer to the recording chamber (except for the CaMKII inhibitor studies, see below), and made in CA1 *striatum radiatum* area with a Pt/Ir recording electrode (FHC, Bowdoinham, ME). A bipolar Pt/Ir electrode was used to stimulate Schaffer collateral/commissural afferents with a stimulus duration of 100 μs . Stimulus response curves were obtained at the beginning of each experiment and these were not different between mutants. Subsequent stimulation was performed at 1/3 of the maximum response. A stable baseline was recorded before the onset of each experiment. Similar to the previous study⁴, we used a 10 theta-burst stimulation protocol in the presence of D-APV (2-amino-5-phosphonovalerate, 50 μM , Tocris) to measure synaptic augmentation. The 10 Hz experiments were done in the presence of D-APV and picrotoxin (100 μM , Tocris), and on mini-slices in which CA3 area was removed to prevent epileptic discharges. The input/output curves of **Supplementary fig. 3** were obtained in the presence of D-APV, prior to recording augmentation.

KN92, KN93 (10 μM) and Ant-AIP-II (4 μM) were obtained from Calbiochem. Experiments using CaMKII inhibitors were performed at 32°C with a perfusion rate of 5–6 mL/minute. These slices were pre-incubated with the drug under these conditions in the recording chamber for at least 1 hour before the experiment was started. Control slices were treated in the same way, except that either no drug or KN92 was present. The efficacy of KN93 and AIP was tested by their ability to impair LTP induction (**Supplementary figure 1**). All LTP experiments were performed at a stimulation strength 2/3 of maximum.

Analysis of presynaptic vesicle distribution

The size of the readily releasable pool (RRP) was estimated by quantitative electron microscopy of asymmetric synapses on dendritic spines of CA1 pyramidal neurons. We quantified the number of clear, round synaptic vesicles in contact and within one vesicle diameter from the presynaptic active zone. This morphologically defined set of vesicles is thought to correlate with the readily-releasable pool of quanta^{13,16,17}. We used a random sampling method from single thin sections as described¹⁴, since we previously showed that data obtained with this method correlates well with an unbiased serial sectioning approach¹⁸. Only complete profiles of nonperforated asymmetric synapses on dendritic spines within *striatum radiatum* of area CA1 were photographed. The parameters measured in each synapse were: (1) the length of the active zone; (2) presynaptic terminal area, (3) total number of small (~50 nm) clear and round synaptic vesicles per terminal; and (4) the number of docked vesicles per active zone. The docked vesicles are defined as those up to one-vesicle-diameter (~50 nm) distance from the active zone, according to criteria developed by Reese and colleagues¹⁶, because these vesicles have been shown to be depleted during sustained, repetitive activity. For the synaptic sizes (active zone length, terminal bouton area) we quantified 70 wt, 53 CaMKII-KO and 54 T305D synapses (from 2 mice of every genotype). For the vesicle distribution analysis we quantified 21/13/10 synapses respectively. This method was previously validated by comparing it to serial sectioning¹⁸.

Western blot analysis

Synaptosomes were isolated as described previously⁷. The concentration of the synaptosomes was adjusted to 1 mg/ml. Western blots were probed with antibodies directed against Thr286/287- α/β -CaMKII (#06-881, 1:5000; Upstate Cell Signaling Solutions), Anti-Phospho-Ser603 Synapsin I (p1560-603, 1:1000; PhosphoSolutions), Synapsin I (AB1543P, 1:10,000; Chemicon), β CaMKII (CB- β 1, 1:2000; Zymed), δ CaMKII (sc-5392, 1:200; Santa Cruz), γ CaMKII (sc-1541, 1:1000; Santa Cruz) Calmodulin (#465, 1:500, Swant) and Actin (MAB1501R, 1:2000; Chemicon). Blots were first probed with the antibody of interest and after stripping (Restore western blot stripping buffer; Pierce) re-probed with the loading control antibody. Western blots were quantified using NIH-Image.

Data analysis and statistics

The experimenter was blind to the genotype until the experiment and analysis were completed. Error bars in graph indicate the standard error of mean. Sample size numbers in the graphs indicate the number of slices, and this number was also used for statistical comparisons. ANOVA's were used for morphological studies and for determining the augmentation (5 seconds after the tetanus) and for determining the depletion (at the 100th stimulus). Repeated measures ANOVA were used for statistical analysis of the synaptic transmission curves, and for the entire augmentation and 10Hz curves, followed by a post-hoc Fisher's PLSD analysis if necessary.

Compromise Power Analyses was performed to determine the statistical power of the morphological studies using G*Power (Erdfelder E, et al (1996) GPOWER: A general power analysis program. Behavior Research Methods, Instruments, and Computers 28:1-11). This analysis gave values of statistical power larger than 0.95 (i.e. 95% confidence of accepting the null hypothesis when it is true).

Literature cited

1. Bennett, M.K., Erondy, N.E. & Kennedy, M.B. *J. Biol. Chem.* **258**, 12735-44 (1983).
2. Benfenati, F. *et al. Nature* **359**, 417-20 (1992).
3. Erondy, N.E. & Kennedy, M.B. *J Neurosci* **5**, 3270-7 (1985).
4. Chapman, P.F., Frenguelli, B.G., Smith, A., Chen, C.M. & Silva, A.J. *Neuron* **14**, 591-7 (1995).
5. Hinds, H.L., Goussakov, I., Nakazawa, K., Tonegawa, S. & Bolshakov, V.Y. *Proc Natl Acad Sci U S A* **100**, 4275-80 (2003).
6. Giese, K.P., Fedorov, N.B., Filipkowski, R.K. & Silva, A.J. *Science* **279**, 870-3 (1998).
7. Elgersma, Y. *et al. Neuron* **36**, 493-505 (2002).
8. Silva, A.J., Stevens, C.F., Tonegawa, S. & Wang, Y. *Science* **257**, 201-6 (1992).
9. Elgersma, Y., Sweatt, J.D. & Giese, K.P. *J Neurosci* **24**, 8410-5 (2004).
10. Zucker, R.S. & Regehr, W.G. *Annu Rev Physiol* **64**, 355-405 (2002).
11. Sumi, M. *et al. Biochem Biophys Res Commun* **181**, 968-75 (1991).
12. Ishida, A., Kameshita, I., Okuno, S., Kitani, T. & Fujisawa, H. *Biochem Biophys Res Commun* **212**, 806-12 (1995).
13. Schikorski, T. & Stevens, C.F. *Nat Neurosci* **4**, 391-5 (2001).
14. Tyler, W.J. & Pozzo-Miller, L.D. *J Neurosci* **21**, 4249-58 (2001).
15. Borst, J.G. & Sakmann, B. *Nature* **383**, 431-4 (1996).
16. Dickinson-Nelson, A. & Reese, T.S. *J Neurosci* **3**, 42-52 (1983).
17. Pozzo-Miller, L.D. *et al. J Neurosci* **19**, 4972-83 (1999).
18. Kushner, S.A. *et al. J Neurosci* **25**, 9721-34 (2005).
19. Hinds, H.L., Tonegawa, S. & Malinow, R. *Learn. Mem.* **5**, 344-54 (1998).
20. Zhang, L. *et al. J Neurosci* **25**, 7697-707 (2005).
21. Lengyel, I. *et al. Eur J Neurosci* **20**, 3063-72 (2004).

Chapter 4

Rescue of neurological deficits in a mouse model for Angelman syndrome by reduction of alphaCaMKII inhibitory phosphorylation

Published in

Nature Neuroscience 2007 March 10(3), 280-282

Rescue of neurological deficits in a mouse model for Angelman syndrome by reduction of α CaMKII inhibitory phosphorylation

Geeske M van Woerden¹, Karen D Harris², Mohammad Reza Hojjati¹, Richard M Gustin³, Shenfeng Qiu², Rogerio de Avila Freire¹, Yong-hui Jiang⁴, Ype Elgersma¹ & Edwin J Weeber^{2,3}

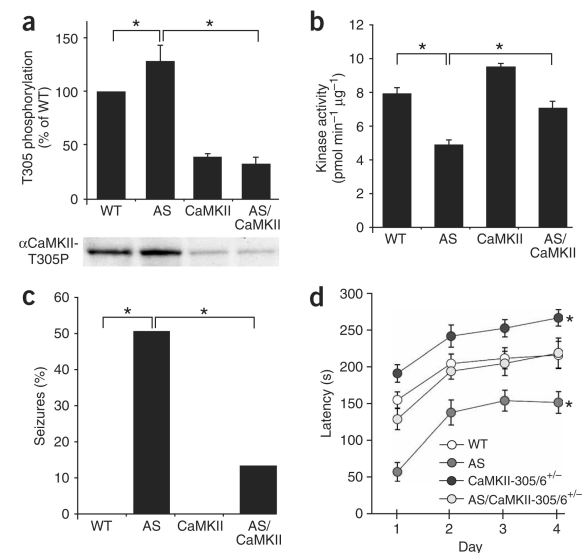
Angelman syndrome (AS) is a severe neurological disorder characterized by mental retardation, motor dysfunction and epilepsy. We show that the molecular and cellular deficits of an AS mouse model can be rescued by introducing an additional mutation at the inhibitory phosphorylation site of α CaMKII. Moreover, these double mutants no longer show the behavioral deficits seen in AS mice, suggesting that these deficits are the direct result of increased inhibitory phosphorylation of α CaMKII.

Angelman syndrome is caused by loss of function of imprinted genes on human chromosome 15q11–13 or by mutations in the *UBE3A* gene, which resides in this region^{1–4}. Imprinting of this gene results in exclusive expression of the maternal allele in hippocampal neurons and cerebellar Purkinje cells⁵. The *UBE3A* gene encodes the ubiquitin protein ligase E3A, also known as E6-AP, but its role remains elusive. Heterozygous mice with a maternally inherited *Ube3a* mutation (here called 'AS mice') show seizures and motor and cognitive abnormalities similar to the symptoms of AS individuals⁶. Biochemical analysis of these mice indicates that calcium/calmodulin-dependent kinase type 2

(CaMKII) activity is reduced and that phosphorylation of the inhibitory Thr305 and Thr306 site is increased⁷. Because increased inhibitory phosphorylation of CaMKII has a severe impact on neuronal function^{8–10}, we investigated whether the increased phosphorylation is directly responsible for the major deficits seen in AS. Female AS mice were crossed with heterozygous males that carried the targeted α CaMKII-*T305V/T306A* mutation, which prevents inhibitory phosphorylation of α CaMKII (designated as CaMKII-305/6^{+/-} mice; **Supplementary Methods** online). This resulted in offspring with four genotypes: wild-type mice, AS mutants, α CaMKII-305/6^{+/-} mutants and AS/CaMKII-305/6^{+/-} double mutants. As reported previously⁷, western blot analysis of hippocampal lysates showed a significant increase of Thr305 phosphorylation in AS mice (130%; $P < 0.05$ Fisher's protected least-significant difference, PLSD). In contrast, inhibitory phosphorylation was significantly reduced in CaMKII-305/6^{+/-} mutants (40%, $P < 0.001$) and in AS/CaMKII-305/6^{+/-} double mutants (**Fig. 1a** and **Supplementary Fig. 1** online). Moreover, the decreased kinase activity of the AS mutants was restored to near wild-type levels in the AS/CaMKII-305/6^{+/-} double mutants (**Fig. 1b**). Thus, these mutants are suitable for determining the extent to which increased inhibitory phosphorylation of CaMKII underlies the neurological phenotype of AS mice.

All the mutants appeared healthy, but adult (>2 months) AS mice showed a small (20%) but significant increase in body weight

Figure 1 Reduction of α CaMKII inhibitory phosphorylation rescues CaMKII activity and reduces both seizure propensity and motor performance deficits associated with AS. (a) CaMKII Thr305 phosphorylation is reduced in hippocampal lysates of AS/CaMKII-305/6^{+/-} double mutants. (b) Restoration of CaMKII activity in hippocampal synaptosomes of AS/CaMKII-305/6^{+/-} double mutants. (c) Propensity to audiogenic seizures of AS mutants is reduced in AS/CaMKII-305/6^{+/-} double mutants. (d) Opposing effects of the AS and CaMKII-305/6^{+/-} mutations on performance on the accelerating rotarod. Asterisks indicate significant differences from wild-type mice. Error bars represent s.e.m. All animal experiments were approved by the Dutch Ethical Committee, or in accordance with Institutional Animal Care and Use Committee guidelines. See text and **Supplementary Methods** for statistics, experimental details and number of subjects used.



¹Erasmus MC, University Medical Centre, Department of Neuroscience, Dr. Molewaterplein 50, PO Box 2040, 3000 CA, Rotterdam, The Netherlands. ²Department of Molecular Physiology and Biophysics. ³Department of Pharmacology, Vanderbilt University, 754 Robinson Research Building, Nashville, Tennessee 37235, USA.

⁴Department of Molecular and Human Genetics, Baylor College of Medicine, One Baylor Plaza, Houston, Texas 770301, USA. Correspondence should be addressed to Y.E. (y.elgersma@erasmusmc.nl).

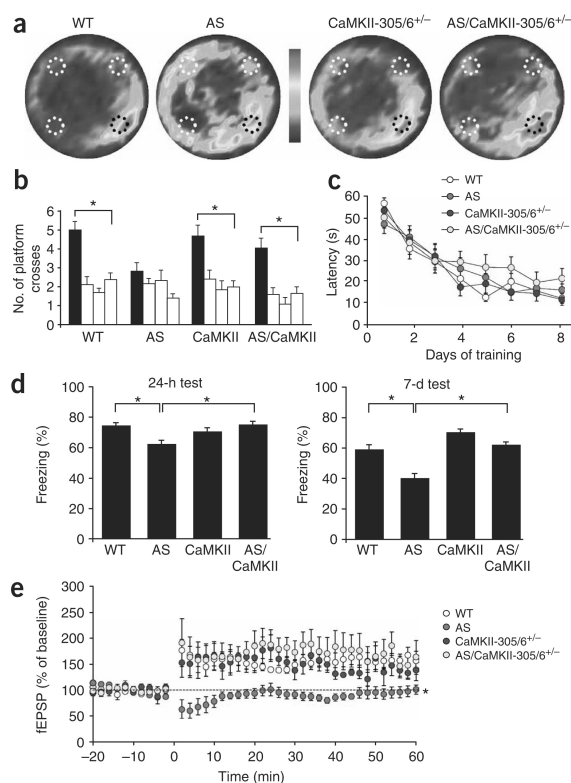


Figure 2 Hippocampal learning and plasticity of AS mice is rescued by the CaMKII-305/6^{+/-} mutation. Learning in the Morris water maze. **(a)** A probe trial shows that AS mice's search for the platform is less focused, as compared with wild-type and CaMKII-305/6^{+/-} mice. The plots are a visual representation of all search tracks combined, in which the color indicates the mean time spent at a certain position. The black circle indicates the target platform position used during training. The other (virtual) positions are indicated in white. **(b)** Quantification of the platform positions as indicated in **a**. Bars represent target position, adjacent right, opposite and adjacent left positions, respectively. Asterisks indicate that target position crossing happened significantly more than crossing of the other positions. **(c)** Escape latency to reach the platform shows no difference between the mutants. **(d)** AS mutants show impaired contextual conditioning. Freezing was assessed either 24 h or 7 d after conditioning. **(e)** LTP deficits of AS mice are rescued by the CaMKII-305/6^{+/-} mutation. Error bars represent s.e.m. See text and **Supplementary Methods** for statistics, experimental details and number of subjects used.

significant difference between genotypes ($F_{3,31} = 6.9$, $P < 0.005$ repeated measures ANOVA): AS mice stayed on the rotarod for significantly less time than their wild-type littermates ($P < 0.0001$ Fisher's PLSD; **Fig. 1d**). In contrast, CaMKII-305/6^{+/-} mutants performed better than wild-type mice ($P < 0.005$), whereas AS/CaMKII-305/6^{+/-} mice performed normal (wild type versus AS/CaMKII-305/6^{+/-}, $P = 0.5$). These results suggest that regulation of inhibitory phosphorylation of CaMKII is critical for motor coordination performance and that the increased phosphorylation directly underlies the motor performance deficits of AS mice.

The *UBE3A* gene is also imprinted in the hippocampus⁵. The important function of α CaMKII in hippocampus-dependent learning⁸ makes it likely that the increased inhibitory phosphorylation of α CaMKII underlies the cognitive deficits in AS individuals and mice⁶. Hippocampus-dependent learning was first assessed using the Morris water maze task. A probe trial given after 6 d of training showed a significant difference between genotypes when the number of target platform crossings was compared between mutants ($F_{3,66} = 3.7$, $P < 0.05$ ANOVA). Indeed, whereas wild type and CaMKII-305/6^{+/-} mutants showed significantly more crossings of the target platform position as compared with the other positions, AS mice did not (wild type, $P < 0.0001$; CaMKII-305/6^{+/-}, $P < 0.0001$; AS, $P = 0.16$, paired *t*-test between target and average of other positions; **Fig. 2a,b**). The learning deficit of AS mutants was not due to impaired motor performance or decreased motivation to escape, as all mutants showed similar escape latencies in the hidden platform task ($F_{3,31} = 0.8$, $P = 0.5$ repeated measures ANOVA, **Fig. 2c**) as well as in the visible platform task (**Supplementary Fig. 3** online). Moreover, the swim speed of AS mice was similar to that of wild-type mice, and the spatial learning deficits were overcome by additional training (**Supplementary Fig. 3**). Notably, the spatial learning deficits of AS mice at day 6 were again completely rescued by the CaMKII-305/6^{+/-} mutation, as the AS/CaMKII-305/6^{+/-} double mutants showed a highly selective search strategy (target crossing versus average of other positions, $P < 0.0001$, paired *t*-test).

Hippocampus-dependent learning was also assessed using contextual fear conditioning. Context-dependent memory was tested 24 h or 7 d following training (**Fig. 2d**). A significant difference between genotypes was observed at both time points, with AS mice freezing significantly less than any other group (24 h: $F_{3,25} = 9$, $P < 0.0005$ ANOVA, all $P < 0.01$ Fisher's PLSD; 7 days: $F_{3,25} = 26$, $P < 0.0001$ ANOVA, all $P < 0.0001$ Fisher's PLSD). In contrast, CaMKII-305/6^{+/-} mutants showed significantly more freezing in the 7-d memory test (all $P < 0.05$ Fisher's PLSD), but not in the 24-h memory test. Once more, the phenotype was rescued by the AS/CaMKII-305/6^{+/-} double

($P < 0.005$ Fisher's PLSD; **Supplementary Fig. 2** online). Although obesity is not a characteristic feature of the disease, it occurs in 15% of AS children¹¹ and in the majority of AS children carrying the *Ube3a* mutation¹². Moreover, obesity is a common feature of children with a previously unrecognized form of AS¹³. Increased body weight was absent in AS/CaMKII-305/6^{+/-} double mutants ($P > 0.3$). As α CaMKII expression is restricted to neurons, these results suggest that the increased body weight of AS mice has a neurological basis and is caused by increased α CaMKII Thr^{305/306} phosphorylation.

Epilepsy is a common feature of AS^{11,14}. As epilepsy is absent in some AS individuals and is background dependent in AS mice⁸, several genes seem to be involved in the development of this phenotype. Nevertheless, as reduced α CaMKII activity can result in epilepsy⁸, the increased CaMKII inhibitory phosphorylation could potentially contribute to the increased seizure propensity of AS mice. Using audiogenic stimulation, we observed seizures in 50% of the AS mice, whereas no seizures were observed in wild-type mice or CaMKII-305/6^{+/-} mutants. Notably, there was a 75% reduction of seizure propensity in AS/CaMKII-305/6^{+/-} double mutants as compared with the AS mutants ($P < 0.05$ Pearson's test, **Fig. 1c**). This suggests that the increased inhibitory phosphorylation of CaMKII strongly contributes to the increased seizure susceptibility of the AS mutants.

Motor coordination deficits are common in all AS individuals and mice^{6,14}. The *UBE3A* gene is imprinted in cerebellar Purkinje cells⁵, and we have shown that α CaMKII is essential for cerebellar motor learning and Purkinje cell plasticity¹⁵. Therefore, these deficits could well be caused by dysregulation of cerebellar CaMKII. Motor performance of the mutants was assessed using an accelerating rotarod. There was a

mutation (wild type versus AS/CaMKII-305/6^{+/-}, 24 h; $P = 0.6$; 7 days: $P = 0.4$ Fisher's PLSD). Because cued conditioning was normal in the AS mice (**Supplementary Fig. 4** online), we conclude that AS mice have a hippocampal learning deficit and that the mutant phenotype can be rescued by decreasing α CaMKII inhibitory phosphorylation.

Inhibitory phosphorylation of α CaMKII is important in setting the threshold for the induction of long-term potentiation (LTP); homozygous CaMKII-305/6 mice show increased LTP at subthreshold stimulation and normal LTP when a strong stimulation protocol is applied⁹. In contrast, AS mice show a striking LTP deficit, which is rescued by a strong stimulation protocol^{6,7}. To directly test whether the LTP deficit of AS mice is due to excessive Thr^{305/306} phosphorylation, we measured LTP in hippocampal slices of the mutants. Consistent with previous findings, AS mice showed a severe LTP deficit compared with wild-type mice ($F_{3,87} = 0.3$, $P < 0.0001$ ANOVA, all $P < 0.001$ Fishers PLSD; **Fig. 2e**). LTP was normal in the CaMKII-305/6^{+/-} mice ($P = 0.5$ Fishers PLSD), as well as in the AS/CaMKII-305/6^{+/-} double mutants ($P = 0.4$ Fishers PLSD), suggesting that the plasticity deficits of AS mice are the result of increased inhibitory phosphorylation of CaMKII.

Although further research is needed to link E6-AP to CaMKII inhibitory phosphorylation, here we report a functional connection between CaMKII and a human learning and memory disorder. This study provides insight into the molecular basis of the motor, seizure and cognitive facets observed in Angelman syndrome.

Note: Supplementary information is available on the Nature Neuroscience website.

ACKNOWLEDGMENTS

The authors thank M. Elgersma and M. Aghadavoud Jolfaei for technical support. This work was supported by the Netherlands Organization for Scientific Research (NWO-ZonMW), Hersenstichting Nederland (HsN), Netherlands Epilepsy Fund and the Nina Foundation/Angelman Vereniging.

COMPETING INTERESTS STATEMENT

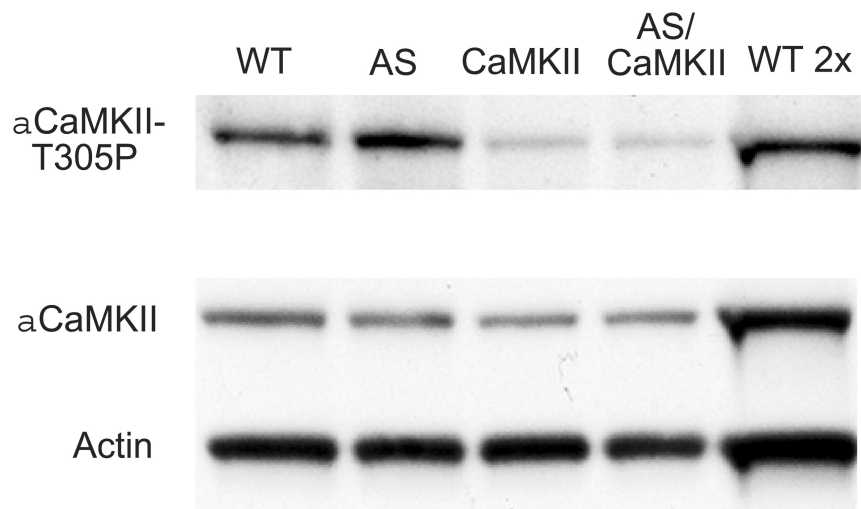
The authors declare that they have no competing financial interests.

Published online at <http://www.nature.com/natureneuroscience>

Reprints and permissions information is available online at <http://npg.nature.com/reprintsandpermissions>

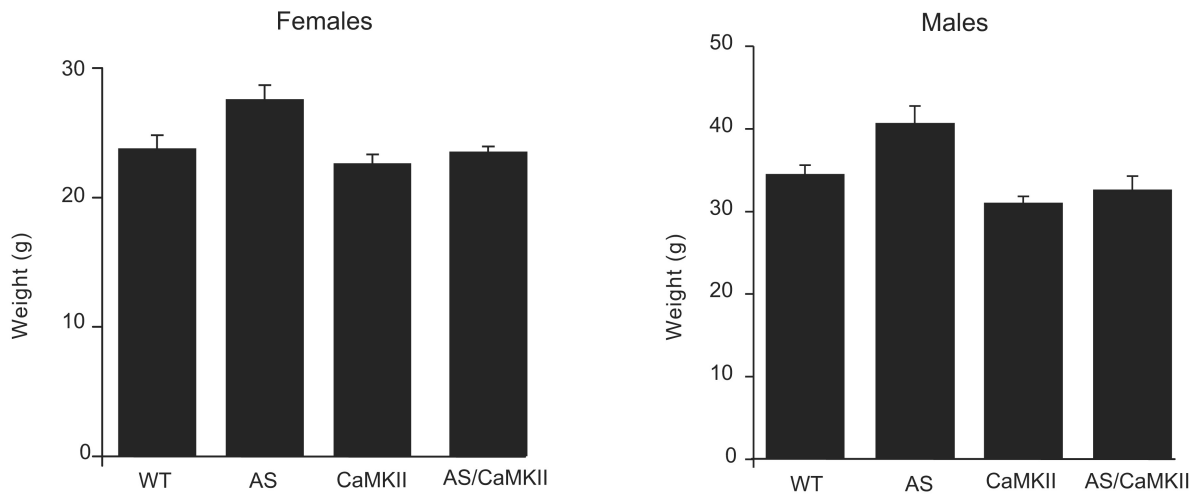
1. Knoll, J.H. *et al.* *Am. J. Med. Genet.* **32**, 285–290 (1989).
2. Sutcliffe, J.S. *et al.* *Genome Res.* **7**, 368–377 (1997).
3. Matsuura, T. *et al.* *Nat. Genet.* **15**, 74–77 (1997).
4. Kishino, T., Lalonde, M. & Wagstaff, J. *Nat. Genet.* **15**, 70–73 (1997).
5. Albrecht, U. *et al.* *Nat. Genet.* **17**, 75–78 (1997).
6. Jiang, Y.H. *et al.* *Neuron* **21**, 799–811 (1998).
7. Weeber, E.J. *et al.* *J. Neurosci.* **23**, 2634–2644 (2003).
8. Elgersma, Y., Sweatt, J.D. & Giese, K.P. *J. Neurosci.* **24**, 8410–8415 (2004).
9. Elgersma, Y. *et al.* *Neuron* **36**, 493–505 (2002).
10. Zhang, L. *et al.* *J. Neurosci.* **25**, 7697–7707 (2005).
11. Smith, A. *et al.* *J. Med. Genet.* **33**, 107–112 (1996).
12. Moncla, A. *et al.* *J. Med. Genet.* **36**, 554–560 (1999).
13. Gillissen-Kaesbach, G. *et al.* *Eur. J. Hum. Genet.* **7**, 638–644 (1999).
14. Clayton-Smith, J. *Am. J. Med. Genet.* **46**, 12–15 (1993).
15. Hansel, C. *et al.* *Neuron* **51**, 835–843 (2006).

Supplementary Fig. 1 Van Woerden et al.



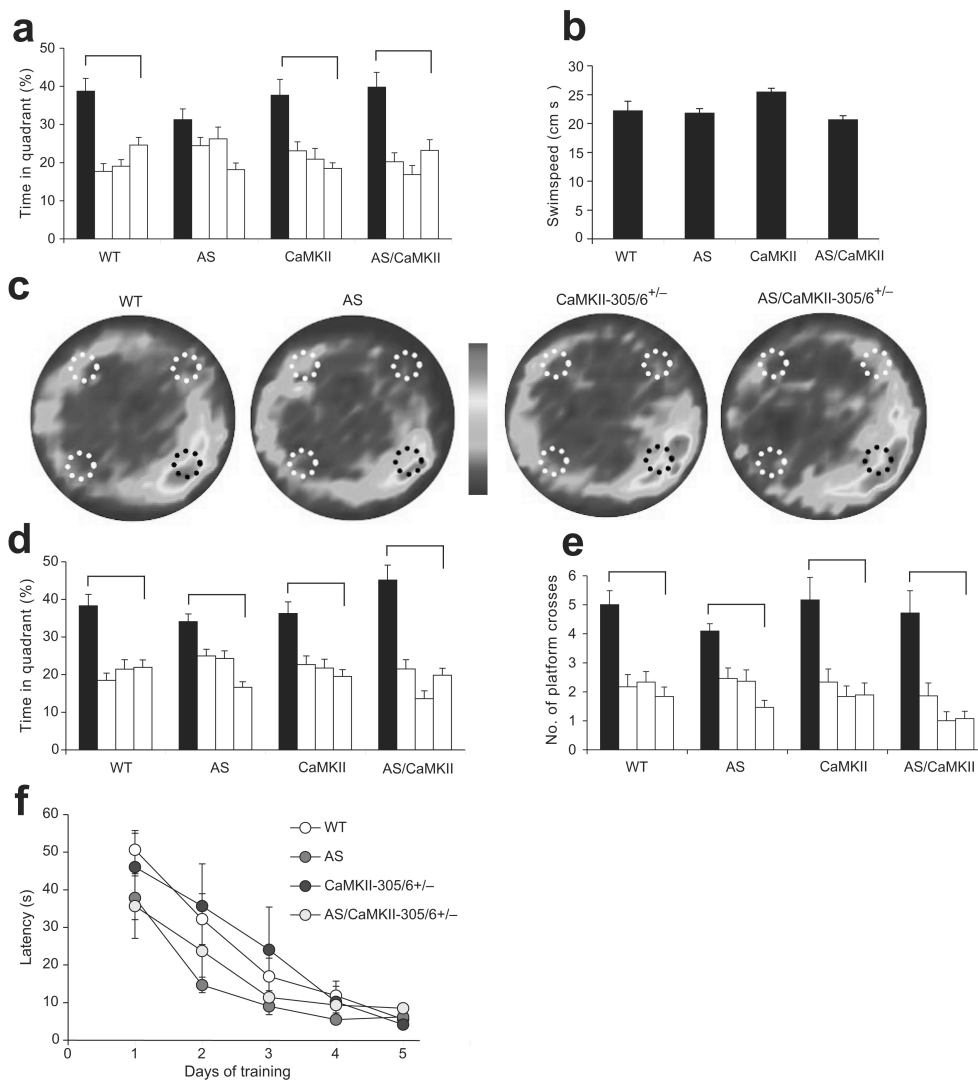
Decreased inhibitory phosphorylation in hippocampal lysates of AS/CaMKII-305/6^{+/-} double mutants. AS mice show significantly increased CaMKII-T305 phosphorylation, compared to their WT littermates, which is decreased when crossed with CaMKII-305/6^{+/-} mice. Western blots were first probed with antibodies directed against Thr305-CaMKII and after stripping re-probed with CaMKII and Actin. To ensure that the staining was within the linear range, the wild-type samples were also loaded at two fold higher concentration.

Supplementary Fig. 2 Van Woerden et al.



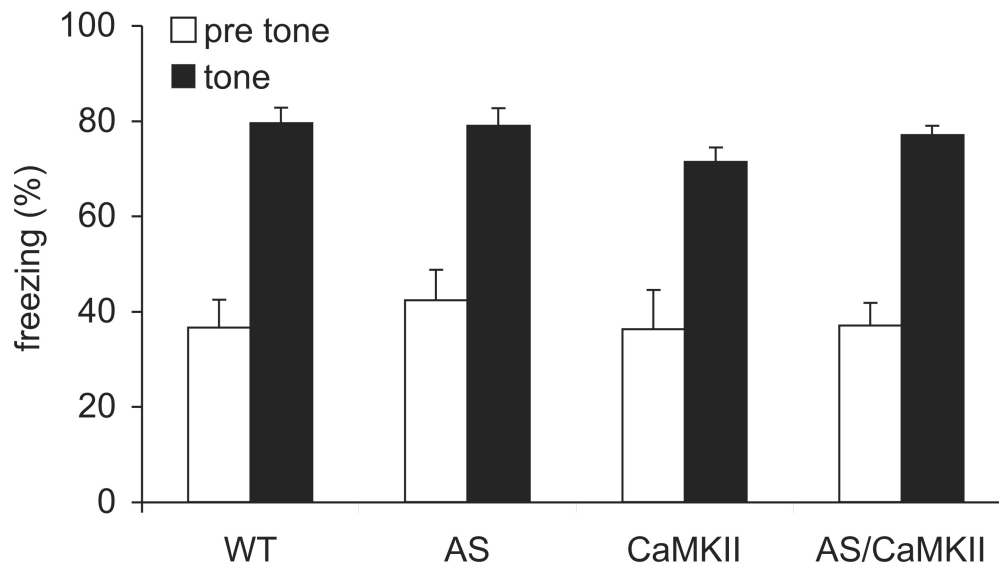
The increased bodyweight in AS mice returns to WT level in AS/CaMKII-305/6^{+/-} mice. AS mice show a small but significant ($P < 0.005$) increase in bodyweight (females (2.5 months old): $F_{3,48} = 5.6$, $P < 0.005$, males (4 months old): $F_{3,13} = 9.6$, $P < 0.005$ ANOVA; Post hoc analysis: all $P < 0.005$ Fisher's PLSD), which was absent in AS/CaMKII-305/6^{+/-} double mutants ($P > 0.3$ for males and females). Error bars represent SEM.

Supplementary Fig. 3 Van Woerden et al.



Learning of the hidden platform (a-e) and visible (f) platform watermaze. AS mice show impaired hippocampal learning at the probe trial given at day 6 compared to their wild type littermates, which is improved after two additional training days. (a) During the probe trial at day 6 AS mice do not spend significantly more time in the target quadrant as compared to all the other quadrants, whereas the AS/CaMKII-305/6^{+/-} mice show high preference for the target quadrant. (b) The learning impairment of the AS mice cannot be ascribed to motor impairments or motivational problems, as they swim as fast as their wild type littermates. Only the CaMKII-305/6^{+/-} mice tend to swim faster. (c,d,e) At the probe trial given at day 8, the AS mice caught up with their littermate controls and showed selective searching as judged from the time spent in target quadrant (d) and from the number of platform crosses (e). To exclude that AS mice have visual or motivational problems that could account for the impaired learning, a visible watermaze was performed and the escape latency was determined. This task shows no effect of genotype ($F_{3,14}=1.4$, $P=0.3$ repeated measures ANOVA). Error bars represent SEM.

Supplementary Fig. 4 Van Woerden et al.



AS mice show no deficits in cued conditioning. Cued conditioning test was used to assess whether the contextual conditioning phenotype of the AS mice was hippocampus-dependent. Cued conditioning did not reveal any difference between the different mutants, indicating that the contextual phenotype found in AS mice is indeed hippocampus-dependent ($F_{3,34} = 0.6$, $P = 0.6$ repeated measures ANOVA). Error bars represent SEM.

Material and Methods

Breeding of mutants.

Mutants with the *Ube3a* null mutation (designated as AS mice) and mutants carrying the targeted α CaMKII-T305V/T306A mutation which prevents phosphorylation at these residues (designated as CaMKII-305/6^{+/-} mice) were developed as described previously^{1,2}. All experiments described in this paper were carried out using hybrid mice in the mixed 129/Sv-C57BL/6 background. To that end, male α CaMKII-305/6^{+/-} mutants in the C57BL/6 background were crossed with female AS mutants in the 129/Sv background (weight, rotarod, watermaze) or with female AS mutants in the 129/Sv-C57BL/6 background (epilepsy, fear conditioning, LTP).

Mice were genotyped when they were 7-10 days, but the experimenter remained blind for the genotype during data collection and the initial analysis. Genotypes were again established after all experiments were done and the code was then broken to perform the final statistical analysis. All experiments were done with 2-4 month old littermates that were housed in groups of 2-3 per home cage. Genotype groups were approximately sex and age matched. Single-housed mice were excluded for the behavioral studies. The mice were kept on a 12h light/dark cycle, with food and water available ad libitum. The behavioral experiments were performed during the light period of the cycle.

Western blot analysis of the phosphorylation state of CaMKII.

Lysates were prepared by quickly dissecting the hippocampus followed by homogenation in lysis buffer (10mM TRIS-HCl 6.8, 2.5% SDS, 2mM EDTA and protease and phosphatase inhibitor cocktails (Sigma)). Lysates were then adjusted to 1 mg/ml, and 10 μ g was used for SDS-PAGE analysis and Western blotting. Western blots were first probed with antibodies

directed against Thr305- α CaMKII (pB60², 1:5000) and after stripping re-probed with α CaMKII (MAB3119, 1:10000; Chemicon), and Actin (MAB1501R, 1:2000; Chemicon). Blots were quantified using NIH-Image using the α CaMKII signal as loading control, and normalized against wild-type. The number of mice used: WT (4); AS (4); CaMKII-306/5^{+/-} (4); AS/CaMKII-305/6^{+/-} (4).

CaMKII Activity Measurement

Mice were sacrificed by cervical dislocation and hippocampi were quickly isolated in ice-cold cutting solution and sonicated in cold homogenization buffer containing 4 mM HEPES, 320 mM sucrose and protease inhibitor cocktail (Sigma, Saint Louis, MO). The homogenates were centrifuged at 1500 g for 10 min. The supernatant was then centrifuged at 16000 g for 20 min to yield a pellet containing the crude synaptosome fraction. This fraction was resuspended in 200 μ l homogenization buffer to measure the Ca²⁺/calmodulin dependent CaMKII activity using the assay kit from Millipore Inc. (14-217). The number of mice used: WT (6); AS (6); CaMKII-306/5^{+/-} (6); AS/CaMKII-305/6^{+/-} (6).

Weight and seizure susceptibility

Female AS mice started to show increased bodyweight after 2 months, whereas male AS mice started to become significantly heavier after 4 months. Number of mice used: females (8-9 weeks): WT (13); AS (7); CaMKII-305/6^{+/-} (10); AS/CAMKII-305/6^{+/-}, (13). Males (16-18 weeks): WT (4); AS (3); CaMKII-305/6^{+/-} (6); AS/CaMKII-305/6^{+/-} (4). To assess seizure susceptibility we induced audiogenic seizures by vigorously scratching scissors across the

metal grating of the mouse cage lid for 20 seconds, or shorter if a seizure developed before that time. The number of mice used in this paradigm: WT (11); AS (10); CaMKII-305/6^{+/-} (12); AS/CaMKII-305/6^{+/-} (15).

Motor performance.

We tested motor function in F1 mice using the accelerating rotarod (4-40 rpm, in 5 minutes; model 7650, Ugo Basile Biological Research Apparatus, Varese, Italy). Mice were given two trials per day with a 45-60 min inter trial interval for 4 consecutive days. For each day we calculated the average of the time spent on the rotarod, or of the time until the mouse made 3 consecutive rotations on the rotarod. Maximum duration of a trial was 5 min. The number of mice used: WT (10); AS (7); CaMKII-305/6^{+/-} (10); AS/CaMKII-305/6^{+/-} (8).

Water Maze.

To test spatial memory we used the Water Maze. Prior to the test mice were handled extensively (2 min/day; 5 days). Our pool is 1.2 m in diameter and has an 11 cm diameter platform submerged 1 cm below the water surface. The water is painted milk-white with non-toxic paint and water temperature is kept constant at 26°C. We use dimmed lighting, and mouse-tracking is performed using SMART version 2.0 (Panlab, Barcelona, Spain). Mice were given 2 trials per day, with 30 sec inter trial interval for 8 consecutive days. At a training session, the mouse was first placed on the platform for 30 sec. Then it was placed in the water at a pseudo-random start position and it was given a maximum of 60 seconds to find the platform. If the mouse did not find the platform within 60 seconds, it was placed back on the platform. After 30 seconds on the platform, this training procedure was repeated once more. The platform position remained at the same position during all trials.

One hour after the training on day 6 and day 8, a probe trial was given to test spatial learning. Mice were placed on the platform for 30 seconds, after which the platform was removed from the pool and the mice were placed in the pool at the opposite side of the previous platform position. The mice were then allowed to search for the platform for 60 seconds. The number of mice used for this paradigm: WT (18); AS (11); CaMKII-306/5^{+/-} (18); AS/CaMKII-305/6^{+/-} (14).

The visible water maze was performed done in the same way as the hidden platform water maze, except that this time the platform was flagged with a small cue on top the platform. The number of (naïve) mice used for this paradigm: WT (6); AS (5); CaMKII-306/5^{+/-} (4); AS/CaMKII-305/6^{+/-} (3).

Fear Conditioning.

Fear conditioning was performed in a testing chamber (26 × 22 × 18 cm; San Diego Instruments, San Diego, CA) made of Plexiglas equipped with a grid floor via which the foot shock could be administered and a CCD camera to monitor activity. The conditioning chamber was placed inside a soundproof isolation cubicle. Training and testing occurred in the presence of white light and white noise. Each mouse was placed inside the conditioning chamber for 150 seconds before the onset of a 2 s foot shock (0.5 mA). After 150 seconds, a second foot shock was delivered, and the mouse was returned to its home cage after another 2.5 min. Testing of context-dependent fear was performed either 24 hours or 1 week after the conditioning in the same context.

For cued conditioning, each mouse was placed inside the conditioning chamber for 2 min before the onset of a conditioned stimulus (CS; an 85 dB tone), which lasted for 30 s. training occurred in the presence of white light and white noise. A 2 s US foot shock (0.5 mA) was delivered immediately after the termination of the CS. Each mouse remained in the chamber for an additional 120 s, followed by another CS–US pairing. Each mouse was returned to its home cage after another 2.5 min. Cued fear conditioning was tested in the presence of a masked context consisting of a small Plexiglas cube attached to an opaque Plexiglas floor insert, different lighting conditions, and a vanilla odor. Each mouse was placed in this novel context for 3 min at approximately 24 h after training, and they were exposed to the CS for another 3 min.

Freezing behavior was recorded and processed by SDI Photobeam Activity System software throughout each testing session. The mouse was considered to be freezing after a lack of movement for 2 s. Number of animals used: 24 hours context: WT (6); AS (6); CaMKII-305/6^{+/-} (8); AS/CaMKII-305/6^{+/-} (9) ; 1 week context: (WT (7); AS (8); CaMKII-305/6^{+/-} (7); AS/CaMKII-305/6^{+/-} (8). 24 hours cued: WT (11); AS (11); CaMKII-305/6^{+/-} (7); AS/CaMKII-305/6^{+/-} (9) ;

Shock threshold was assessed by placing the animal in the conditioning chamber and by delivering foot shocks starting at 0.075 mA and increasing by 0.05 mA every 30 s. The experiment was terminated at the shock intensity sufficient to induce vocalization. There was no difference in shock sensitivity between the groups ($F_{3,75}=0.53$, $p=0.9$ ANOVA).

Hippocampal slice preparation and electrophysiology

The brain was quickly removed and placed in ice-cold high sucrose cutting solution containing (in mM): 110 sucrose, 60 NaCl, 3 KCl, 28 NaHCO₃, 1.25 NaH₂PO₄, 7 MgCl₂, 0.5 CaCl₂, 0.6 sodium ascorbate, and 5 D- glucose, pH 7.3–7.4. Horizontal 400 μ m sections were cut in sucrose cutting solution using a Vibratome. The slices were stored in 95% O₂/5% CO₂-equilibrated artificial CSF containing (in mM): 125 NaCl, 2.5 KCl, 1.25 NaH₂PO₄, 28 NaHCO₃, 1.0 MgCl₂, 2.0 CaCl₂, and 10 D- glucose, (pH 7.3-7.4) and kept at room temperature for at least 1 hour before switching to the interface chamber supported by a nylon mesh and allowed to recover for a minimum of 1 hour prior to recording. The chamber was kept at 32 ± 0.5 °C with a laminar ACSF flow rate of 2–3 ml/min. Extracellular field recordings were obtained from area CA1 of the stratum radiatum. Stimulations were supplied with a bipolar Teflon-coated platinum electrode and recordings were obtained with the use of a glass microelectrode field with ACSF with tip diameter about 1 μ m (1–4 M Ω electrical resistance). Tetani used to evoke CA1 LTP consisted of two trains of 100 Hz stimulation for 1s with each train separated by a 20s interval. Stimulus intensities were adjusted to give pEPSPs (population excitatory postsynaptic potentials) with slopes that were <50% of the maximum determined from an input/output curve. Potentiation was measured as the normalized increase of the mean pEPSP for the duration of the baseline recording. Experimental results were obtained from those slices that exhibited stable baseline synaptic transmission for a minimum of 30 min prior to the delivery of the LTP- inducing stimulus. For recording we used an Axon 1320 Digidata data acquisition hardware operated by Axon pClamp 9.2 software. We used maximally two slices per mouse. The number of slices used for the experiment are: WT (11); AS (6); CaMKII-305/6^{+/-} (6); AS/CaMKII-305/6^{+/-} (6).

Statistical analysis.

StatView data analysis software was used for statistical analysis. An ANOVA or repeated measures ANOVA was used for multiple group data, to test for the effect of genotype. If this was significant, the data was further analyzed using the Fisher PLSD Post Hoc test. All figure data represents mean \pm SEM. An analysis with a value of $p < 0.05$ was considered to be statistically significant (indicated by an asterisk in the figures).

References

1. Jiang, Y.H. et al. Mutation of the Angelman ubiquitin ligase in mice causes increased cytoplasmic p53 and deficits of contextual learning and long-term potentiation. *Neuron* 21, 799-811 (1998).
2. Elgersma, Y. et al. Inhibitory autophosphorylation of CaMKII controls PSD association, plasticity, and learning. *Neuron* 36, 493-505 (2002).

Chapter 5

The neuron-specific NF1 exon 9a is essential for theta-frequency LTP and learning

Mohammad Reza Hojjati^{1,2}, Geeske M. van Woerden¹, Alcino J. Silva³, and Ype Elgersma¹

¹Department of Neuroscience, Erasmus University Medical Center, Dr. Molewaterplein 50, 3015 GE, Rotterdam, The Netherlands. ²Department of Physiology, Shahrekord University of Medical Sciences, Kashani Blvd, Shahrekord, 88155, Iran. ³Department of Neurobiology, Psychiatry and psychology, Brain Research Institute, 695 Charles Young Drive South, University of Carolina, LA, USA

Abstract

Neurofibromatosis type 1 (NF1) is one of the most common inherited single-gene disorders affecting cognitive function. The NF1 gene encodes a large amino acid protein called neurofibromin, which functions as a Ras GTP-ase activating protein (GAP). Although NF1 is expressed in all cells of the brain, expression of NF1 containing the small alternatively spliced exon 9a is restricted to neurons, and this isoform is particularly highly expressed in the forebrain. This exon is not part of the GAP domain and its function is unknown. To study the role of the NF1-Ex9a isoform in cognitive function, we generated a mouse lacking the NF1-Ex9a isoform and show that they demonstrate spatial learning deficits in the Morris water maze task and impaired LTP induced at theta frequency. Our finding suggest that exon 9a is essential for the function of NF1 in spatial learning and hippocampal plasticity, and that the role of NF1 in neuronal function is not restricted to its function as a GAP protein.

Introduction

Neurofibromatosis type I (NF1) is one of the most common single gene disorders (1 in 3500) affecting cognitive function (Huson et al., 1988; Poyhonen et al., 2000). 40 to 60% of children with NF1 have learning disabilities ranging from mild cognitive impairment to attention deficit disorder (North et al., 1997). The phenotype of NF1 is highly variable, with several organ systems affected. Affected individuals present with pigmentary abnormalities and an increased risk of developing both benign and malignant tumors (Gutmann et al., 1997).

NF1 is caused by a mutation within the NF1 gene located on chromosome 17 in humans (O'Connell et al., 1989). The highest level of NF1 gene expression is seen in neural tissues (Daston et al., 1992). The NF1 gene encodes a large amino acid protein, which is called neurofibromin. Neurofibromin has several properties and functions, including Ras GTPase-activating protein activity (Ras-GAP activity) (Xu et al., 1990), adenylyl cyclase modulation (Guo et al., 1997), microtubule binding (Xu and Gutmann, 1997), and regulation of actin filament reorganization (Ozawa et al., 2005).

There are three major alternatively spliced exons of the NF1 gene: exon 9a, 23a, and 48a. The NF1 isoform containing exon 48a is highly expressed in adult and embryonic cardiac and muscle tissues, but not in the adult brain (Gutmann et al., 1995a). In contrast, the most commonly expressed alternative isoform NF1-Ex23a (NF1 type II) is particularly highly expressed in astrocytes (Huynh et al., 1994; Gutmann et al., 1995b). This isoform has been shown to have decreased Ras-GAP activity (Danglot et al., 1995; Gutmann et al., 1995b; Geist and Gutmann, 1996). Mice lacking exon 23a show specific hippocampal learning impairments, but other forms of learning, embryological development and tumor suppression were unaffected by this mutation (Costa et al., 2001). However, to what extent the cognitive deficits are caused by neuronal or astrocyte dysfunction is not clear. Interestingly, expression of neurofibromin containing exon 9a, NF1-Ex9a, is restricted to neurons (Geist and Gutmann, 1996). Previous studies have shown that the NF1-Ex9a isoform is highly expressed in the forebrain (striatum, cortex, and hippocampus) beginning in the first week of postnatal life (Geist and Gutmann, 1996; Gutmann et al., 1999). Exon 9a encodes only 10 amino acids, and is present in the N-terminus of the protein, which is not part of the GAP domain. The importance of this neuronal isoform is unclear. In this study we have generated mice that lack the exon9a, and show that this exon is essential for the role of NF1 in spatial learning and hippocampal plasticity.

Results

NF1^{9a*/9a*} mice are viable and show normal expression level of NF1

To study the role of neuronal NF1 in learning and memory, we introduced a nonsense mutation into exon 9a (fig 1A). Successfully targeted E14 ES cells (identified by Southern blot analysis (fig 1B)) were used to obtain F1 heterozygous NF1^{9a*/9a} mice. These mice were subsequently used to obtain F2 homozygous NF1^{9a*/9a*} mice and wild-type littermate controls. Homozygous NF1^{9a*/9a*} were born at the expected Mendelian frequency, and were undistinguishable from wild-type mice upon examination by an experienced observer.

Expression of neurofibromin in the hippocampus was assessed using western blot analysis. No difference was found in the total amount of NF1 protein expressed in NF1^{9a*/9a*} mice compared to wild type, indicating that introduction of the mutations in exon 9a prevented the incorporation of this exon into the NF1 protein. Therefore this mutant is a good model to study the role of this specific exon in learning and plasticity.

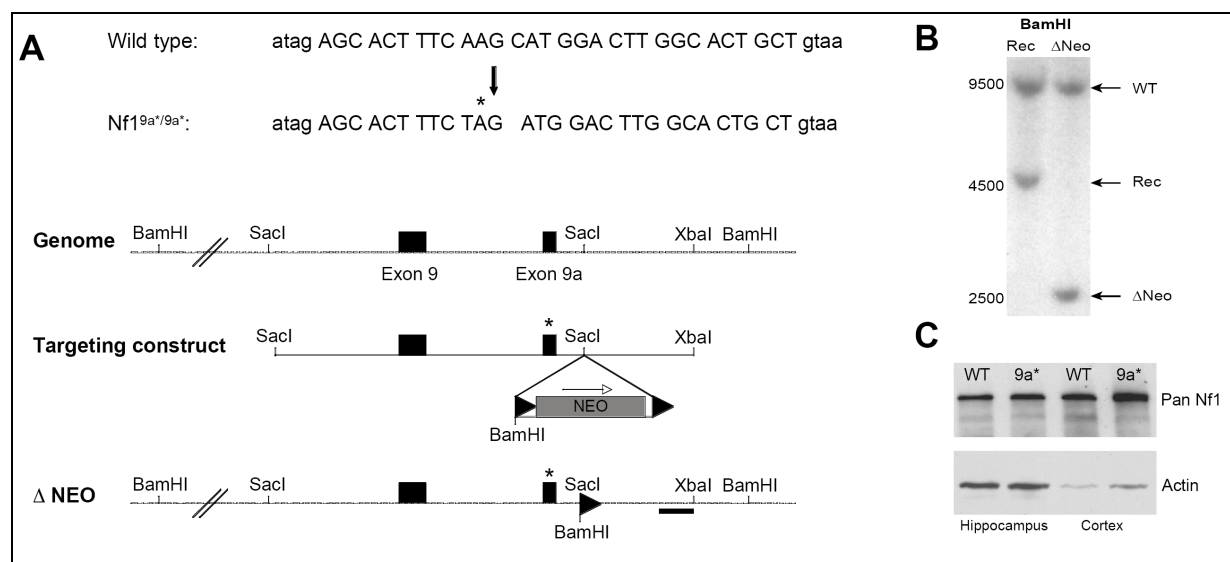


Figure 1. Generation of NF1^{9a*/9a*} mutant mice. **A**, Top: NF1 exon 9a DNA sequence and the introduced NF1^{9a*} mutation. Bottom: schematic diagram of the procedure for generating the exon 9a mutant ES clones. (Top) The wild-type NF1 locus with the location of the exons 9 and 9a depicted as filled boxes. (Middle) Targeting construct used for the generation of the NF1 exon 9a mutations. The asterisk indicates the mutated exon 9a. The LoxP sites flanking the neomycin resistance cassette are depicted as triangles. (Bottom) Mutant NF1 locus after homologous recombination and after the deletion of the neomycin gene by transient transfection of Cre recombinase. Shown in bold are the positions of the BamHI sites used to digest the DNA for Southern blot analysis (**B**). The position of the probe used for the analysis is depicted as a black bar. **B**, Southern blot obtained after BamHI digestion of ES cell DNA after homologous recombination (Rec) and after deletion of the neomycin gene (Δ Neo). The annotation of the obtained bands is indicated with the arrows. The numbers refer to the approximate sizes in base pairs after BamHI digestion. **C**, Western blot analysis of hippocampal and cortical lysates of the NF1^{9a*/9a*} mutants. No difference in expression level of Neurofibromin was found in the mutant compared to the wt samples in both hippocampus and cortex.

NF1^{9a*/9a*} mice show spatial learning deficits

Previous studies have shown that learning disabilities are commonly associated with NF1. For instance, studies in human have shown that individuals affected with NF1 display a wide range of learning disabilities (North et al., 1997). Interestingly, both NF1^{+/-} mice and *Drosophila* mutants show learning and memory deficits (Silva et al., 1997; Guo et al., 2000). Since previous studies have shown that the NF1 Exon 9a isoform is highly expressed in the forebrain (striatum, cortex and hippocampus), it might be that exon 9a isoform plays a role in hippocampal-dependent learning. To investigate this hypothesis, NF1^{9a*/9a*} mice were tested in the Morris water maze task, in which the animal has to find a fixed hidden platform from random departure location. After a handling period of 5 days (2 minutes/day), animals were first trained with four trials per day for 3 days. After the last training trial the mice were given a probe trial at the day 3 and day 5, in which the platform was removed and mice were allowed to search it for 60 s. No differences were observed between wild type and NF1^{9a*/9a*} mice in floating and circling behaviour (The time spent in a 10-cm ring-shaped near the wall of the pool). However, as shown in Figure 2A, in a probe trial was given after 3 days of training, the wild-type mice searched selectively, spending significantly longer time in the target quadrant where the platform was during training, whereas NF1^{9a*/9a*} mice searched randomly and spent significantly less time searching for the platform in the target quadrant (wild type, $P = 0.001$; NF1^{9a*/9a*}, $P = 0.63$, paired t-test between target and average of other positions).

Previous studies showed that additional training alleviates the learning deficits in the NF1^{+/-} and NF1^{23a/-} mice (Silva et al., 1997; Costa et al., 2001). Consistently, the learning impairment in our NF1^{9a*/9a*} mice was improved after two additional training days and the mutant mice searched as selectively as wild-type controls in a probe test at the day 5 (wild type, $P < 0.0001$; NF1^{9a*/9a*}, $P < 0.0001$, paired t-test between target and average of other positions; Figure 2B). The learning deficit of NF1^{9a*/9a*} mice was not due to impaired motor performance or decreased motivation to escape, as they showed similar escape latencies to reach the platform in the hidden platform task and also swam as fast as their wild type littermates (data not shown). Moreover, the swim path length in NF1^{9a*/9a*} mice is comparable with the wild type mice (ANOVA, $F(1,27) = 0.46$, $P = 0.5$, Figure 2,C; ANOVA, $F(1,27) = 0.26$, $P = 0.6$, Figure 2,D).

Basic synaptic transmission is normal in NF1^{9a*/9a*} mice

Previous experiments with NF1^{+/-} mutants showed a decrease in input-output function of extracellularly recorded EPSPs at Schaffer-collateral/CA1 synapse (Costa et al., 2002). To investigate whether hippocampal basic synaptic transmission has changed in NF1^{9a*/9a*} mice, field excitatory postsynaptic potentials (fEPSPs) were recorded from CA1 area of hippocampus. We first tested the synaptic efficacy in both wild type and NF1^{9a*/9a*} mice by stimulating the Schaffer collateral fibers at different stimulation strengths ranging from 10 to

100 μ A. As seen in Figure 3,A-C, synaptic transmission did not appear to be altered in NF1^{9a*/9a*} mutants (Presynaptic fiber volley: $F(1,36)=0.01$, $P = 0.92$; postsynaptic fEPSP: $F(1,98) = 0.28, P = 0.59$). The ratio of the presynaptic fiber volley amplitude to the excitatory postsynaptic potential slope was not different between slices prepared from wild type and NF1^{9a*/9a*} mice (Figure 3,C). Next, we measured paired-pulse facilitation (PPF), a presynaptic form of short-term plasticity. Paired pulse stimulating at different interstimulus intervals (from 10 to 400 ms) showed no significant difference between NF1^{9a*/9a*} and wild type mice (Repeated Measures ANOVA, $F(1,50) = 0.2$, $P = 0.6$, [Figure 3,D](#)), suggesting that presynaptic function in NF1^{9a*/9a*} mice is normal.

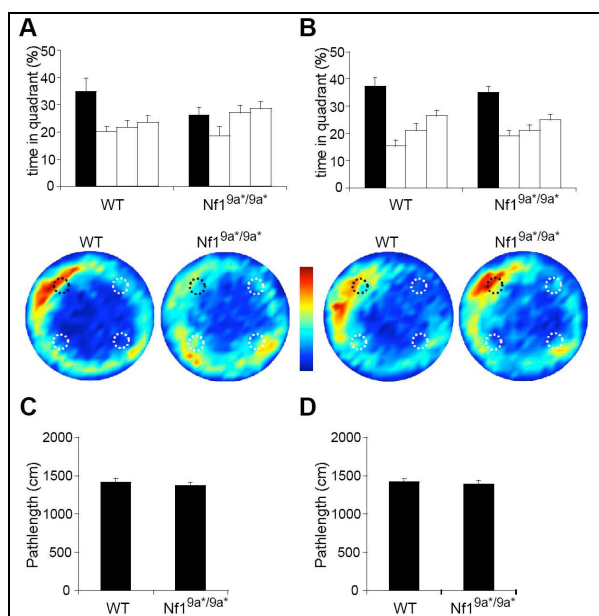


Figure 2. Hippocampal learning is reduced in NF1^{9a*/9a*} mice. NF1^{9a*/9a*} mutants show impaired hippocampal learning at the probe trial given at day 3 compared to their wild type littermates (A), which is improved after two additional training days (B). At the probe trial given at day 5 (B), the NF1^{9a*/9a*} mice caught up with their littermate controls and showed selective searching as judged from the time spend in target quadrant. Path length of NF1^{9a*/9a*} mice was not different from WT mice suggesting no deficits in swimming (C-D).

Long term potentiation is impaired in NF1^{9a*/9a*} mice

Learning is thought to require activity-dependent synaptic modifications in neuronal networks. To determine whether changes in synaptic plasticity might account for the spatial learning impairments of NF1^{9a*/9a*} mutants, we examined long-term potentiation (LTP) at

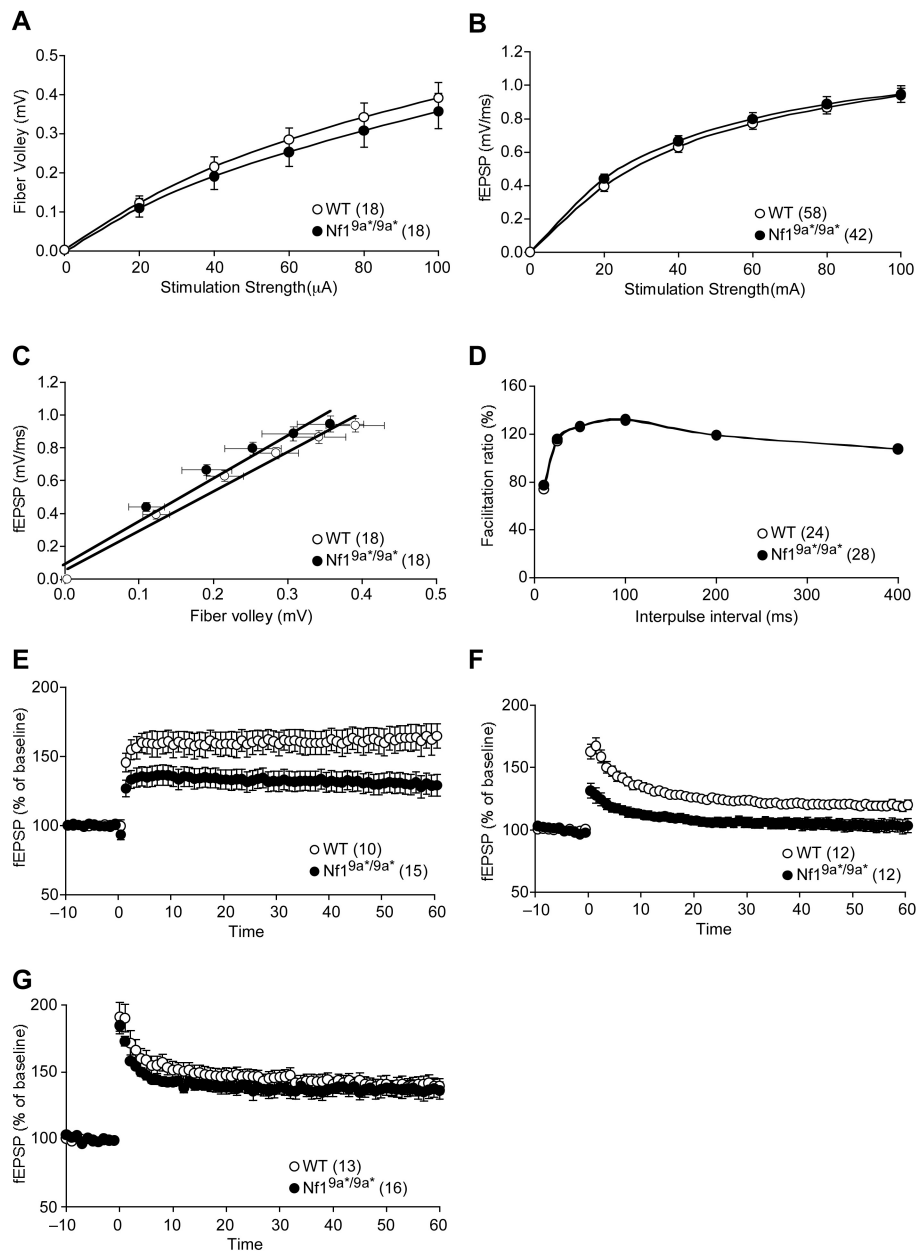


Figure 3. Synaptic transmission (A-C), Paired Pulse Facilitation (D) and long-term potentiation at Schaffer Collateral CA1 synapses in NF1^{9a*/9a*} mice. A-C, Basal synaptic transmission was normal in WT and NF1^{9a*/9a*} littermates. Plots show the presynaptic fiber volley as a function of stimulation strength (A), the fEPSP as a function of stimulation strength (B), the fEPSP as a function of the evoked presynaptic fiber volley (C). D, Paired-pulse facilitation was normal in NF1^{9a*/9a*} mice for intervals from 10-400 ms. E-G, LTP was reduced when induced by 10 Hz (E) and two-TBS stimulation (F), but not by 100Hz (G) stimulation.

Schaffer collateral/CA1 synapses in hippocampal slices from these mice. We first induced LTP using a 10 Hz stimulation protocol (100 stimuli/10s). This protocol elicited a significantly lower LTP in NF1^{9a*/9a*} mutants than that triggered in wild-type mice. (ANOVA $F(1,23) = 8.09, P < 0.01$, Figure 3E). We also used two-theta burst stimulation protocol to induce LTP in the hippocampal slices from wild type and mutant mice. As shown in Figure 3F, two-theta burst LTP in NF1^{9a*/9a*} mice is significantly lower than that measured in wild-type littermates (ANOVA $F(1,22) = 6.95, P = 0.01$). We also examined LTP induced under high-frequency stimulation (100 Hz for 1s). Consistent with the data from NF1^{+/-} mice (Costa et al., 2002), LTP induction showed equivalent potentiations in wild type and NF1^{9a*/9a*} mice using 100 Hz stimulation (ANOVA $F(1,27) = 0.12, P = 0.77$, Figure 3G).

Discussion

Several lines of evidence have shown that learning impairment is a common characteristic of neurofibromatosis type 1 (NF1). Most of these studies have pointed at the importance of the regulation of Ras by NF1 (Costa et al., 2001; Costa et al., 2002). However, it has recently been shown in flies that the role of NF1 in neuronal function is not restricted to its GAP function (Ho et al., 2007). Our experiments using NF1^{9a*/9a*} mutants suggest that the N-terminal exon 9a is critical for the role of NF1 in neuronal function, and thus confirm that the role of NF1 in neuronal function is not restricted to Ras regulation. Interestingly, in contrast to NF1^{+/-} mice (Costa et al., 2002), NF1^{9a*/9a*} mice showed no difference in basal transmission suggesting that the underlying molecular deficits may indeed be different from NF1^{+/-} mice. However, LTP induced by 10 Hz and theta-burst stimulation (TBS) protocols was deficient in NF1^{9a*/9a*} mutants but not at 100 Hz stimulation, which is consistent with the previous data from NF1^{+/-} mice (Costa et al., 2002). The theta burst stimulation protocol (TBS) is more physiological and mimics the *in vivo* activity of hippocampal neurons during exploratory behaviour (Larson et al., 1986). It has been suggested that LTP induced by TBS is more sensitive to changes in GABA-mediated inhibition than is LTP induced by high frequency stimulation (Chapman et al., 1998). In addition, results from a previous study showed an increase in GABA-mediated inhibition leads to LTP deficits in NF1^{+/-} mice (Costa et al., 2002). Future experiments will be required to investigate whether GABA-mediated inhibition is also underlying the learning and LTP deficits in the NF1^{9a*/9a*} mutants, or whether the impairments are due to other affected cellular mechanisms.

Methods

Generation of NF1 exon 9a mutant mice

NF1 mutant ES cells were generated as follows: A 1.5 Kb intronic DNA fragment was obtained by PCR using primers designed within exon 9 and exon 9a of the NF1 gene. This fragment was used to screen a C57Bl6 genomic DNA library. A 6 Kb fragment encoding exon9 and exon 9a was obtained. A PGK neomycin cassette flanked by LoxP sites was inserted in the SacI site, which is approximately 500 bp downstream of the exon 9a (Fig 1A). To make the neuronal specific deletion of *NF1 9a* (*NF1*^{9a*}), a stop codon as well as a frameshift mutation was introduced within exon 9a, by PCR based site directed mutations (Fig 1A). After transfection of R1 embryonic stem cells (derived from 129/Sv substrain (Nagy et al., 1993)) and selection with G418, targeted clones (approximately 4 %) were identified by Southern blot analysis. After checking the presence of the mutations by PCR/restriction analysis and sequencing, the PGK neo cassette was removed by a secondary transient transfection with pBS185 (Gibco) encoding the Cre recombinase. F1 heterozygous mice were obtained by injection of the ES cells into blastocysts of C57BL/6J mice, and crossing the resulting chimeras with C57/BL6^{tac}. F2 offspring used for behavioral analyses were obtained by subsequent crossing of the F1 heterozygous mice.

Western blotting

Lysates were prepared by quickly taking out the hippocampus of the mutant mice and homogenisation in lysis buffer (10mM TRIS-HCl 6.8, 2.5% SDS, 2mM EDTA and protease and phosphatase inhibitor cocktails (Sigma)). The concentration of the lysates was adjusted to 1 mg/ml. Western blots were probed with antibodies directed against Neurofibromin (sc-67, 1:200, Santa Cruz Biotechnology) and Actin (MAB1501R, 1:2000; Chemicon).

Water Maze

To test spatial memory we used a standard water maze task. Prior to the test, mice were handled extensively (2 min/day; 5 days). After the handling period, mice were trained in a circular water tank (120 cm in diameter, 40 cm high) to find an escape platform (11 cm of diameter) 1 cm below the surface of the water. The pool contained water (26 °C) made opaque by the addition of a non-toxic paint. Both the pool and the surrounding distal cues were kept fixed during all experiments. We use dimmed lighting, and mouse-tracking is performed using SMART version 2.0 (Panlab, Barcelona, Spain). Mice were given 4 trials per day, with 1 hour inter trial interval for 5 consecutive days. A trial consists of 2 training sessions where the mouse was first placed on the platform for 30 sec. Then it was placed in the water at a pseudo-random start position and it was given a maximum of 60 seconds to find the platform. If the mouse did not find the platform within 60 seconds, it was placed back on the platform. After 30 seconds on the platform, this training procedure was repeated. The platform position remained at the same position during all trials. One hour after the training on day 3 and day 5, a probe trial was given to test spatial learning. Mice were placed

on the platform for 30 seconds, after which the platform was removed from the pool and the mice were placed in the pool at the opposite side of the previous platform position. The mice were then allowed to search for the platform for 60 seconds.

Electrophysiology

Electrophysiological recordings were performed on adult mice and the experimenter was blind to genotype. After the animals had been sacrificed, hippocampi were removed in ice-cold artificial cerebrospinal fluid (ACSF), and sagittal hippocampal slices (400 μm) were prepared using a vibratome. Hippocampal slices were maintained in artificial cerebrospinal fluid (ACSF) at room temperature for at least 1.5 hour to recover before experiments were initiated. Then they were transferred to a submerged 4-chamber field recording set-up and perfused continuously at a rate of 2mL/minute with ACSF equilibrated with 95% O₂, 5% CO₂ at 30°C. ACSF contained (in mM) 120 NaCl, 3.5 KCl, 2.5 CaCl₂, 1.3 MgSO₄, 1.25 NaH₂PO₄, 26 NaHCO₃ and 10 D-glucose. Extracellular recording of field excitatory postsynaptic potentials (fEPSPs) was started 20 minutes after transfer to the recording chamber, in CA1 striatum radiatum area with a Pt/Ir recording electrode (FHC, Bowdoinham, ME). In all experiments, a bipolar Pt/Ir electrode was used for every chamber to stimulate Schaffer collateral/commissural afferents every minute. All stimulus pulses were 100 μs in duration and two-third of the maximum fEPSP. Stimulus response curves were obtained at the beginning of each experiment. For input-output curves, we applied different stimulation strengths from 10 to 100 μA . After a 10-min stable baseline recording, LTP (10Hz or two-theta burst) was induced.

References:

- Chapman CA, Perez Y, Lacaille JC (1998) Effects of GABA(A) inhibition on the expression of long-term potentiation in CA1 pyramidal cells are dependent on tetanization parameters. *Hippocampus* 8:289-298.
- Costa RM, Yang T, Huynh DP, Pulst SM, Viskochil DH, Silva AJ, Brannan CI (2001) Learning deficits, but normal development and tumor predisposition, in mice lacking exon 23a of Nf1. *Nat Genet* 27:399-405.
- Costa RM, Federov NB, Kogan JH, Murphy GG, Stern J, Ohno M, Kucherlapati R, Jacks T, Silva AJ (2002) Mechanism for the learning deficits in a mouse model of neurofibromatosis type 1. *Nature* 415:526-530.
- Danglot G, Regnier V, Fauvet D, Vassal G, Kujas M, Bernheim A (1995) Neurofibromatosis 1 (NF1) mRNAs expressed in the central nervous system are differentially spliced in the 5' part of the gene. *Hum Mol Genet* 4:915-920.
- Daston MM, Scrable H, Nordlund M, Sturbaum AK, Nissen LM, Ratner N (1992) The protein product of the neurofibromatosis type 1 gene is expressed at highest abundance in neurons, Schwann cells, and oligodendrocytes. *Neuron* 8:415-428.
- Geist RT, Gutmann DH (1996) Expression of a developmentally-regulated neuron-specific isoform of the neurofibromatosis 1 (NF1) gene. *Neurosci Lett* 211:85-88.
- Guo HF, The I, Hannan F, Bernards A, Zhong Y (1997) Requirement of Drosophila NF1 for activation of adenylyl cyclase by PACAP38-like neuropeptides. *Science* 276:795-798.

- Guo HF, Tong J, Hannan F, Luo L, Zhong Y (2000) A neurofibromatosis-1-regulated pathway is required for learning in *Drosophila*. *Nature* 403:895-898.
- Gutmann DH, Zhang Y, Hirbe A (1999) Developmental regulation of a neuron-specific neurofibromatosis 1 isoform. *Ann Neurol* 46:777-782.
- Gutmann DH, Geist RT, Rose K, Wright DE (1995a) Expression of two new protein isoforms of the neurofibromatosis type 1 gene product, neurofibromin, in muscle tissues. *Dev Dyn* 202:302-311.
- Gutmann DH, Geist RT, Wright DE, Snider WD (1995b) Expression of the neurofibromatosis 1 (NF1) isoforms in developing and adult rat tissues. *Cell Growth Differ* 6:315-323.
- Gutmann DH, Aylsworth A, Carey JC, Korf B, Marks J, Pyeritz RE, Rubenstein A, Viskochil D (1997) The diagnostic evaluation and multidisciplinary management of neurofibromatosis 1 and neurofibromatosis 2. *Jama* 278:51-57.
- Ho IS, Hannan F, Guo HF, Hakker I, Zhong Y (2007) Distinct functional domains of neurofibromatosis type 1 regulate immediate versus long-term memory formation. *J Neurosci* 27:6852-6857.
- Huson SM, Harper PS, Compston DA (1988) Von Recklinghausen neurofibromatosis. A clinical and population study in south-east Wales. *Brain* 111 (Pt 6):1355-1381.
- Huynh DP, Nechiporuk T, Pulst SM (1994) Differential expression and tissue distribution of type I and type II neurofibromins during mouse fetal development. *Dev Biol* 161:538-551.
- Larson J, Wong D, Lynch G (1986) Patterned stimulation at the theta frequency is optimal for the induction of hippocampal long-term potentiation. *Brain Res* 368:347-350.
- Nagy A, Rossant J, Nagy R, Abramow-Newerly W, Roder JC (1993) Derivation of completely cell culture-derived mice from early-passage embryonic stem cells. *Proc Natl Acad Sci U S A* 90:8424-8428.
- North KN, Riccardi V, Samango-Sprouse C, Ferner R, Moore B, Legius E, Ratner N, Denckla MB (1997) Cognitive function and academic performance in neurofibromatosis. 1: consensus statement from the NF1 Cognitive Disorders Task Force. *Neurology* 48:1121-1127.
- O'Connell P, Leach R, Cawthon RM, Culver M, Stevens J, Viskochil D, Fournier RE, Rich DC, Ledbetter DH, White R (1989) Two NF1 translocations map within a 600-kilobase segment of 17q11.2. *Science* 244:1087-1088.
- Ozawa T, Araki N, Yunoue S, Tokuo H, Feng L, Patrakitkomjorn S, Hara T, Ichikawa Y, Matsumoto K, Fujii K, Saya H (2005) The neurofibromatosis type 1 gene product neurofibromin enhances cell motility by regulating actin filament dynamics via the Rho-ROCK-LIMK2-cofilin pathway. *J Biol Chem* 280:39524-39533.
- Poyhonen M, Kytola S, Leisti J (2000) Epidemiology of neurofibromatosis type 1 (NF1) in northern Finland. *J Med Genet* 37:632-636.
- Silva AJ, Frankland PW, Marowitz Z, Friedman E, Laszlo GS, Cioffi D, Jacks T, Bourtschuladze R (1997) A mouse model for the learning and memory deficits associated with neurofibromatosis type I. *Nat Genet* 15:281-284.
- Xu GF, Lin B, Tanaka K, Dunn D, Wood D, Gesteland R, White R, Weiss R, Tamanai F (1990) The catalytic domain of the neurofibromatosis type 1 gene product stimulates ras GTPase and complements ira mutants of *S. cerevisiae*. *Cell* 63:835-841.
- Xu H, Gutmann DH (1997) Mutations in the GAP-related domain impair the ability of neurofibromin to associate with microtubules. *Brain Res* 759:149-152.

Chapter 6

Spatial navigation impairment in mice lacking cerebellar LTD: a motor adaptation deficit?

Published in

Nature Neuroscience 2005 October 8(10), 1292-1294

Spatial navigation impairment in mice lacking cerebellar LTD: a motor adaptation deficit?

Eric Burguière¹, Angelo Arleo^{1,4}, Mohammad reza Hojjati^{2,3}, Ype Elgersma², Chris I De Zeeuw², Alain Berthoz¹ & Laure Rondi-Reig¹

L7-PKCI transgenic mice, which lack parallel fiber–Purkinje cell long-term depression (LTD), were tested with two different mazes to dissociate the relative importance of declarative and procedural components of spatial navigation. We show that L7-PKCI mice are deficient in acquisition of an adapted goal-oriented behavior, part of the procedural component of the task. This supports the hypothesis that cerebellar LTD may subserve a general sensorimotor adaptation process shared by motor and spatial learning functions.

Spatial navigation offers a suitable framework to study the ability of animals to adapt their behavior to a specific context, defined here as the combination of the multimodal information sensed by the animal and its internal state at a specific time. Spatial navigation requires at least two complementary processes: (i) the development of a spatial representation of the environment (declarative component), enabling the animal to encode the spatiotemporal relationships among environmental cues or events, and (ii) the acquisition of a motor behavior adapted to the context in which navigation takes place (procedural component), permitting the execution of optimal (direct) trajectories toward rewarding locations¹. Testing of several cerebellar animal models in spatial navigation tasks² (Supplementary Note) has suggested that the cerebellum has a role in mediating the procedural component of spatial navigation. In this study, we focused on the cellular mechanisms subserving the contribution of the cerebellum in spatial learning. Our working hypothesis is that cerebellar LTD that occurs at the parallel fiber–Purkinje cell synapses and is required for the acquisition of classical conditioning tasks³ may also be necessary for the acquisition of efficient trajectories toward a spatial goal through a basic and common process of sensorimotor adaptation.

We used the L7-PKCI transgenic mice model⁴, which allows specific inactivation of parallel fiber–Purkinje cell LTD, to investigate the potential role of this cellular mechanism during spatial navigation (Supplementary Methods; all experiments were performed in compliance with European Union Council animal ethics guidelines). L7-PKCI mutants are known to have intact motor capabilities and normal electrophysiological properties of Purkinje cells^{5,6}

(Supplementary Note). Likewise, we did not observe any abnormalities in the sensorimotor reflexes, physical characteristics or general behavior of L7-PKCI mice (Supplementary Table 1). Hippocampal functions (synaptic transmission and plasticity), known to be essential for navigation tasks, were normal in L7-PKCI mice (Supplementary Fig. 1).

In order to dissociate the relative importance of the declarative and procedural components of navigation, we used two different behavioral tasks: the Morris water maze and a new task called the ‘starmaze’ (Fig. 1). In both cases, the animal has to find a fixed hidden platform from random departure locations, which requires the declarative capability to learn a spatial representation of the environment. Yet, in contrast to the Morris water maze task, the starmaze allows the animal to swim only within alleys guiding its movement. This helps the animal to execute goal-directed trajectories effectively, and reduces the procedural demand of the task.

To compare the navigation performances of L7-PKCI mice ($n = 14$) and their control littermates ($n = 15$) when solving the hidden-platform version of the Morris water maze, we used three standard parameters: (i) the mean escape latency, which measures the time the animal takes to reach the target and estimates its ability to learn the navigation task; (ii) the search score, which describes the goal-oriented trajectory quantitatively⁷, and (iii) circling behavior, defined as the time spent in a 10-cm annulus near the wall of the pool, already interpreted as a deficit in the procedural component of the spatial task⁸.

Both the mean escape latency and the search score of L7-PKCI mice were significantly higher than those in wild-type mice (ANOVA, $F_{1,27} = 14.2$, $P < 0.001$; and ANOVA, $F_{1,27} = 19.3$, $P < 0.001$; Fig. 2a). The

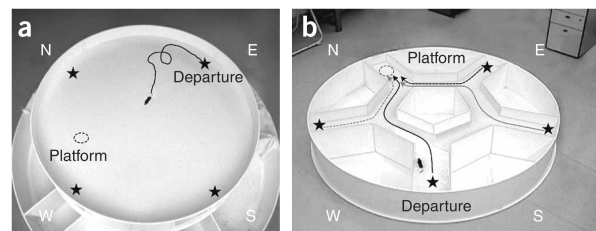


Figure 1 Comparison of two spatial navigation tasks. Both the Morris water maze (a) and the allocentric version of the starmaze task (b) require mice to find an escape platform (dashed circle) submerged under opaque water. To locate the platform efficiently, animals have to use the configuration of cues located outside the apparatus. In both tasks, animals are trained to reach the platform from four randomly selected departure points (black stars). Similar to the Morris water maze, solving the starmaze task implies spatial learning capabilities. In contrast, in the starmaze, animals are constrained to swim within alleys that guide their movements, which reduces the possible deviations from an ideal trajectory.

¹Laboratoire de Physiologie de la Perception et de l'Action, UMR CNRS 7152, 11 place Marcelin Berthelot, Collège de France, 75005 Paris, France.

²Department of Neuroscience, Erasmus MC, 3000 DR, Rotterdam, The Netherlands. ³Department of Physiology, Shahrekord University of Medical Sciences, Iran.

⁴Present address: Neuroscience Group, Sony Computer Science Laboratory, 6 rue Amyot, 75005 Paris, France. Correspondence should be addressed to L.R.-R. (laure.rondi-reig@college-de-france.fr).

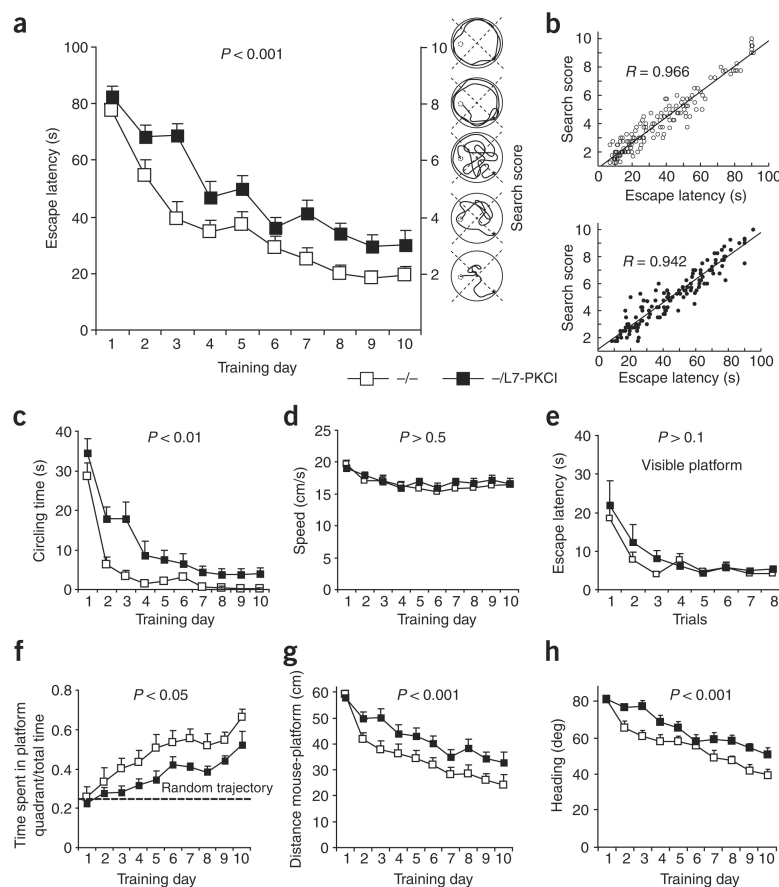


Figure 2 Inactivation of LTD in L7-PKCI mice affected their performance in the Morris water maze task. **(a)** The mean escape latencies of controls and mutants (open and filled squares, respectively) were similar at the beginning of training (day 1). However, controls improved their performance significantly better than mutants over time. The behavioral patterns corresponding to the search scores are illustrated by the cartoon trajectories on the right side: the lower the score, the better the searching behavior. The search scores of L7-PKCI mice were significantly higher than those of control animals. **(b)** The search scores and the escape latencies were highly correlated for both control (top) and mutant (bottom) mice, suggesting that the longer time-to-goal needed by L7-PKCI mice was due to non-optimal searching trajectories. **(c)** L7-PKCI mutants showed a significantly larger amount of circling behavior over training, which has been interpreted as a deficit in the procedural component of navigation⁷. **(d)** The mean swimming speeds of controls and mutants remained comparable over the entire training period. **(e)** Mutants are not impaired when solving the visible platform version of the Morris water maze (that is, the visual guidance navigation task). **(f)** The mean ratio of the time spent within the target quadrant to the total duration of the trial of both controls and mutants increased significantly above the random trajectory level during training. However, controls improved their ratio significantly better than L7-PKCI mice. **(g)** The mouse-platform distance parameter demonstrated that mutants followed significantly longer trajectories than controls. **(h)** The mean angular deviation between ideal and actual trajectory showed that mutants had a deficit in maintaining their body locomotion oriented toward the platform during navigation.

escape latency measure and the search score method were highly correlated for both groups of animals ($R = 0.966$, $P < 0.001$, and $R = 0.942$, $P < 0.001$, for wild-type mice and mutants, respectively; **Fig. 2b**). The circling times of the LTD-deficient mutants were also significantly longer than those of wild types (ANOVA, $F_{1,27} = 11.6$, $P < 0.01$; **Fig. 2c**). These results showed that L7-PKCI mice were impaired in solving the Morris water maze task. This spatial navigation impairment was due neither to a deficit in swimming speed (ANOVA, $F_{1,27} = 0.46$, $P > 0.5$; **Fig. 2d**) nor to a deficit in visual guidance abilities (ANOVA, $F_{1,27} = 1.2$, $P > 0.1$; **Fig. 2e**).

The ratio between the time spent in the target quadrant and the duration of the trial provides an estimate of the ability of an animal to locate the platform. Both groups of mice spent significantly more time in the target quadrant than in any other quadrant (ANOVA, $F_{1,9} = 15$, $P < 0.0001$), which suggested that both control and L7-PKCI mice were able to acquire a memory of the localization of the platform. However, an inter-group comparison of this ratio as a function of learning showed that L7-PKCI mice spent significantly less time than controls within the target quadrant (ANOVA, $F_{1,27} = 5.1$, $P < 0.05$; **Fig. 2f**). To investigate this difference and to assess the accuracy of the mice's goal-oriented behavior during learning, we calculated the average mouse-to-platform distance during a trial for both control and L7-PKCI mice (**Fig. 2g**). L7-PKCI mice showed a longer mean distance relative to the platform than control animals over the entire

training period (ANOVA, $F_{1,27} = 16.6$, $P < 0.001$). This result indicated that the trajectories of L7-PKCI mice toward the platform were less direct than those used by control mice. This issue was further investigated by computing the ongoing egocentric angle ($\phi(t) \in [0^\circ, 180^\circ]$) between the optimal direction towards the target and the actual motion direction of the animal. The larger the angle ϕ , the bigger the

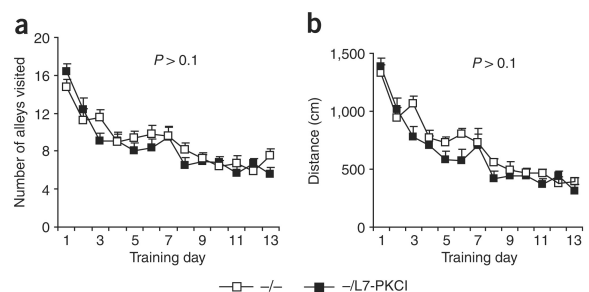


Figure 3 L7-PKCI mutants were not impaired in solving the allocentric version of the star maze task. **(a)** The mean number of alleys visited during a trial was not significantly different between control and mutant mice. **(b)** The distance swum to reach the target was not significantly different between the two groups.

deviation between the ideal goal-directed trajectory and the actual trajectory. Both groups significantly decreased their mean angular deviation from the ideal trajectory over training (ANOVA, $F_{1,9} = 29.4$, $P < 0.0001$; Fig. 2h). However, L7-PKCI mice showed significantly higher deviations than control mice (ANOVA, $F_{1,27} = 14.9$, $P < 0.001$). The statistical correlation between the mean angular deviation measure and the search score parameter was significant for both wild-type mice and mutants ($R = 0.871$, $P < 0.001$, and $R = 0.839$, $P < 0.001$, respectively).

The results obtained with the Morris water maze may suggest that L7-PKCI mice could learn to locate the platform (declarative component) but that they executed non-optimal goal-directed trajectories (procedural component; see **Supplementary Fig. 2** for a qualitative comparison between the searching behavior of controls and mutants over training). To test this hypothesis, we used a task requiring declarative capabilities but with a lower procedural demand than the Morris water maze: the allocentric starmaze task (**Supplementary Methods**). This task, similar to the Morris water maze, has been shown to depend on intact hippocampal function (L. Rondi-Reig *et al.*, *Soc. Neurosci. Abstr.*, 329.2, 2004). To assess the ability of mice to learn the starmaze task, we observed the number of visited alleys and the mean distance swum before finding the platform. Over time, both L7-PKCI mice ($n = 15$) and control mice ($n = 11$) significantly improved their ability to reach the platform quickly (ANOVA, $F_{1,24} = 7.45$, $P < 0.0001$). No statistical difference was observed between the two groups in the number of visited alleys (ANOVA, $F_{1,24} = 0.64$, $P > 0.1$, Fig. 3a) or the mean distance swum to reach the platform (ANOVA, $F_{1,24} = 2.56$, $P > 0.1$, Fig. 3b; see **Supplementary Fig. 3** for a qualitative representation of the similar behavior of controls and mutants).

The results obtained with the starmaze strengthened our hypothesis that the declarative component was not affected in L7-PKCI mice. The absence of a deficit when the trajectory was guided corroborated the results obtained with the Morris water maze, which suggested that L7-PKCI mice were unable to adapt their goal-oriented behavior effectively.

The parallel fiber–Purkinje cell LTD mechanism is likely to constitute a core process underlying cerebellar learning, and it has been proposed to contribute to both motor and cognitive learning⁹. It has been demonstrated that L7-PKCI mutants have response deficits in both adaptation of the vestibulo-ocular reflex⁴ and eyelid conditioning tasks¹⁰. In addition, cerebellar LTD seems most prominently involved in rapid learning of well-timed movements with specific amplitudes. Our results corroborate previous spatial navigation studies with other cerebellar models^{8,11} and suggest that parallel fiber–Purkinje cell LTD participates in the procedural component of navigation (**Supplementary Note**).

How could the same cellular mechanism (that is, parallel fiber–Purkinje cell LTD) be involved in motor learning as well as more cognitive processes such as spatial learning? Several cognitive processes can be considered on the basis of the same sensorimotor coupling scheme observed in classical motor learning¹². Spatial navigation requires a linkage between the spatial context (including sensory inputs and internal state information) and the explorative response (motor output) characterized by the animal's trajectory. Although the

spatial context may be conveyed by the mossy fiber–granule cell–parallel fiber pathway relaying information from the pontine nuclei¹³, errors in the explorative response may be mediated by the climbing fiber signals that originate from the olivary subnuclei that are innervated by descending projections from the mesodiencephalic junction and cerebral cortex¹⁴. As induction of parallel fiber–Purkinje cell LTD requires conjunctive activation of the parallel fiber and climbing fiber pathways, this form of synaptic plasticity could be responsible for the establishment of this linkage¹². Thus, the cerebellum may mediate a general learning function to create a context-response linkage adapted to the task¹⁵. During spatial learning, the subject could establish an appropriate context-response coupling resulting in effective motor behavior (for example, in the execution of optimal trajectories to the target). At the cerebellar level, procedural learning may result from a classical control learning scheme in which the feedback loop allows the system to converge towards an adapted context-motor linkage (**Supplementary Fig. 4**). The absence of parallel fiber–Purkinje cell LTD in L7-PKCI mice could result in an accumulation of errors over time (that is, during the execution of a goal-directed trajectory) due to the absence of continuous context-dependent corrections of the motor signals. From a behavioral point of view, the accumulation of these errors would lead to a drift during unconstrained (not guided) navigation as in the Morris water maze task, but it would be irrelevant in the starmaze task owing to the reduced number of possible goal-directed trajectories.

Note: Supplementary information is available on the Nature Neuroscience website.

ACKNOWLEDGMENTS

The authors thank M. Rutteman, V. Gautheron and F. Maloumian for technical support. L.R.-R. is supported by the Action Concertée Initiative 'Neurosciences intégratives et computationnelles' (NIC 0083), the Institut Fédératif de Recherche 52 'Transduction du signal: molécules à action centrale et périphérique', and the 'Groupement d'Intérêt Scientifique Longévité' (grant L0201). A.B. is supported by the Laboratoire Européen des Neurosciences de l'Action (LENA). C.I.D.Z. is supported by Nederlandse Organisatie voor Wetenschappelijk Onderzoek, the European Economic Community and Neuro-Bsik.

COMPETING INTERESTS STATEMENT

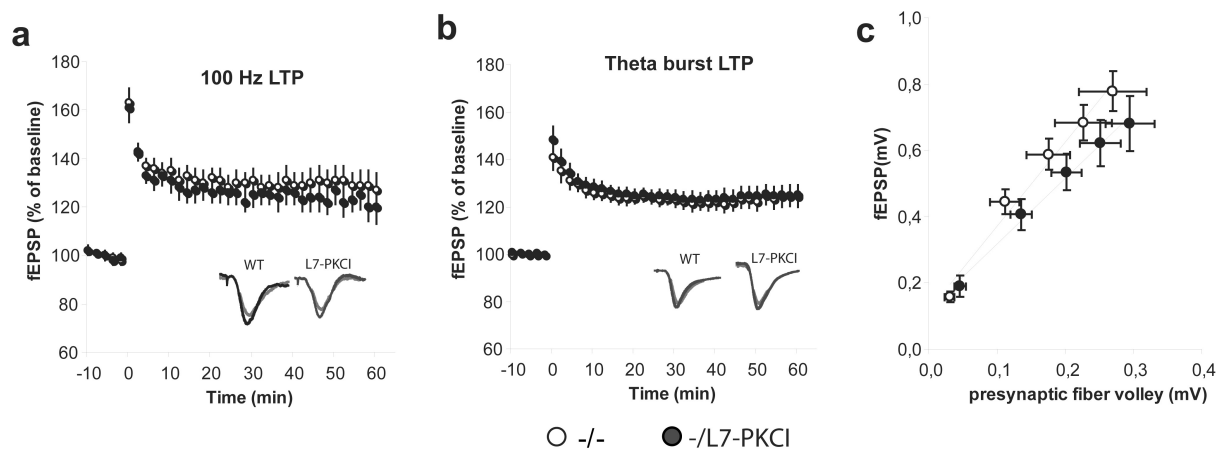
The authors declare that they have no competing financial interests.

Published online at <http://www.nature.com/natureneuroscience/>

Reprints and permissions information is available online at <http://npg.nature.com/reprintsandpermissions/>

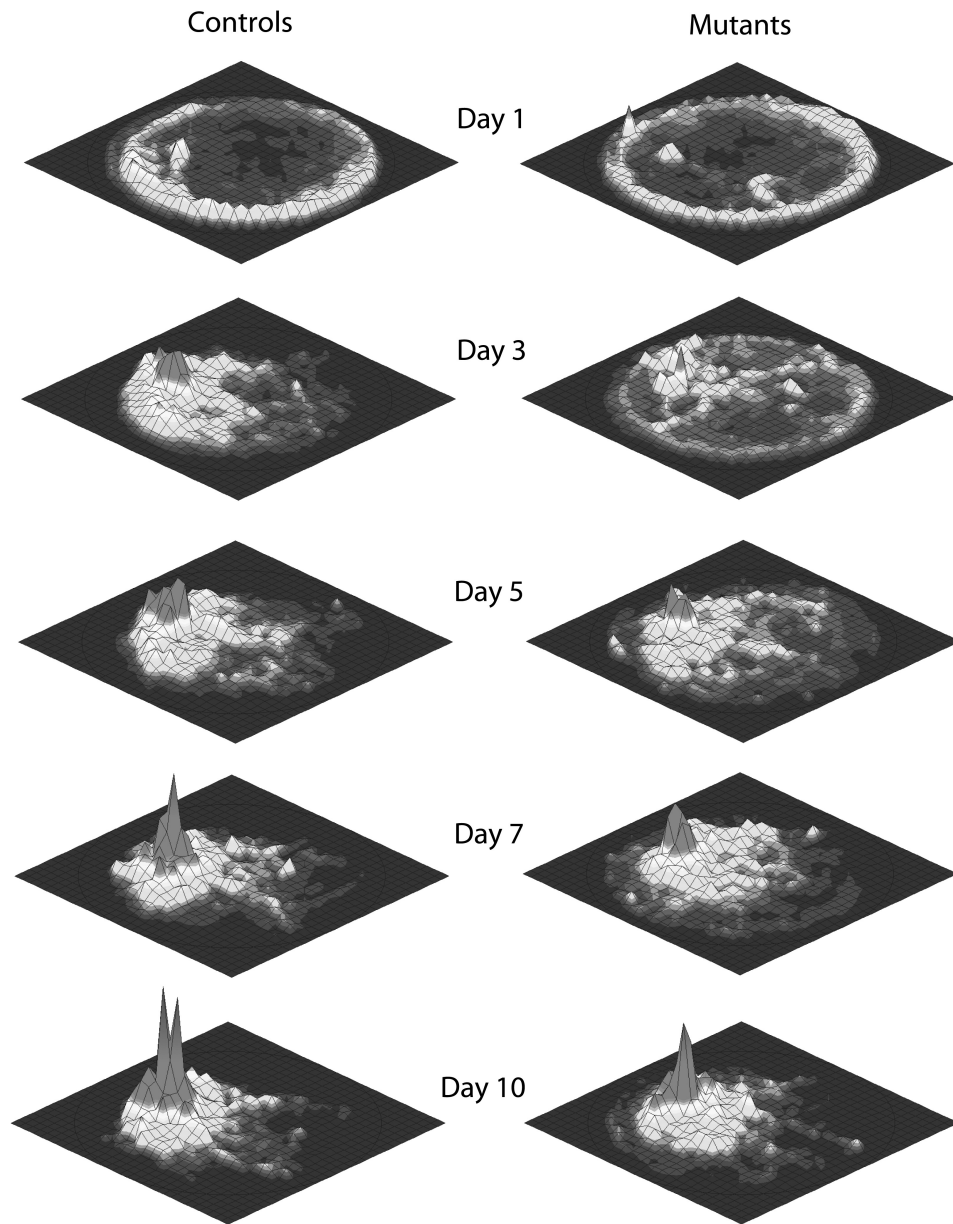
1. Schenk, F. & Morris, R.G. *Exp. Brain Res.* **58**, 11–28 (1985).
2. Rondi-Reig, L. & Burguiere, E. *Prog. Brain Res.* **148**, 199–212 (2005).
3. Thompson, R.F. *et al. Int. Rev. Neurobiol.* **41**, 151–189 (1997).
4. De Zeeuw, C.I. *et al. Neuron* **20**, 495–508 (1998).
5. Goossens, H.H. *et al. Eur. J. Neurosci.* **19**, 687–697 (2004).
6. Goossens, J. *et al. J. Neurosci.* **21**, 5813–5823 (2001).
7. Petrosini, L., Molinari, M. & Dell'Anna, M.E. *Eur. J. Neurosci.* **8**, 1882–1896 (1996).
8. Leggio, M.G. *et al. Exp. Brain Res.* **127**, 1–11 (1999).
9. Ito, M. *Physiol. Rev.* **81**, 1143–1195 (2001).
10. Koekkoek, S.K. *et al. Science* **301**, 1736–1739 (2003).
11. Martin, L.A., Goldowitz, D. & Mittleman, G. *Eur. J. Neurosci.* **18**, 2002–2010 (2003).
12. Ito, M. *Rev. Neurol. (Paris)* **149**, 596–599 (1993).
13. Thach, W.T., Goodkin, H.P. & Keating, J.G. *Annu. Rev. Neurosci.* **15**, 403–442 (1992).
14. De Zeeuw, C.I. *et al. Trends Neurosci.* **21**, 391–400 (1998).
15. Thach, W.T. *Int. Rev. Neurobiol.* **41**, 599–611 (1997).

Supplementary Figure 1

**Hippocampal functions are not impaired in L7-PKCI.**

Although the L7/PCP2 promoter restricts the expression of the PKCI transgene to Purkinje cells, it was conceivable that the unidentified integration site of the transgene may affect the expression of genes required for hippocampal plasticity and function. We directly assessed hippocampal plasticity by examining long-term potentiation (LTP) at the Schaffer collateral-CA1 synapse in acute hippocampal slices. We focused on the Schaffer collateral pathway because many previous studies have demonstrated that LTP at this synapse is crucial for learning contextual and spatial information. **(a)** LTP was first induced using a commonly used 100 Hz stimulation protocol. We found no significant differences between LTP induced in wild-type (WT) mice as compared to PKCI littermate mice (WT: 11 slices, 4 mice; PKCI: 17 slices, 5 mice; ANOVA $F_{1,26} = 0.65$, $P = 0.42$). **(b)** We then assessed the level of LTP induction using five theta-burst stimulation (TBS), which mimics the in vivo activity of hippocampal neurons during exploratory behavior and might be more sensitive to reveal changes in plasticity. Again, LTP in control mice was indistinguishable from LTP in PKCI mice (WT: 12 slices, 4 mice; PKCI: 13 slices, 5 mice; ANOVA $F_{1,23} = 0.01$, $P = 0.93$). At the bottom of **(a, b)**, representative traces are shown at baseline (red line) and at 60 min after LTP induction (black line) (left, WT; right, PKCI). **(c)** Finally, also synaptic transmission was not significantly different between mutants and controls (WT: 17 slices, 4 mice; PKCI: 18 slices, 5 mice; presynaptic fiber volley: $F_{4,132} = 0.04$, $P = 0.99$; postsynaptic fEPSP: $F_{4,132} = 1.21$, $P = 0.31$). Plots show the fEPSP as a function of the evoked presynaptic fiber volley, at 20, 40, 60, 80, 100 μ A stimulation. The line represents the calculated trend line.

Supplementary Figure 2

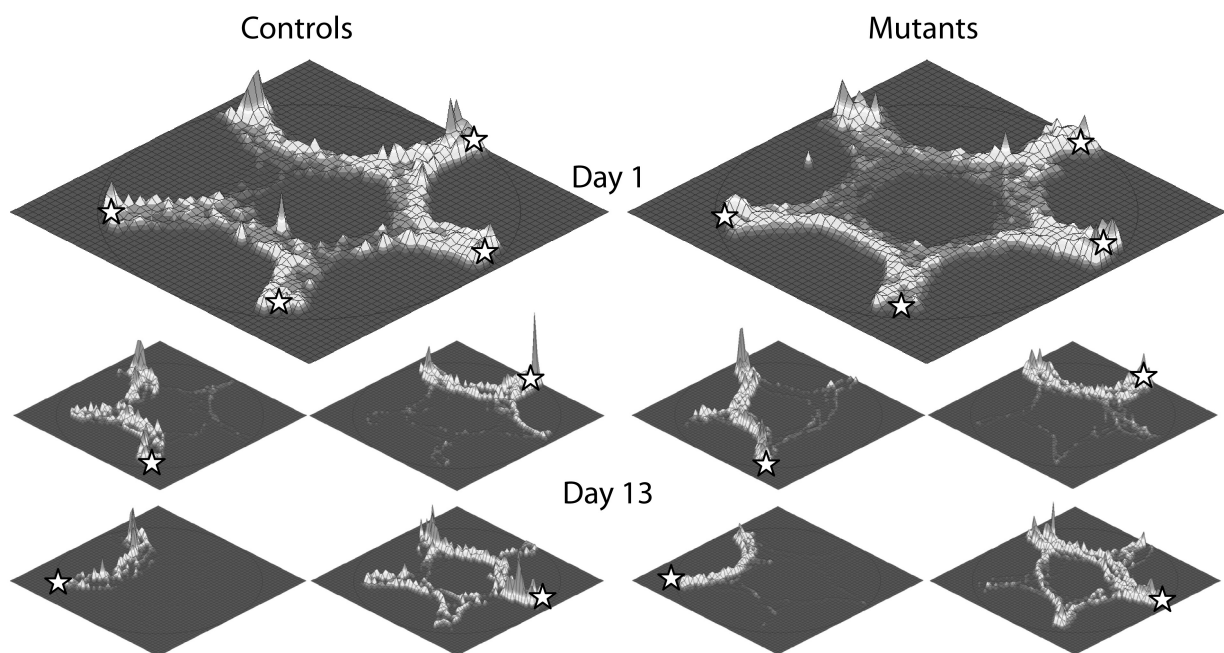


Three-dimensional diagrams of the mean time spent by control and mutant mice at each location of the maze at different training phases.

Qualitative representations of the time (z axis) spent on average by the two groups of animals in the different areas of the pool (x-y axes) at different learning phases (days 1, 3, 5, 7 and 10). Spatial locations were sampled by means of a grid of resolution 30 x 30 (each grid cell is about 5 x 5 cm). The value associated to each grid cell was obtained by normalizing the time spent in the cell region with respect to the duration of each trial, then averaging over all day trials and over all the animals of a group.

These three-dimensional plots show that, when solving the Morris water maze task, mutant mice had larger searching zones than control animals during the whole learning period.

Supplementary Figure 3



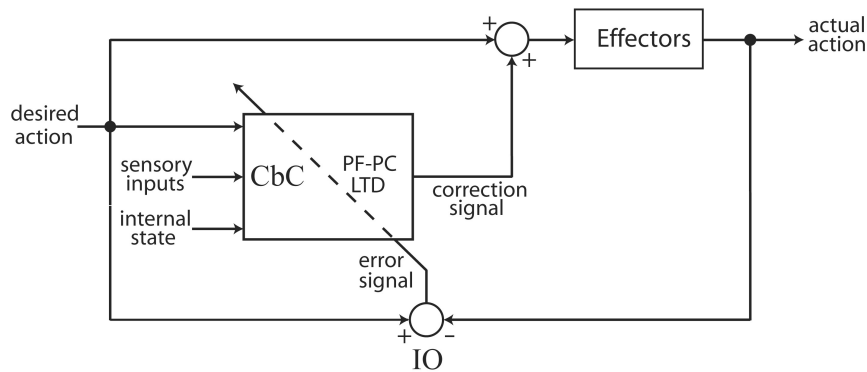
Three-dimensional diagrams showing the mean time spent by the two groups of animals at each location of the Sarmaze at the beginning (day 1) and at the end (day 13) of training.

The white stars indicate the departure positions. Spatial locations were sampled by means of a grid of resolution 50 x 50 (each grid cell is 4 x 4 cm). The value associated to each grid cell was obtained by normalizing the time spent in the cell region with respect to the duration of each trial, and subsequently averaging over all day trials and over all the animals of a group.

On day 1, both groups of mice visited the different alleys of the maze regardless of the starting position (**top left and top right**). No direct trajectory from the departure point to the platform was observed. After 13 days of training, control mice learned to swim directly from each of the departure points to the platform (**bottom left**). Similarly, L7-PKCI mice learned to find the location of the platform through direct pathways from each of the four departure points (**bottom right**).

These plots confirmed that control and mutant mice had a comparable behavior when solving the Sarmaze task.

Supplementary Figure 4



Abstract model describing the error-based cerebellar learning hypothesis (adapted from Ito, M. New concepts in cerebellar function. *Rev. Neurol. (Paris)* 149, 596-599 (1993)).

This theoretical model can be applied to study the process of sensory-response adaptation underlying both basic motor learning and higher cognitive learning. Contextual information (i.e., multimodal sensory signals, animal's internal state, and desired action) enters the cerebellar cortex (CbC) via the mossy fiber – granule cell – parallel fiber pathway. The inferior olive (IO) generates an error signal based on the discrepancy between desired and actual action, and conveys this information to the cerebellum via the climbing fibers. The convergence of both contextual and error signals at precise timing can induce Long-Term synaptic Depression (LTD) at the parallel fiber – Purkinje cell (PF-PC) synapses. This learning process can lead to the acquisition of the optimal sensory-response linkage and, then, it allows the cerebellum to compensate for the error dynamically. In the case of spatial navigation, this can result in the optimization of the goal-directed trajectory performed by the animal. Specific inactivation of the PF-PC LTD mechanism would impair cerebellar learning and disrupt the correction signal. This would result in non-optimal spatial behavior due to cumulative error over time.

Supplementary Table 1

Sensorimotor reflexes	Mutants	Controls	Physical characteristics	Mutants	Controls
Cage movement	15/15	14/14	Presence of whiskers	15/15	14/14
Whisker response	15/15	14/14	Palpebral closure	0/15	0/14
Eyeblink	15/15	14/14	Piloerection	0/15	0/14
Ear twitch	15/15	14/14	Body weight (g)	26.6 +/- 0.3	26.4 +/- 0.9
General behavior observations			Equilibrium and motor abilities		
Wild running	0/15	0/14	Hanging test (sec)	44.4 +/- 8.6	50.7 +/- 12.6
Freezing	0/15	0/14	Static rotarod (sec)	18.3 +/- 3.2	15.7 +/- 3.2
Licking	12/15	13/14	Unstable platform (sl/min)	0.76 +/- 0.15	0.97 +/- 0.12
Jumping	0/15	0/14	Hole board (st/min)	1.8 +/- 0.5	2.6 +/- 0.3
Defecation	3/15	4/14	Anxiety		
Urination	2/15	3/14			
Sniffing	15/15	14/14			
Rearing	15/15	14/14			
Move around entire cage	15/15	14/14	Time in the open arms (%)	16.0 +/- 2.2	13.1 +/- 2.0
			Number of entrances in the open arms (%)	34.2 +/- 3.0	31.2 +/- 3.0

General appearance and motor abilities of mice.

No abnormalities were observed in the sensory-motor reflexes, physical characteristics, and general behavior of L7-PKCI mice. Importantly, balance and motor ability tests including unstable platform and hanging tests showed no statistical difference between mutants ($n = 14$) and controls ($n = 15$) (unpaired T-test, $P > 0.05$). Similarly, the anxiety test did not reveal any statistical difference (unpaired T-test, $P > 0.05$) between mutants and control mice.

Abbreviations: sl for slip and st for stumble.

SUPPLEMENTARY METHODS

Experimental subjects

Heterozygous transgenic L7-PKCI (-/L7-PKCI) mice and their wild-type (-/-) littermates were used for this study. In the L7-PKCI mouse, the pseudosubstrate PKC inhibitor, PKCI, is selectively expressed in Purkinje cells under the control of the *pcp-2* (L7) gene promoter¹. All animals were bred in a C57BL/6 mouse strain background and were housed in standard conditions (12h light/12h dark, water and food *ad libitum*). Both control and transgenic L7-PKCI mice underwent experiments between 3.5 to 6 months. All the behavioral analyses were performed blind with respect to the genotype of the mice. All experiments were performed in compliance with the European ethical animal committee.

Behavioral experiments

According to the S.H.I.R.P.A. protocol for comprehensive phenotype assessment², all animals were tested by a series of experiments run sequentially. The first screen was a set of behavioral tests concerning general appearance and neurological reflexes. The second screen aimed to detect eventual motor, equilibrium or anxiety differences between control and mutant mice. The third screen assessed their spatial navigation abilities. We tested 14 mutants and 15 controls for the Morris water maze task, and 15 mutants and 11 controls underwent the starmaze task.

General appearance and neurological reflexes

Animals were tested for gross abnormalities that could interfere with their behavior in the navigation tasks. General appearance was evaluated by observing the presence of whiskers, the absence of palpebral closure and pilo-erection. Body weight was recorded. Each mouse was then placed for three minutes in an unfamiliar standard mouse cage for observation of any abnormal spontaneous behavior. Examples of aberrant actions include wild running, abnormal jumping or grooming, and frozen immobility. Three neurological reflexes were studied according to established protocols³. Approaching the eye and touching the ear with the tip of a clean cotton swab tested the eyeblink reflex and the ear twitch reflex, respectively. The whisker-orienting reflex was tested by lightly brushing the whiskers of a freely moving animal with a small paintbrush.

Basic motor skills

A series of tests was carried out in order to compare control and L7-PKCI transgenic mice in terms of motor and equilibrium abilities.

Muscle strength was tested by hanging the mouse by its two anterior paws on a rod (25 cm long, 0.3 cm in diameter) located 1 m above a thick carpet to cushion falls. The time the animal hung on a wire without falling was recorded⁴.

To quantify dynamic balance, we used the rotarod apparatus in a fixed position. The rotarod apparatus consists of a wooden horizontal rod 3 cm in diameter and 50 cm long. The animal was placed at the middle of the non rotating rod, its body axis perpendicular to the rod longitudinal axis. The time the animal remained on the rod was recorded. Each trial ended either when the animal fell or after 180 s (in accordance with the rotarod protocol). This test measures the *dynamic* balance because the animal can anticipate and even prevent any fall⁴. We used an unsteady platform⁵ to quantify *static* balance. Mice had to remain still on a narrow unsteady elevated platform, which could tilt by 30° in every direction. The slip frequency on the board was calculated for three trials per animal.

To assess both exploratory behavior and motor coordination, a hole-board was designed⁴ by deriving it from the one used by⁶ with cerebellar mutant mice. It consists of an experimental box (35 x 35 x 25 cm), with a raised (2 cm) platform in which 36 holes (2 cm in diameter, arranged in a 6 x 6 array) have been drilled. The mouse was placed in the middle of the platform and its behavior was video-recorded. Walking time and number of stumbles were counted. To control the possibility that mice stumbled more often simply because they were more active on the hole-board, the number of stumbles per minute of walking time was calculated. This stumble frequency was considered as a measure of motor coordination⁷.

Anxiety test

The classical elevated “+” maze⁸ was employed for this test. It is a cross-shaped maze with two high-walled arms and two wall-less arms. Each arm is 24 cm long and 8 cm wide. Walls are 20 cm high. The whole apparatus was elevated 1 m above the floor. Previous studies have shown that anxious mice spend more time in the walled arms rather than in the open ones. Anxiolytic treatment significantly increases the number of entries in open arms, whereas anxiogen reduces it⁹. We measured the percentage of number of entries and the percentage of time spent by

the animals in the open arms. An entry was considered effective when the animal placed its four paws in the arm. The test lasted 5 min.

Navigation tasks

Two different apparatus were employed for the navigation tasks: the Morris water maze¹⁰ and the allocentric version of the Starmaze task (L. Rondi-Reig *et al.*, Soc. Neurosci. Abstr., 329.2, 2004) (**Fig. 1**).

The Morris water maze task.

Mice were trained in a circular water tank (150 cm in diameter, 40 cm high) to find an escape platform (10 cm of diameter) hidden 1 cm below the surface of the water at a fixed location (**Fig. 1a**, NW quadrant). The pool contained water (21 °C) made opaque by the addition of an inert and nontoxic product (Accusan OP 301). Both the pool and the surrounding distal cues were kept fixed during all experiments. Each mouse underwent one training session per day consisting of four trials. The starting position (North, East, West, or South) was randomly selected with each quadrant sampled once a day. At the beginning of each trial, the mouse was released at the starting point (black stars in **Fig. 1a**) and made facing the inner wall. Then, it was given a maximum of 90 s to locate and climb onto the escape platform. If the mouse was unable to find the platform within the 90 s period, it was taken to the platform by the experimenter. In either case, the mouse was allowed to remain on the platform for 30 s. Animals received 40 training trials over 10 days.

The measured parameters were: (i) the average time necessary to reach the platform (i.e., mean escape latency); (ii) the search score¹¹; (iii) the average speed; (iv) the amount of circling (i.e., the time spent in a 10 cm annulus near the wall of the pool); (v) the mean distance of the mouse relative to the platform, averaged over trials as well as over the entire training period; (vi) the ratio between the time spent in the target quadrant (i.e., the quadrant containing the platform) and the duration of the trial; (vii) the "mean angular deviation" (i.e., the angle between the optimal direction towards the target and the actual motion direction of the animal). For each trial, we computed the mean deviation $\bar{\phi}_i = \langle \phi(t) \rangle_{t \in [0, T_i]}$, where i is the trial and T_i denotes the duration of the trial. Then, we averaged over all the trials performed in one day by all the subjects of the same group of animals.

After training, mice underwent the visible platform task. A proximal cue was placed on the top of the submerged platform, which was positioned at one of four possible locations (North, East, West, and South). To solve this task, animals had to learn that the proximal cue (beacon) indicated the location of the platform. The starting position of the animal was fixed and located at the center of the circular water tank. The test was performed during two consecutive days with four trials a day. The four possible locations of the platform were randomly sampled each day. The time needed by the mice to reach the platform was measured.

The allocentric (multiple departures) version of the Starmaze task.

The Starmaze is an aquatic maze with five alleys forming a central pentagonal ring with a side distance of 37 cm and five peripheral alleys radiating from this pentagonal ring (**Fig. 1b**). Each radial alley is 47 cm long and 25 cm wide. The entire maze (204 cm diameter) is filled with water that has been made opaque with an inert and nontoxic product (Accuscan OP 301). The maze was placed at a fixed location inside a large room (50 m²) with fixed 3D extra-maze cues. We used a random-departure protocol (similar to that employed for the Morris water maze) lasting 13 days and forcing the animal to use an allocentric strategy to perform the task. The platform was always located at the end of alley 7. The mouse was placed at the end of a randomly selected radial arm not containing the platform (i.e. 1, 3, 5, and 9). Each mouse was given four trials per day, each trial corresponding to a different departure arm. If an animal was not able to find the platform within a 90 s period, it was taken to the platform by the experimenter. In either case, the animal was left for 30 s on the platform. The measured parameters were the distance traveled and the number of alleys visited by the animal in order to find the platform.

Electrophysiological recording

Sagittal hippocampal slices (400 µm) were placed in a submerged 4-chamber recording set-up and perfused continuously at a rate of 1.5 mL/min with artificial cerebrospinal fluid (ACSF) equilibrated with 95% O₂, 5% CO₂ at 30°C. ACSF contained (in mM) 120 NaCl, 3.5 KCl, 2.5 CaCl₂, 1.3 MgSO₄, 1.25 NaH₂PO₄, 26 NaHCO₃, 10 D-glucose. Extracellular recordings of field excitatory postsynaptic potentials (fEPSPs) were made in CA1 stratum radiatum with Pt/Ir electrodes (FHC, Bowdoinham, ME). In all experiments, a bipolar Pt/Ir electrode was used to stimulate the Schaffer collateral/commissural afferents prodromically every minute. All stimulus

pulses were 100 μ s in duration and one- (100 Hz) or two-thirds (theta burst LTP) of the maximum fEPSP, which was assessed first by an input-output curve. Average stimulation strength and baseline fEPSP were similar between genotypes for all of the experiments conducted. For LTP, statistical comparisons were made using the number of slices as sample size.

Data acquisition and statistical analysis

Data acquisition was performed by means of a video recording system and a tracking software. Data processing (e.g., the computation of the assessed parameters) was automated via a MATLAB batch program developed in our laboratory. Data were analyzed with the Statview 5.0 software by means of *T*-test and repeated measure analysis of variance (ANOVA). The significant threshold of tests was fixed at 5 % ($p < 0.05$ was significant). All data are presented as mean \pm S.E.M.

References

1. De Zeeuw, C. I. et al. *Neuron* **20**, 495-508 (1998).
2. Crawley, J. N. *Neuropeptides* **33**, 369-375 (1999).
3. Paylor, R. et al. *Learn. Mem.* **5**, 302-316 (1998).
4. Rondi-Reig, L. et al. *Neuroscience* **77**, 955-963 (1997).
5. Hilber, P., Lalonde, R., & Caston, J. J. *J. Neurosci. Methods* **88**, 201-205 (1999).
6. Guastavino, J. M. *Physiol Behav.* **32**, 225-228 (1984).
7. Rondi-Reig, L. & Mariani, J. *Brain Res. Bull.* **57**, 85-91 (2002).
8. Pellow, S. et al. *J. Neurosci. Methods* **14**, 149-167 (1985).
9. Lister, R. G. *Psychopharmacology (Berl)* **92**, 180-185 (1987).
10. Morris, R. et al. *Nature* **297**, 681-683 (1984).
11. Petrosini, L., Molinari, M., & Dell'Anna, M. E. *Eur. J. Neurosci.* **8**, 1882-1896 (1996).

SUPPLEMENTARY NOTES

1. Previous studies with cerebellar models.

Several types of cerebellar animal models have been tested in spatial navigation tasks: mutant mice¹, hemocerebellectomized rats², and rats with cerebellar input lesions³. All cerebellar animals showed impaired learning capabilities when tested with the classical Morris water maze, a task in which the animal has to find a fixed hidden platform from either multiple or a unique starting position⁴. The consensus that emerged from these studies points toward a role⁵ of the cerebellum in mediating the procedural component of the spatial navigation function. Likewise, recent data suggested that the procedural impairment observed in cerebellar animals could also induce a more cognitive impairment since the acquisition of a declarative spatial memory relies on the learning of a correct explorative behavior⁶⁻⁸.

2. Electrophysiological properties of the L7-PKCI mouse model.

De Zeeuw and colleagues have demonstrated that adult L7-PKCI mutant mice have intact baseline discharges of Purkinje cells and no persistent multiple climbing fiber innervation⁹. In fact, even during an optokinetic reflex task, which can be used during visuo-vestibular training, both simple spike and complex spike responses of Purkinje cells appear normal¹⁰.

2. Procedural learning and PF-PC LTD mechanism.

Procedural learning can be defined as the process that permits to execute a new action properly¹¹. In particular, this action has to be optimal with respect to the task to be solved. Our hypothesis of a role of PF-PC LTD in the procedural component of navigation was inspired by the theory that considers the cerebellar learning process as an error based system¹²⁻¹⁴. Marr-Albus-Ito theory postulates that the climbing fibers convey error information to the parallel fiber - Purkinje cell synapses and trigger a modulation of their strength via the LTD mechanism. Ito showed that in VOR adaptation experiments PF-PC LTD is likely to constitute the neural substrate of such an error-driven motor learning process¹⁵. In the case of spatial navigation, the trajectory performed by the animal must be adapted to the spatial context and optimized to lead directly to the goal.

References

1. Lalonde, R. & Botez, M. I. *Brain Res.* **398**, 175-177 (1986).
2. Petrosini, L., Molinari, M., & Dell'Anna, M. E. *Eur. J. Neurosci.* **8**, 1882-1896 (1996).
3. Rondi-Reig, L. et al. *Behav. Brain Res.* **132**, 11-18 (2002).
4. Petrosini, L., Leggio, M. G., & Molinari, M. *Prog. Neurobiol.* **56**, 191-210 (1998).
5. Leggio, M. G. et al. *Exp. Brain Res.* **127**, 1-11 (1999).
6. Gandhi, C. C. et al. *Behav. Brain Res.* **109**, 37-47 (2000).
7. Joyal, C. C., Strazielle, C., & Lalonde, R. *Behav. Brain Res.* **122**, 131-137 (2001).
8. Mandolesi, L. et al. *Eur. J. Neurosci.* **18**, 2618-2626 (2003).
9. Goossens, J. et al. *J. Neurosci.* **21**, 5813-5823 (2001).
10. Goossens, H. H. et al. *Eur. J. Neurosci.* **19**, 687-697 (2004).
11. Hikosaka, O. et al. *Trends Neurosci.* **22**, 464-471 (1999).
12. Marr, D. *J. Physiol* **202**, 437-470 (1969).
13. Albus, J. *Math. Biosci.* **10**, 26-61 (1971).
14. Ito, M. (1984).
15. Ito, M. & Kano, M. *Neurosci. Lett.* **33**, 253-258 (1982).

Chapter 7

General Discussion

7.1 General discussion

The overall aim of the studies described in this thesis was to obtain greater understanding of the molecular and cellular mechanisms underlying spatial learning, focusing on hippocampal learning and plasticity. To elucidate the role of several presynaptic and postsynaptic mechanisms that modulate hippocampal and cerebellar learning, we made use of various mouse mutants in our studies. One of these mutants gave us the opportunity to investigate how a specific presynaptic change affects pre- and postsynaptic plasticity and learning. As described in chapter 2, we made use of transgenic mice expressing a constitutively active form of H-ras protein (H-ras^{G12V}). We demonstrated that this protein is abundantly localized to axon terminals. We further demonstrated that this mutation resulted in a higher density of docked neurotransmitter vesicles in the excitatory terminals, an increased frequency of mEPSCs, and increased paired-pulse facilitation. We also showed that this presynaptic change leads to a postsynaptic change, that is, an increased long-term potentiation following high frequency stimulation. Moreover, H-ras^{G12V} mice showed a dramatic enhancement in both spatial learning and contextual fear conditioning.

What are the molecular mechanism underlying these effects? Ras is a potent upstream activator of ERK. In turn, ERK is known to phosphorylate synapsin I, an abundant presynaptic protein associated with synaptic vesicles and implicated to be involved in the organizing the vesicle pool. Indeed, we found that ERK-dependent phosphorylation of synapsin I was significantly elevated in H-ras^{G12V} mice. Moreover, we showed that the LTP enhancement of the H-ras^{G12V} mice was dependent upon the presence of synapsin I, making this the most likely downstream target of the presynaptic H-Ras/ERK pathway. Nevertheless, we cannot exclude that some of the presynaptic effects observed in this study, are caused by activation of other downstream targets of H-Ras or ERK. To investigate this, the entire study could be repeated in the H-ras^{G12V} / synapsin I double mutant. However such a study is not very attractive for four reasons: First, it would require a side-by-side analysis of four different groups of mutants (wild-type mice, the two single mutants, and the double mutant). Second some of the measures would be confounded by the fact that the loss of synapsin I itself causes changes in several presynaptic measures (e.g. PPF, vesicle pool organization). Third, synapsin I is also regulated by CaMKII and PKA. Thus loss of synapsin I could cause phenotypes that are not directly mediated by the ERK phosphorylation site. Fourth, deletion of synapsin I occurs in all cell-types and may cause developmental effects. In contrast, H-ras^{G12V} expression is driven by the α CaMKII promoter, which restricts expression to relatively mature excitatory neurons.

Therefore, to prove that synapsin I phosphorylation by ERK modulates the observed pre-synaptic and postsynaptic phenotypes another option is more attractive. A transgenic synapsin I mutant could be generated, in which the constitutive phosphorylation of synapsin I at the ERK site is mimicked. If pre-synaptic changes and learning enhancements in these mice are the same as what we have found in H-ras^{G12V} mice, our hypothesis will be supported more strongly.

It is actually quite surprising that the effects of the H-ras^{G12V} mutation appeared to be restricted to the presynaptic site, since there is overwhelming evidence for a postsynaptic ERK signalling pathway. How did this specificity arise? There are three major Ras isoforms in the brain, H-Ras (which we found to be the most abundant one) N-Ras, and K-Ras. It could be that H-Ras is mostly present in the axons whereas K-Ras and N-Ras are mostly present in the dendrites. A detailed immuno-cytochemistry study could shed more light on this issue. In addition it would be interesting to investigate the phenotype of a K-Ras or N-Ras gain of function mutant. This might well result in major post-synaptic changes without affecting presynaptic plasticity.

In chapter 3 we investigated the role of α CaMKII in presynaptic plasticity. But in contrast to chapter 2, in which we concluded that a change in the ERK phosphorylation of synapsin I affected several pre- and postsynaptic measures; we did not find such a role for α CaMKII-dependent synapsin I phosphorylation. Specifically, we were unable to find a correlation between α CaMKII-dependent synapsin I phosphorylation and CaMKII-dependent presynaptic measures such as synaptic fatigue and augmentation. This raised the question to what extent α CaMKII activity was required for these measures. Using targeted genetic mutations and competitive inhibitors to prevent Ca/CaM binding, we demonstrated unambiguously that α CaMKII autophosphorylation and its Ca/CaM-dependent activation are not required for normal short-term presynaptic plasticity. However these measurements do not exclude the possibility that some remaining α CaMKII basal activity is still required. However, the observation that augmentation and synaptic fatigue are not affected by the AIP inhibitor (which blocks basal activity) or by a mutation (T305D) that blocks CaMKII autophosphorylation, this option is not very likely. The best way to settle this would be the 'kinase-dead' α CaMKII-K42R mutant, in which the catalytic site of α CaMKII is mutated. Recently, this mutant has been generated by Y. Yamagata, (SFN 2006 abstract- The role of protein phosphorylation in brain functions revealed by inactivated α CaMKII knock-in mouse). Importantly, while α CaMKII protein is totally inactive in these mice, augmentation was normal (Y. Yamagata, personal communication). This finding confirms our conclusion and indicates a structural (non-enzymatic) role for α CaMKII in presynaptic short-term plasticity measures such as

augmentation and synaptic fatigue during repetitive 10Hz stimulation. It would now be very interesting to investigate to which proteins CaMKII is able to bind, and which domains are required for such an interaction. Co-immunoprecipitations and two-hybrid screens would help to address these questions.

Does our finding mean that presynaptic α CaMKII activity is not important at all? A recent study in cultured hippocampal neurons showed that presynaptic CaMKII activity was required for changing the glutamate-induced mEPSC frequency and amplitude, as well as for the number of presynaptic functional boutons. (Ninan and Arancio, 2004). In addition, it was shown that CA3-CA3 LTP in culture organotypic slices required the activation of presynaptic CaMKII (Lu and Hawkins, 2006). These findings could indicate that presynaptic α CaMKII activity is required for other presynaptic measures, in particular in those measures that involve a longer time scale. However, given the experimental approach one should be careful to draw such firm conclusions. A better approach that would directly test this hypothesis would be to generate a mutant with CA3 restricted deletion of α CaMKII and measure the effect on long-term potentiation and learning. We have recently generated such a mutant and are now in the process of analyzing these mice.

Even though α CaMKII is essential for normal plasticity and learning, the gene has not yet been linked to a cognitive disorder. That may seem surprising, but the most common mutation (heterozygous loss of a gene) may get unnoticed since α CaMKII expression is very restricted both with respect to its onset and region (postnatal and only in neurons). Thus a loss-of-function mutation in humans would probably result in a mild cognitive deficit without any other identifiable deficits, similar to what is seen in α CaMKII heterozygous mice. Such a mutation is likely not to get diagnosed. In contrast, a gain of function mutation or a dominant negative mutation may result in a much more severe cognitive phenotype that could also affect other neuronal functions such as motor coordination. Indeed, in Chapter 4 we provide evidence that the neurological symptoms associated with Angelman Syndrome (AS) are caused by the dominant negative effect of α CaMKII deregulation. A mouse model for Angelman Syndrome shows reduced CaMKII activity and increased phosphorylation of the CaMKII inhibitory T305 and T306 site (Weeber et al., 2003). By crossing the AS mouse with α CaMKII-T305V/T306A mutant mice, in which inhibitory phosphorylation of CaMKII is reduced, we were able to show that the increased inhibitory phosphorylation is directly responsible for the major deficits observed in AS. The molecular and cellular deficits of the AS mouse were rescued by preventing the inhibitory phosphorylation of CaMKII at T305 and T306. We showed that reduction of α CaMKII inhibitory phosphorylation rescues CaMKII activity and reduces both seizure propensity and motor performance deficits associated with AS.

In addition, we were able to rescue the plasticity and learning deficits. Thus, deregulation of α CaMKII phosphorylation seems to be the primary cause for the neurological deficits associated with Angelman syndrome. Even though this finding is very important, it is not immediately clear how these findings can lead to prevent or rescue the cognitive deficits in AS patients. CaMKII seems a precarious protein to be used as a drug target. Moreover, we have not yet proven whether the deficits are reversible at a time when most children get diagnosed (after one or two years of age). To address this, a new mutant has to be made that allows us to silence the Ube3a gene until the mouse is adult. Thus, the mouse would first show the symptoms of AS, but after the gene is switched on the mutant phenotype should revert to a wild-type phenotype. Recently, this genetic approach has been successfully applied to a mouse model of Rett syndrome (Guy et al., 2007).

To identify targets for a pharmaceutical intervention, it is also pivotal to understand the link between α CaMKII inhibitory phosphorylation and Ube3a. Is Ube3a controlling the activity of a phosphatase? And if so, why does that only affect CaMKII function, whereas other kinases seem to work fine? This question has not been answered yet, and extensive proteomics studies in which Ube3a mouse brains are directly compared with wild-type brains will be needed to reveal the precise mechanism linking CaMKII and Ube3a.

Most human cognitive disorders are associated with mutations in genes involved in signal transduction. Neurofibromatosis 1 (NF1) is one of these diseases and with an incidence of 1:1500 it is one of the most common cognitive disorders linked to a single gene mutation (Ozonoff, 1999). We investigated a mouse model of this disorder in chapter 5. Neurofibromin, the protein encoded by the NF1 gene, has several functions, serving as a GTP-ase activating protein (GAP) as well as modulating adenylate cyclase and microtubule binding activity (Costa et al., 2002). GAP proteins (such as NF1) normally convert Ras protein from the active form (GTP-bound) to the inactive guanosine diphosphate-bound form. Hence, mutations in a GAP encoding gene, would be expected to increase the activity of Ras and consequently leads increased activity of its downstream ERK signalling pathway. This is consistent with the report that learning deficits can be rescued in a mouse model of NF1 by genetic and pharmacologic manipulations that decrease Ras function (Costa et al., 2002). As we showed in chapter 2, Ras activation in excitatory neurons leads to increased transmitter release, increased LTP, and increased hippocampal learning. Since NF1 is a GAP protein and changes active Ras to inactive Ras, one may expect that NF1 mutants must show the same responses seen in H-Ras^{G12V} mice. In contrast, mice lacking the NF1-9a isoform show LTP and learning deficits with no changes in presynaptic plasticity. The reason for this difference is probably caused by the

differences in localization between the transgenic Ras gene and NF1. In H-Ras^{G12V} mice we used the CaMKII promoter, which restricts expression to the excitatory neurons of the forebrain. In contrast, studies on NF1^{+/-} mutants suggest that NF1 is mostly affecting inhibitory neurons (Costa et al., 2002). Indeed, LTP deficits in the NF1^{+/-} mutant have been rescued using GABA inhibitors, suggesting that this increased GABA release might be responsible for plasticity and learning deficits in NF1. Whether this is also the case for the Exon9a isoform remains to be investigated. However since exon 9a is not part of the GAP domain it is likely that this part of the protein is not involved in the regulation of Ras. Therefore it is questionable whether the deficits of the NF1-9a mutant are comparable to the NF1^{+/-} mutant. Studies in which GABA release is measured by determining IPSC frequency could shed more light on this. In addition, it could be tested whether the LTP deficits in the NF1-9a mutant can also be rescued by applying GABA inhibitors. Finally, it would be interesting to investigate with which other protein(s) the exon 9a containing N-terminal part of NF1 is interacting. Co-immunoprecipitation of NF1 with and without exon 9a followed by a proteomics analysis could be used to investigate this. In addition, we could look for binding partners using a two-hybrid screen. Finally, it would be interesting to know whether NF1 patients have been identified with mutations in exon9a or in the adjacent exons. This would strengthen our observation that this is an important exon. However, if such patients are not found, one could argue that such patients may not receive the clinical NF1 diagnosis (i.e presence of café-au-lait spots and neurofibromas), since the exon 9a isoform is only expressed in neurons.

Most studies in this thesis (from chapter 2 to chapter 5) have focused on the hippocampus, which is known to be critically involved in spatial learning. However, in chapter 7 we investigated to what extent the cerebellum is involved in spatial navigation. Several types of cerebellar animal models have been tested in spatial navigation tasks, including mutant mice (Lalonde and Botez, 1986), hemi-cerebellectomized rats (Petrosini et al., 1996), and rats with cerebellar input lesions (Rondi-Reig et al., 2002). All cerebellar animal models showed impaired learning capabilities when tested with the classical Morris water maze. Although these studies point toward a role for cerebellum in mediating the procedural component of the spatial navigation function (Leggio et al., 1999), they suffer from some limitations. For example, in addition to a learning deficit these cerebellar animal models also show a motor performance deficit, caused by lesions (Petrosini et al., 1998; Leggio et al., 1999; Mandolesi et al., 2001; Colombel et al., 2004) or cerebellar degeneration, as a result of spontaneous mutations (Lalonde and Botez, 1986; Lalonde et al., 1988; Lalonde et al., 1996; Lalonde and Strazielle, 2003; Martin et al., 2003; Martin et al.,

2004). To overcome these limitations, a transgenic mouse (called L7-PKCI) has been produced (De Zeeuw et al., 1998) in which the pseudosubstrate PKC inhibitor, PKC[19–31], was selectively expressed in Purkinje cells under the control of the *pcp-2(L7)* gene promoter. De Zeeuw and colleagues showed a complete block of LTD induction in these mice. Importantly, these mice have no motor performance deficits and normal electrophysiological properties of Purkinje cells. We used these mice in our study and found that their general behaviour, physical characteristics or sensorimotor reflexes are normal. Electrophysiological experiments in CA1 area of these mice showed normal hippocampal function as well. To investigate the impact of a parallel fiber-LTD deficit on spatial navigation, we used two different behavioural tasks (The Morris water maze and the star maze) and showed that these mice are able to encode the spatiotemporal relationships among environmental cues or events (declarative component), but they are unable to adapt their goal-directed behaviour (procedural component) effectively. This suggests that the cerebellum may also have an important role in goal directed behavior and confirm a role for cerebellar LTD in spatial learning. This finding highlights the importance of using several tests before concluding that a deficit in maze learning is caused by a hippocampal deficit. It would also be interesting to see if our finding with the L7-PKCI mutant can be extended to other mutants with impaired cerebellar LTD. Since it was recently shown that α CaMKII is required for cerebellar LTD as well (Hansel et al., 2006), it would be interesting to test maze and context learning in a Purkinje cell specific knock-out of α CaMKII, and compare these results with a hippocampal CA1 specific α CaMKII knock-out. In such a study we could directly assess the relative importance of the hippocampus and cerebellar in spatial learning.

7.2 References

- Colombel C, Lalonde R, Caston J (2004) The effects of unilateral removal of the cerebellar hemispheres on spatial learning and memory in rats. *Brain Res* 1004:108-115.
- Costa RM, Federov NB, Kogan JH, Murphy GG, Stern J, Ohno M, Kucherlapati R, Jacks T, Silva AJ (2002) Mechanism for the learning deficits in a mouse model of neurofibromatosis type 1. *Nature* 415:526-530.
- De Zeeuw CI, Hansel C, Bian F, Koekkoek SK, van Alphen AM, Linden DJ, Oberdick J (1998) Expression of a protein kinase C inhibitor in Purkinje cells blocks cerebellar LTD and adaptation of the vestibulo-ocular reflex. *Neuron* 20:495-508.
- Guy J, Gan J, Selfridge J, Cobb S, Bird A (2007) Reversal of neurological defects in a mouse model of Rett syndrome. *Science* 315:1143-1147.
- Hansel C, de Jeu M, Belmeguenai A, Houtman SH, Buitendijk GH, Andreev D, De Zeeuw CI, Elgersma Y (2006) α CaMKII Is essential for cerebellar LTD and motor learning. *Neuron* 51:835-843.

- Lalonde R, Botez MI (1986) Navigational deficits in weaver mutant mice. *Brain Res* 398:175-177.
- Lalonde R, Strazielle C (2003) Motor coordination, exploration, and spatial learning in a natural mouse mutation (nervous) with Purkinje cell degeneration. *Behav Genet* 33:59-66.
- Lalonde R, Lamarre Y, Smith AM (1988) Does the mutant mouse *lurcher* have deficits in spatially oriented behaviours? *Brain Res* 455:24-30.
- Lalonde R, Filali M, Bensoula AN, Monnier C, Guastavino JM (1996) Spatial learning in a Z-maze by cerebellar mutant mice. *Physiol Behav* 59:83-86.
- Leggio MG, Neri P, Graziano A, Mandolesi L, Molinari M, Petrosini L (1999) Cerebellar contribution to spatial event processing: characterization of procedural learning. *Exp Brain Res* 127:1-11.
- Lu FM, Hawkins RD (2006) Presynaptic and postsynaptic Ca(2+) and CamKII contribute to long-term potentiation at synapses between individual CA3 neurons. *Proc Natl Acad Sci U S A* 103:4264-4269.
- Mandolesi L, Leggio MG, Graziano A, Neri P, Petrosini L (2001) Cerebellar contribution to spatial event processing: involvement in procedural and working memory components. *Eur J Neurosci* 14:2011-2022.
- Martin LA, Goldowitz D, Mittleman G (2003) The cerebellum and spatial ability: dissection of motor and cognitive components with a mouse model system. *Eur J Neurosci* 18:2002-2010.
- Martin LA, Escher T, Goldowitz D, Mittleman G (2004) A relationship between cerebellar Purkinje cells and spatial working memory demonstrated in a *lurcher*/chimera mouse model system. *Genes Brain Behav* 3:158-166.
- Ninan I, Arancio O (2004) Presynaptic CaMKII is necessary for synaptic plasticity in cultured hippocampal neurons. *Neuron* 42:129-141.
- Ozonoff S (1999) Cognitive impairment in neurofibromatosis type 1. *Am J Med Genet* 89:45-52.
- Petrosini L, Molinari M, Dell'Anna ME (1996) Cerebellar contribution to spatial event processing: Morris water maze and T-maze. *Eur J Neurosci* 8:1882-1896.
- Petrosini L, Leggio MG, Molinari M (1998) The cerebellum in the spatial problem solving: a co-star or a guest star? *Prog Neurobiol* 56:191-210.
- Rondi-Reig L, Le Marec N, Caston J, Mariani J (2002) The role of climbing and parallel fibers inputs to cerebellar cortex in navigation. *Behav Brain Res* 132:11-18.
- Weeber EJ, Jiang YH, Elgersma Y, Varga AW, Carrasquillo Y, Brown SE, Christian JM, Mirnikjoo B, Silva A, Beaudet AL, Sweatt JD (2003) Derangements of hippocampal calcium/calmodulin-dependent protein kinase II in a mouse model for Angelman mental retardation syndrome. *J Neurosci* 23:2634-2644.

Summary

Understanding the molecular and cellular mechanisms underlying learning and memory is one of the most exciting topics in the field of Neuroscience. Learning is thought to occur through activity-dependent synaptic modification in the neuronal network. The hippocampus, is an excellent structure to study synaptic plasticity and learning, because of its anatomy and network. Most of the studies in this thesis were performed on the hippocampus to unravel the molecular and cellular mechanisms underlying spatial learning.

Molecular and cellular studies of mechanisms underlying mammalian learning and memory have focused almost exclusively on postsynaptic function. However, in *chapter 2* we reveal a presynaptic mechanism that modulates learning and synaptic plasticity in mice. Using transgenic mice expressing a constitutively active form of H-ras (H-rasG12V), we studied the H-Ras/ERK/Syn I pathway and showed that in these mice ERK-dependent phosphorylation of synapsin I is increased and causes several presynaptic changes.

Calcium-calmodulin dependent protein kinase II (CaMKII) is a protein kinase, which detects Ca^{2+} signals and can phosphorylate many target proteins as well as itself. This auto-phosphorylation is critical for its role in LTP and learning. However, in *chapter 3* we show that although CaMKII is required for normal presynaptic function, its ability to phosphorylate itself, or other proteins does not appear to be necessary for its presynaptic role. This suggests that CaMKII plays a structural (non-enzymatic) role and may explain why this kinase is so abundant.

The phosphorylation of CaMKII appears to be deregulated in Angelman syndrome, a severe neurological disorder. Specifically, phosphorylation at CaMKII-Thr305/Thr306 appears to be increased which results in self-inhibition of CaMKII. However to what extent the neurological deficits can be attributed to the increased self-inhibition was not known. In *chapter 4* we provide strong evidence that the major neurological symptoms are directly attributable by this increased self-inhibited form of CaMKII.

In *chapter 5* we studied one of the most common single-gene disorders affecting cognitive function in human, neurofibromatosis type 1 (NF1). We investigated the importance of the alternatively spliced exon 9a in NF1 function. This exon is not a part of GAP domain and its function is unknown. We created a mouse lacking the NF1-Ex9a isoform and showed that these mice have hippocampal learning deficits and impaired LTP. It does appear that this exon is critical for the role of NF1 in synaptic function and this suggest that NF1 may play an additional role besides Ras regulation.

The hippocampus is not the only structure involved in spatial learning. Other structures have also been implicated in spatial learning. In *chapter 6*, we made use of L7-PKCI transgenic mice, which lack parallel fiber-Purkinje cell LTD, to test the involvement of the cerebellum. This study strongly suggested a role for the cerebellum in goal directed behavior.

Samenvatting

Het ontrafelen van de moleculaire en cellulaire processen die ten grondslag liggen aan leren en geheugen is waarschijnlijk een van de grootste uitdagingen in de Neurowetenschappen. Leren vindt o.a. plaats door synaptische modificaties in de neuronale netwerken. Vanwege zijn ideale anatomie, grote plasticiteit en de essentiële rol in ruimtelijk leren is de hippocampus bij uitstek geschikt om de moleculaire en cellulaire processen die betrokken zijn bij dit leerproces te bestuderen.

De meeste studies richten zich op de moleculaire en cellulaire processen van de post-synaptische neuron. Echter, in hoofdstuk 2 laten we zien dat er ook een presynaptic mechanisme is dat het leren en de plasticiteit kan moduleren. Door gebruik te maken van transgene H-ras (H-rasG12V) muizen, vonden we dat de H-Ras/ERK/Syn I signaal route belangrijk is voor het reguleren van neurotransmitter afgifte en voor plasticiteit en leren.

Calcium-calmodulin afhankelijke kinase II (CaMKII) is een kinase dat Ca^{2+} signalen kan detecteren, en daarna vele andere eiwitten en ook zichzelf kan fosforyleren. Met name deze zelf-fosforylatie is belangrijk voor plasticiteit en leren. Echter, in hoofdstuk 3 laten we zien dat pre-synaptisch CaMKII zijn rol in neurotransmitter afgifte ook kan vervullen zonder dat het zichzelf of andere eiwitten kan fosforyleren. Dus pre-synaptisch CaMKII speelt met name een structurele (niet enzymatische) rol. Dit kan verklaren waarom er zoveel CaMKII in de cel zit.

De auto-fosforylatie van CaMKII is aangedaan in de ernstige neurologische aandoening Angelman Syndroom. Met name blijkt er te veel CaMKII-Thr305/Thr306 auto-fosforylatie te zijn, hetgeen resulteert in te veel zelfremming van CaMKII. In hoofdstuk 4 laten we zien dat deze verhoogde zelfremming direct verantwoordelijk is voor de meeste neurologische symptomen van Angelman Syndroom.

In hoofdstuk 5 richten we ons op Neurofibromatose, een van de meest voorkomende erfelijke aandoeningen die leerproblemen veroorzaakt. NF1 reguleert de hoeveelheid actief Ras in een neuron. We hebben onderzocht wat het belang was van de NF1 isoform die exon 9a bevat. We vonden dat zonder dit exon, NF1 zijn rol in plasticiteit en leren niet goed kan vervullen. Omdat exon 9a buiten het Ras regulatie gebied van NF1 zit concludeerden we, dat NF1 meer doet in de neuron dan alleen Ras reguleren.

De hippocampus is niet het enige deel van het brein dat belangrijk is voor ruimtelijk leren. In hoofdstuk 5 hebben we de bijdrage van de kleine hersenen bestudeerd. Door gebruik te maken van een L7-PKCI transgene muis die geen parallel-vezel LTD meer vertoont, konden we aantonen dat deze cerebellaire plasticiteit essentieel is voor het bereiken van een bepaalde plaats.

List of Publications

1. Zarrindast, M.R., **Hodjati, M.R.**, Pejhan, A. and Soleimannejad, E. (1996). Bupropion induces sniffing: a possible dopaminergic mechanism. *European Neuropsychopharmacology*. 6, 299-303.
2. Kushner, S. A., Elgersma, Y., Murphy, G. G., Jaarsma, D., van Woerden, G. M., **Hojjati, M. R.**, Cui, Y., LeBoutillier, J. C., Marrone, D. F., Choi, E. S., *et al.* (2005). Modulation of presynaptic plasticity and learning by the H-ras/extracellular signal-regulated kinase/synapsin I signaling pathway. *The Journal of Neuroscience*. 25, 9721-9734.
3. Burguiere, E., Arleo, A., **Hojjati, M.R.**, Elgersma, Y., De Zeeuw, C. I., Berthoz, A., and Rondi-Reig, L. (2005). Spatial navigation impairment in mice lacking cerebellar LTD: a motor adaptation deficit? *Nature Neuroscience*. 8, 1292-1294.
4. Van Woerden, G. M., Harris, K. D., **Hojjati, M. R.**, Gustin, R. M., Qiu, S., de Avila Freire, R., Jiang, Y. H., Elgersma, Y., and Weeber, E. J. (2007). Rescue of neurological deficits in a mouse model for Angelman syndrome by reduction of alphaCaMKII inhibitory phosphorylation. *Nature Neuroscience*. 10, 280-282.
5. **Hojjati, M.R.**, Geeske M. van Woerden, William J. Tyler, Karl Peter Giese, Alcino J. Silva, Lucas Pozzo-Miller and Ype Elgersma. (2007). Kinase activity is not required for α CaMKII-dependent presynaptic plasticity at hippocampal CA3-CA1 synapses. *Nature Neuroscience*. 10(9): 1125-1127.
6. **Hojjati, M.R.**, Geeske M. van Woerden, Alcino J. Silva, and Ype Elgersma. The neuron-specific NF1 exon 9a is essential for theta frequency LTP and learning. Submitted

Curriculum Vitae

The author of this thesis was born on 10 June 1965 in Najafabad, Esfahan in Iran. He graduated from high school in 1983, in Najafabad. He moved to Ahvaz, a city in South of Iran, to study his Bachelor of Science (B.Sc) in Biology. He finished his B.Sc. in 1987. From 1991-1994, he studied Human Physiology and got his first Master of Science (M.Sc.) from Tarbiat Modarres University in Tehran. His research, "The effect of Bupropion on sniffing behaviour in rats", was conducted under supervision of Dr. M.R. Zarrindast. In July 1994, he was employed at Shahrekord University of Medical Sciences to teach Physiology for medical and undergraduate students. His marriage with M. Namavar was in 1994 and now they have two children. He continued his teaching at the University from 1994 till 2003, when he got a scholarship from Iranian Ministry of Health, Treatment, and Medical Education to follow his education leading to the Ph.D. in Molecular Physiology. He then moved with his family to the Netherlands, where he began his M.Sc./Ph.D. projects in the department of Neuroscience, at the Erasmus Medical Center under supervision of Dr. Y. Elgersma and Prof.dr. Chirs de Zeeuw. He finished his second Master of Science (M.Sc.) in Neuroscience in 2005 and then continued to the Ph.D. degree. After his graduation he will go back to Iran to do research and teaching in his country.

Acknowledgements

First of all, thank to The God, the Beneficent and the Merciful who created Humans as his best creatures. After that, I would like to thank my promoter Prof.dr. Chris de Zeeuw for giving me the opportunity to work as a PhD student at the Neuroscience department. I am sure you still remember your questions and my answers in our first conversation, when I called you from Iran. To me it seems like yesterday, but it was 4.5 years ago that I started the application procedure. Without your support I could not finish my Ph.D. on time. Thanks for your support and your positive view.

I also would like to express my sincere appreciation to my co-promoter, Dr. Ype Elgersma who allowed me to work in his lab. It was surprising for me when you said that you would come to the airport on the first day of my arrival to the Netherlands. That day the weather was rainy, windy and very cold, but your warm welcome made it an unforgettable day for my friend and I. During my stay in the Netherlands, whenever I had problems you were always helpful to me and tried your best to solve the problems. I have to express my special thank to you because of your guidance, advices and of course for buying the four chambers setup. It helped me to finish the projects much quicker compared to the old setup. I learnt a lot from you in our weekly group meetings, journal clubs or our individual discussions. You taught me how to look at the science and to do research. I have been working as a teacher for about 9 years, but working in your lab gave me the opportunity to improve my technical abilities as well. I know I am still in preliminary steps, but I hope I can combine my teaching and research abilities and be useful for my country. Thanks a lot for your patience and support during last 4 years.

Furthermore, I would like to thank the promotiecommissie and grote promotiecommissie for reading this thesis, specially to Prof.dr. Gerard Borst for his critical reading and helpful comments.

Many thanks to Prof. Dr. Heinz Beck in Germany (Bonn), who let me to work in his lab and test the effect of the CaMKII inhibitors, and thanks to Malte, for his technical help during my stay in that lab. Thanks to Dr. Steven Kushner for critically discussions.

Thanks to all members of the Ype's lab, from the former members (specially Robert, Susan Ketelaars and Mitja) to the new member of the lab (Azar). Special thanks to Minetta for organizing, ordering and collecting mice for me, for your hospitality when I came to your house and of course for the donation of some of your house stuffs in the first year of my stay in the Netherlands.

Thanks to Rogerio, you and Geeske trained me to do the water maze and fear conditioning experiments. Many thank to Gabrielle for training immuno-histochemistry and Mehrnosh for genotyping the mice. Susan, Marija, Manja and Petra you all were friendly with me and I appreciate your collaborations and helpful talks.

Geeske, you not only were very helpful for me, but also for most of the people in the lab. Everybody in the department knows that you work very hard and have enough data to finish your PhD. I am sure you will have a nice thesis with nice articles. Thanks for your patience whenever I had a question about the mutant mice, and thanks for reading the thesis and for your comments.

Many thanks, to my two roommates Lianne and Nils, who made our room pleasant for work. You always were good friends for me, and gave me very good advices and help. You translated a lot of forms and letters from IND, City Hall, University and other organizations. Sometimes I was ashamed to ask you for more translation, but I have to say that the Netherlands needs a real revolution to solve the bureaucracy in some organizations! Thanks again to Nils for reading the thesis and giving the comments. You easily work with two multi-chamber setups at the same time and record 12 to 16 slices per day. You showed that you are an expert in field recording and a good alternative for Mohammad! Thank you for accepting to be one of my paranimfs.

Many thanks to Loes, Edith and also Moshe (who has left the department), for coordinating MSc. Neuroscience and administrative works, and thanks to Annette, Eric, Ria and Kenneth for arranging the orders, and also to Hans for his technical support. Thanks to Eddie for his help in scanning my files, computer service and for writing the Kandel's book figures on a CD for me.

I also have to thank all group leaders in the department who taught me during my Master course, especially Christian to let me learn patch clamp for a while in his lab, and thanks to Ragu and Simone for their help with patching. Thanks to Joan Holstege to let us use his printer, to Freek for his advices for printing the thesis, to Heiko for the software, to Erika, Mandy and Elize for their smiles and big laughs and again to Elize for the description of electron microscopy to my friend. Thanks to Rik for his help for making pdf of my thesis.

I should thank a large group of people who work in the Neuroscience department, and because of limited space I cannot mention their names, and also thanks to all of my co-authors.

I would like to express my sincere appreciation to my wife for her encourage, patience and for her prayers. During last four years, she also worked very hard as a teacher for our two children, Fatemeh and Mohammad Mahdi and taught them from group 2 to group 5. Without you I could not be succeed in my work and in my life.

And finally thank to the Iranian Ministry of health, and Shahrekord University of Medical Sciences for giving me the scholarship and financial support to continue my study leading to the PhD. degree in the Netherlands; specially to Ms. Dr. Nafisi in the Ministry of health for her cooperation and arranging my works, and also to Dr. Ali Nasimi, my colleague in Shahrekord University, who accepted to continue teaching physiology untill I finish my study.



Water maze room

Original artwork by Fatemeh (11) & Mohammad Mahdi (8) Hojjati, Rotterdam, 2007